Comparing marine primary production and carbon export methods in the Arctic and NE subarctic Pacific

by

Amanda Timmerman
B.Sc., University of Hawaii Manoa, 2010
M.Sc., University of Hawaii Manoa, 2012

A Dissertation Submitted in Partial Fulfillment
of the Requirements for the Degree of

DOCTOR OF PHILOSOPHY

in the School of Earth and Ocean Sciences

Supervisory Committee

Comparing marine primary production and carbon export methods in the Arctic and NE subarctic Pacific

by

Amanda Timmerman
B.Sc., University of Hawaii Manoa, 2010
M.Sc., University of Hawaii Manoa, 2012

Supervisory Committee

Dr. Roberta Hamme, School of Earth and Ocean Sciences
Supervisor

Dr. Diana Varela, School of Earth and Ocean Sciences
Departmental Member

Dr. Debby Ianson, School of Earth and Ocean Sciences
Departmental Member

Dr. Jim Gower, Department of Geography
Outside Member

Dr. Lauren Juranek, Oregon State University
Affiliate Member

Abstract

Primary production and carbon export connect biogeochemical cycles in the surface waters to the deep. Quantifying rates of production and carbon export are important to understanding the global carbon cycle. There are multiple productivity rate methods, but each measures a different fraction of production. The first type of method is in vitro methods that involve removing water samples from the environment and incubating with an isotopically labelled tracer, such as a nutrient. At the end of the incubation, the amount of enrichment in either the particulates (phytoplankton) or the dissolved oxygen are measured to determine productivity. The second type of method is in situ methods that measure the natural environmental parameters instead of incubations. In this study, the natural isotopic composition and the ratio of gases in the surface water are measured. Comparing in situ versus in vitro methods in the Arctic on a GEOTRACES cruise (July 2015), we identified five reasons to explain why methods do not agree: time of integration, depth of integration, recently shoaled mixed layer, mixing at the base of the mixed layer, and methodological issues. When comparing in vitro methods to each other, filter handling and some as yet unidentified bias causes differences. Comparing methods along Line P (over three years), we hypothesize that excretion of dissolved organic nitrogen, upwelling, bottle effects, mixing, and time of integration are the most important factors that cause disagreement between methods. End of bloom dynamics created an extreme case where method disagreement was most severe.

Applying method comparison in the NE subarctic Pacific (August 2014 – June 2017) helps to understand what drives variability in primary production. Historical data show that chlorophyll-a is low and invariant offshore in the high nutrient low chlorophyll area (HNLC), where iron is limiting. We used satellites and models, which compare well with shipboard data, to expand our spatial and temporal coverage of the offshore HNLC area. Increased chlorophyll a is associated with higher production, higher salinity, and lower temperature. We hypothesize that iron can be supplied to surface waters by offshore fronts, using June 2015 and June 2016 as specific examples. Fronts are locations where temperature, salinity and/or density are rapidly changing, in this particular dissertation a

1°C change over 1/3 degree distance. We identified locations where fronts were located based on Mercator model sea surface temperatures and compared these features to satellite chlorophyll patterns. Our hypothesis is also supported by data from June 2017 where there were no fronts and chlorophyll was uniformly low. Future research should consider fronts as a possible mechanism for increasing productivity in the area. Identifying mechanisms that cause methods to disagree and then applying to biogeochemical regions allows for better understanding of carbon cycling.

Table of Contents

List of Tables

List of Figures

Acknowledgments

First I want to say thank Roberta Hamme for all feedback, mentoring, discussions and patience.

Secondly, thanks to my committee members, Debby Ianson, Laurie Juranek, Diana Varela and Jim Gower for the support and helpful suggestions throughout the last five years. Also thank you to Adrian Marchetti for being my external examiner.

Thank you to Peter Stutton, Francisco Chavez, Marguerite Blum for help with Niskin questions. Thank you to Ben Twining, Peter Morton, Kristin Buck, Andrew Ross for help with trace metal samples. Thanks also for conversations about iron with Christina Schallenberg, Dave Janssen and Jay Cullen. Thank you to Erik Fields for help with Mercator model questions. Thank you for the helpful conversations with Lisa Miller, Frank Whitney, Patrick Cummins, Noel Pelland, Peter Webley, and Angelica Peña. Thank you to Shigenobu Takeda, Saichun Tan and Yoko Iwamoto for helping to point me in the right direction for satellite dust detection.

Thank you for all of the assistance in the field. Thank you so much Marie Robert, Doug Yelland and Roger Francois for being so accommodating to my sampling requests. Thank you to the Captains and crew of the CCGS John P. Tully and Amundsen. Thank you to Mariela for helping with analyzing oxygen and O_2/Ar samples. Thank you to Karina Giesbrecht, Kristina Brown, Marjolaine Blais, Michel Gosselin, Helmuth Thomas, Jean-Eric Tremblay and the Laval people for helping on GEOTRACES. Thank you to Robert and Theresa for being my sampling buddies at 4am. Thank you to IOS folk especially Moira, Mark, Glenn, Melissa, Kenny, Nina, and Tamara. Thanks to everyone else who helped carry incubation bottles and flask trunks up and down stairs. Thank you to Sarah Thornton and Steve Emerson for allowing me to borrow gear.

Thanks for help in the lab especially to Paul Quay, Hilary Palevsky, Johnny Stutsman, Mark Haught, Lianna Teeter, Hollie Johnson, Erin Raftery, Maureen Soon.

Thank you to the SEOS office staff for your support on all things UVic, especially to Allison.

Thank you to Ellen, Rick, Rebecca, Taylor, and Auntie Kay who encouraged me and even listened to my seminar. Thank you to all my friends, especially Sheryl Murdock, Cat Stevens, Theresa Venello, Rianna Burnham, Mina SeyedAli and Trevor Gallagher.

Lastly, thank you to Ross. It's been crazy over the past 5 years and I'm glad you were a part of it.

Chapter 1. Introduction

1.1 Marine productivity

Marine primary productivity is important globally. Through photosynthesis, phytoplankton convert inorganic carbon to organic carbon, contributing about half of the global productivity (Field et al., 1998). However, productivity rates are not uniform across time and space in the global ocean. Seasonally, primary productivity is at a maximum in the spring and a minimum in the winter in the NE Pacific (Palevsky et al., 2016). Spatially in the Pacific Ocean, average net primary production (from ^{14}C incubations) ranges from 13.9±0.5 mol C m^{-2} yr^{-1} near Hawaii, with very little seasonal variation (Brix et al., 2006) to 28±7 mol C m^{-2} yr^{-1} near the Kuroshio current (Palevsky et al., 2016) to even higher values in upwelling zones. Quantifying the variability will help decrease the error when extrapolating rates from single stations to larger spatial and temporal time scales.

1.2 Biological carbon pump

The biological carbon pump, which exports organic carbon from the surface ocean, is an important process in the global carbon cycle. The carbon pump exports organic carbon through the following mechanisms: sinking particles, mixing of dissolved organic matter, and active transport by higher trophic levels (Emerson, 2014; De La Rocha and Passow, 2007), where particle transport is the largest flux (Emerson 2014). The deep ocean is an important reservoir for carbon, because carbon in the ocean's interior is out of contact with the atmosphere for long time scales (Falkowski et al., 2003). Through the carbon pump, the surface water is connected to the deep ocean, creating the vertical carbon gradient. The biological carbon pump plays a role in regulating Earth's climate, where

the atmospheric CO_2 concentration would be ~400 ppm higher without marine production (Falkowski et al., 2003).

1.3 Multiple methods and capturing variability

One issue with quantifying marine production is that there are multiple methods, and each measures a different fraction of production. There are two main types of methods. The first is in situ methods in this dissertation measure the natural gas or isotopic composition of gas in the surface waters; however, other in situ techniques that measure other natural parameters exist. In vitro methods involve removing the sample from its environment, spiking with an isotopically labelled tracer (such as a nutrient), and tracing the change in isotopic composition over time. Additionally, most studies utilize only one method, making it difficult to compare rates across studies.

The first method developed to measure photosynthetic rates of marine phytoplankton measured oxygen evolution (Gaarder and Gran, 1927); however, that method was unable to capture low productivity rates. The science community sought a more accurate technique. The modification of the Winkler method improved the oxygen evolution method; however, additional issues with the method exist (e.g. assumption that respiration is the same in the dark and light). An alternative was developed in the 1950's with the ^{14}C in vitro method (Nielsen, 1952). Briefly, water samples are spiked with ^{14}C labelled bicarbonate and then incubated trying to recreate in situ conditions. At the end of the incubation, the water is filtered and the amount of isotopic enrichment of the particles gives an estimate of primary production. Twenty-five years later, Slawyk et al. (1977) developed another in vitro method using the stable isotope ^{13}C, which became more common in the mid 1980's and provides an alternative to the ^{14}C method (Hama et al.,

1983). For both carbon in vitro methods, the exact fraction of primary production measured is unclear. Studies have shown that these methods measure somewhere between net primary production and gross primary production (Slawyk et al., 1977; Hama et al., 1983; Mousseau et al., 1995; Collos and Slawyk, 1985). Since the ^{14}C method was developed, more in vitro methods have been introduced, including the $^{15}NO_3$, $^{15}NH_4$ (Dugdale and Goering, 1967), and ^{18}O (Grande et al., 1989) methods. In

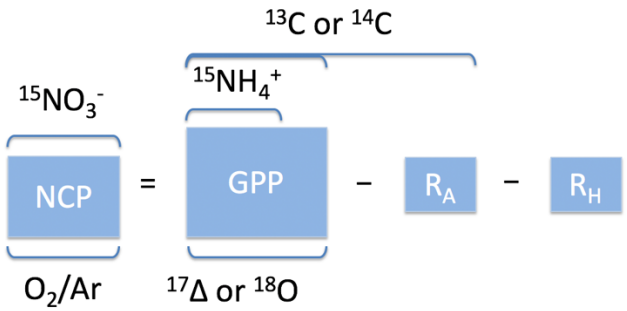

Figure 1.1. Visual representation of what fraction of production each method measures. NCP, GPP, R_A, and R_H represent net community production, gross primary production, respiration by autotrophs, and respiration by heterotrophs, respectively. Methods measuring nitrogen or carbon are labelled on the top of the figure and those measuring oxygen at the bottom. ^{13}C, ^{14}C, $^{15}NO_3^-$, $^{15}NH_4^+$ and ^{18}O are all in vitro methods. O_2/Ar and $^{17}\Delta$ are in situ methods. $^{17}\Delta$ represents the triple oxygen isotopic composition method. Modified figure from Nicholson et al. (2012).

general, samples for in situ methods are easier to collect in the field than in vitro, but require significant processing time in the lab and expensive equipment. In situ methods include mass balance approaches based on oxygen to argon ratios (Craig and Hayward, 1987) and triple oxygen isotopic composition (Luz et al., 1999). Both in situ and in vitro methods have assumptions that are not always upheld, leading to biases. Table 1.1

presents a summary of the methods used in this dissertation, while Figure 1.1 shows which fraction of productivity they measure.

Table 1.1. Synthesis table of the in vitro and in situ methods detailing the time and depth of integration, costs per station, active time in the field and lab, first time the method was used, auxiliary data needed, and what fraction of production is measured. Costs do not include the following: bottles, incubator, filtering rig, beta counter, radiation van, mass spectrometer, consumables, or technician time. The in vitro methods assume five light levels. The in situ methods assume duplicates at one depth within the mixed layer. Time required has three relative quantities: low, medium, and high. The high time frame requires many hours compared to a low time frame of one hour or less.

	In vitro					In situ		
method	**^{14}C**	**^{13}C**	**$^{15}NO_3$**	**$^{15}NH_4$**	**^{18}O**	**O_2/Ar**		**Triple**
Time scale	24 hours					residence time of oxygen in mixed layer		
Depth scale	Mixed layer or euphotic depth					Mixed layer		
Cost	$250 /station	$175 /station	$48 for spike (will last for years)	$62 for spike (will last for years)	$550 /station+ $1500 for analysis	$80 /sample		$160 /sample
Active time in field	medium	medium	medium	medium	high	low		medium
Time in lab	low	medium	medium	medium	high	high		high
First time used	Nielsen, 1952	Slawyk et al., 1977	Dugdale and Goering, 1967	Dugdale and Goering, 1967	Grande et al., 1989	Craig and Hayward, 1987		Luz et al., 1999
Auxiliary data needed	DIC, PAR	PAR	NO_3, PAR	NH_4, PAR	$H_2{}^{18}O$, PAR, ctd data, O_2	wind speed, ctd data		wind speed, ctd data, O_2
Measures	Primary production		New production	Recycled production	Gross primary production	Net community production		Gross primary production

With the wide variety of methods, there are many factors that could cause methods to disagree. Method disagreement is exacerbated when extrapolated to larger spatial and time scales. For example, multiple methods for estimating carbon export do not agree on a global scale, with a range of 5 to 20 Gt C yr^{-1} (Henson et al., 2011), on the order of annual anthropogenic carbon dioxide emission rates (Siegel et al., 2014). However, consistent differences between methods are beginning to emerge, and reasons for method disagreement are becoming clearer. Determining how methods are related will help to identify when biases are important, and may allow comparisons with previous studies to determine long term productivity trends.

1.4 Higher trophic levels

Phytoplankton form the base of the marine food web. Quantifying productivity is important for understanding higher trophic level dynamics. There is debate (e.g. Power, 1992; Verity and Smetacek, 1996) over whether phytoplankton control the higher trophic levels (bottom up) or if grazing by higher trophic levels controls phytoplankton biomass (top down). In reality it might be a mixture of both. Trophic dynamics can impact production rates if top down controls are more important than bottom up. Higher trophic levels also contribute to the biological pump. Zooplankton can graze on phytoplankton, repackaging organic matter into dense fecal pellets that sink quickly (Ducklow et al. 2001). Another way zooplankton contribute to increased export is through feeding within the euphotic zone and then migration to deeper depths (Ducklow et al., 2001). Interestingly, zooplankton fecal pellets could account for a wide range (<5% to almost 50%) of total export in the NE Pacific based on sediment trap data (Wilson et al., 2013).

Similarly, zooplankton could also be eaten and transported deeper by fish and marine mammals.

1.5 Changes in the future

It is unclear how primary production and carbon export will change in the future. Fu et al. (2015) predicted that export will decrease due to increased stratification and decreased nutrient supply from climate change, based on Earth System Models. However, others argue that increased storms could increase mixing (Knutson et al., 2010) and thus increase productivity (e.g. Babin et al., 2004). The Fifth Assessment Report of the Intergovernmental Panel on Climate Change (IPCC) concluded that the biological pump is not understood well enough to determine whether the sign or magnitude of the pump will change in the future (Portner et al., 2014). If the strength and efficiency of the biological pump does change over time, it could affect how carbon is distributed in the ocean and how anthropogenic carbon is taken up by the ocean (Passow and Carlson, 2012). Decreased sea ice coverage and a longer growing season in the Arctic has resulted in increased productivity (Arrigo et al., 2008); however, a mismatch between when prey is abundant and the presence of predators in the area could cause trophic level collapse.

1.6 Regions

This dissertation focuses on three very different regions based on the physical oceanography and biological trends: the subarctic NE Pacific, the Arctic, and the North Atlantic. Grouping according to these three regions is also recommended by Carmack and McLaughlin (2011) based on temperature and salinity relationships and are described as distinct ‘water mass clusters’.

The subarctic NE Pacific's main feature is the Alaska gyre (cyclonic), bounded on the south by the North Pacific Current. The mountain ranges to the east (Cascade and Kluane) trap westerly storm system moisture within the region (Carmack and McLaughlin, 2011). The region can be further split into two subcategories: coastal and offshore. In coastal areas, production is generally limited by macronutrients. Upwelling in the spring and summer brings nutrients to the surface waters, fueling productivity. In juxtaposition, productivity in the offshore region is limited by iron resulting in macronutrients remaining high year round (Whitney et al., 1998; Whitney and Freeland, 1999). Chlorophyll a is lower and less variable offshore compared to the coastal region (e.g. Parslow, 1981; Peña and Varela, 2007). Primary production is at a minimum in the winter and maximum in the spring (e.g. Wong et al. 1995). With the larger scale oceanography being fairly well understood and somewhat uniform, this is an ideal location to conduct method comparison work.

The Arctic region includes the Canadian Arctic Archipelago (CAA). This area can be thought of as an advective ocean with water generally flowing from the Pacific through the Canadian Arctic Archipelago to the North Atlantic (Carmack and Wassmann, 2006; Tremblay et al., 2015) and transporting nutrients from the Barents Sea Opening and Bering Strait throughout the region (Torres-Valdés et al., 2013). The water is modified as it moves through the channels, sills, and islands (Yamamoto-Kawai et al., 2006). Partially because of the varying bathymetry, many dissimilar water masses converge, resulting in a dynamic region. For example, Lancaster Sound contains water from both the Atlantic and Pacific Ocean based on temperature, salinity, and nutrient concentrations (Carmack and McLaughlin, 2011). With the fairly shallow bottom depths at our stations (218 m to 674

m), there could be bathymetry-induced mixing and different water masses in contact with each other. Another consideration within the CAA is that local inputs of river runoff and sea ice melt (Carmack and McLaughlin, 2011) can create salinity stratified regions and rapidly changing stratification and mixing dynamics. With its complicated oceanography, the Arctic is a challenging region for method comparison with many potential causes for methods to be different.

Finally, we classify the Labrador Sea and Baffin Bay within the North Atlantic region. The bathymetry is deeper in the middle of the Labrador Sea and Baffin Bay. Davis Strait (located between the two) is shallower at about 600 m, and about the same depth as the shelf on the outskirts of both. The bottom depth of the stations sampled during this study were greater than 3000 m in the Labrador Sea and ranged from ~1000 m to ~2370 m in Baffin Bay. Baffin Bay has cyclonic circulation (Tang et al., 2004) with less complicated oceanography compared to the CAA. However, the northward flowing Greenland current and the Davis Strait create complicated circulation, allowing different water to be close together (Lobb et al., 2003). This could again complicate method comparison.

1.7 Method comparison studies

Method comparison studies have been conducted in such locations as the Hawaii Ocean Time-series (Quay et al., 2010; Juranek and Quay, 2005; Corno et al., 2005), the North Atlantic (e.g. Chipman et al., 1993; Robinson et al., 2009), Bermuda Atlantic Time Series (e.g. Luz and Barkan, 2000; Luz and Barkan, 2009; Nicholson et al., 2012) and the Southern Ocean (e.g. Hamme et al., 2012; Cassar et al., 2015). These are very different biogeochemical regions, ranging from oligotrophic to high nutrient low chlorophyll areas.

Several method comparison studies have been conducted in the high nutrient low chlorophyll subarctic NE Pacific including the Subarctic Upper Ocean Ecosystem Research (SUPER) program in 1988 and the Joint Global Ocean Flux Study (JGOFS) in the 1990s. In situ and in vitro methods have been compared in the area (Emerson et al., 1993; Giesbrecht et al., 2012; Welschmeyer et al 1993); however, the number of methods was limited and time frames were variable. Emerson et al. (1993) investigated only one month in contrast to Giesbrecht et al. (2012) who sampled three times a year for three years. Both these studies used only two methods that estimate carbon export.

Some studies have measured export in the Arctic, but there are very few method comparisons. Export via ^{234}Th (Cai et al., 2010; Coppola et al., 2002; Moran et al., 1997; Le Moigne et al., 2015) and sediment trap (Coppola et al., 2002) methods has been observed sporadically through space and time. For example, Ulfsbo et al. (2014) compared multiple carbon export methods focusing on underway samples and nutrient drawdown. Stanley et al. (2015) compared two in situ methods. Varela et al. (2013) compared multiple in vitro methods. However, limited Arctic studies (Le Moigne et al., 2015) have compared both in situ and in vitro methods.

1.8 Overview of chapters

There were three main research questions explored in this dissertation.

(1) What are the consistent differences between marine primary production and carbon export methods?

(2) What drives differences between methods?

(3) What causes variability in productivity in the NE subarctic Pacific?

Chapter 2 compares marine primary production and carbon export methods in the Arctic (Question 1). We identify reasons why in situ and in vitro methods do not agree and how they apply to this dataset (Question 2). All data were collected from the 2015 GEOTRACES Arctic cruise utilizing seven methods including both in vitro and in situ methods.

Chapter 3 compares productivity methods in the NE subarctic Pacific (Question 1 and 2). To address these questions, six methods were used along Line P from June and August cruises over three years (six cruises from 2014 to 2017) and five methods on a La Perouse cruise in May 2016.

Chapter 4 examines what drives the spatial and temporal changes in productivity in the NE subarctic Pacific (Question 3). The approach utilizes model, satellite, and shipboard data to put forth a new hypothesis on how fronts control productivity in the high nutrient low chlorophyll *a* area offshore.

Chapter 2. Arctic conditions complicate comparison between in situ and in vitro productivity methods

Key points

1. ^{13}C and ^{14}C bottle incubations are not equivalent on a point-by-point basis during 24-hr incubations
2. Recently shoaled mixed layer can affect in situ versus in vitro method comparison
3. Chlorophyll-a concentration is highly correlated to ^{13}C-PP, ^{14}C-PP and ^{18}O-GPP
4. Primary production integrated to the bottom of the euphotic zone increased with decreasing latitude

Keywords: primary production, carbon export, biological pump, Arctic

2.1 Abstract

Marine primary production produces about half of the oxygen in the atmosphere. The biological pump exports carbon from surface waters to deeper waters. Quantifying these rates is important for understanding the global carbon cycle. Mismatches among multiple productivity methods that should agree complicate quantification. Here we compare two types of methods: in vitro methods, which remove samples from the ocean and incubate them, with in situ methods, which measure natural chemical distributions. We focus on the Labrador Sea, Baffin Bay, and the Canadian Arctic Archipelago during a July 2015 cruise, largely underrepresented regions. We have five hypotheses about what affects in vitro and in situ comparisons: time of integration, depth of integration, recently shoaled mixed layer depth, mixing at the base of the mixed layer, and methodological issues. Regardless of differences, chlorophyll-a concentration is highly correlated with some productivity measurements. We also compare traditional carbon radioisotope (^{14}C) and stable isotope (^{13}C) in vitro methods and find they are not equivalent due to some unidentified bias. Interestingly, we also see latitudinal trends in primary production,

related to PAR and euphotic zone temperature. Consistent difference between methods are emerging and include the underrepresented Arctic.

2.2 Introduction

Quantifying the rate of marine primary production is important on a global scale. During photosynthesis, phytoplankton produce oxygen while converting carbon to organic matter. Half of all global primary production annually occurs in the ocean (Field et al., 1998). Through the biological pump, fixed carbon is transported out of the surface water through the following mechanisms: sinking particles, mixing of dissolved organic matter, and active transport by higher trophic levels (Emerson, 2014). Carbon reaching the deep ocean is out of contact with the atmosphere (Falkowski et al., 2003), sequestered for 100's to 1000's of years (Henson et al., 2012), compared to a residence time on the order of years for carbon remaining in surface waters (Keeling, 1965). The biological carbon pump thus influences Earth's climate, such that atmospheric carbon dioxide concentrations would be about 400 ppm higher without marine production (Falkowski et al., 2003). On an ocean basin scale, the biological pump, and to a smaller extent physical properties, create a vertical carbon gradient in the ocean (Houghton, 2007). Better quantification of current oceanic carbon export and production rates will lead to improved predictions of future atmospheric carbon dioxide concentrations and climate change.

Multiple methods exist for measuring both carbon export and other fractions of production; however, they often disagree for reasons that are still unclear. Such disagreements complicate intercomparison of publications that utilize other methods. For example, multiple methods for quantifying carbon export disagree on a global scale, with

a range from 5 (from ^{234}Th; Henson et al., 2011) to 12.9 GtC yr^{-1} (nitrate uptake; Laws et al., 2000). Given the wide range in global estimates, point measurements of carbon export and their controls need to be better understood before extrapolating to a global scale. More studies are published each year quantifying different fractions of primary production, but how these methods compare to each other is unclear. Through method comparison and intercalibration, a more complete spatial and temporal picture of carbon export and productivity can be obtained. Without this understanding, the undersampling problem may be exacerbated by methodological differences between different studies.

These problems are particularly acute in the Arctic where very few measurements have been taken and even fewer method comparisons have been carried out (e.g. Varela et al., 2013; Le Moigne et al., 2015). The importance of the Arctic to the global biological pump is unclear and likely variable, due to the complicated oceanography in the region. Some studies even exclude the Arctic from their global integrative perspective (e.g. Henson et al. 2011).

The general water flow is from the Pacific through the Canadian Arctic Archipelago (CAA) to the North Atlantic (Carmack and Wassmann, 2006; Tremblay et al., 2015) where it is modified during the transit (Yamamoto-Kawai et al., 2006). The CAA is a dynamic region with complicated oceanography, partially due to varying bathymetry and a network of islands, resulting in many dissimilar water masses converging. There are also freshwater inputs from rivers and sea ice melt (Carmack and McLaughlin, 2011) creating salinity stratified regions with rapidly changing stratification and mixing. With its complicated oceanography, the Arctic is a challenging region for method comparison with many potential causes for methods to be different. The Labrador Sea and Baffin

Bay, within the North Atlantic region, has deeper bathymetry in the center and split by Davis Strait (shallower around 600 m). Baffin Bay has cyclonic circulation (Tang et al., 2004) with less complicated oceanography compared to the CAA. However, the northward flowing Greenland current and the Davis Strait creates more complex circulation, allowing different water to be close together (Lobb et al., 2003) and making method comparison complicated.

Undersampling is the largest problem in quantifying the biological pump. Some time series stations and larger programs (e.g. Joint Global Ocean Flux Study, JGOFS) regularly measured carbon export and production; however, these are only in a handful of places and largely ignore the Arctic. Method comparisons in particular have focused on the Hawaii Ocean time-series (Quay et al., 2010; Juranek and Quay, 2005; Corno et al., 2005), Bermuda Atlantic time-series (Luz and Barkan, 2009; Nicholson et al., 2012), and the North Atlantic (Robinson et al., 2009). With these studies, we are beginning to understand how different methods relate to each other. For example, it appears that in situ methods tend to have higher rates than in vitro methods (e.g. Juranek and Quay, 2005; Giesbrecht et al., 2012; Quay et al., 2010). Some factors already identified that cause disagreement between methods are rapid changes in rates over time (Hamme et al., 2012), productivity levels themselves (Giesbrecht et al., 2012), and the time each method integrates over (Quay et al., 2010). Appropriate spatial and temporal sampling to capture a location depends on factors such as how quickly the environment is changing and whether point measurements adequately capture regional variability.

This chapter will compare estimates for carbon export, primary production, and gross production methods simultaneously in the Arctic, a chronically underrepresented area,

with a focus on three types of comparisons. First, we examine how closely in situ and in vitro methods agree, comparing two methods that estimate carbon export and two methods that estimate gross primary production. We put forth five hypotheses for differences between in situ and in vitro methods. Second, we examine whether ^{13}C and ^{14}C bottle incubations yield equivalent values. Third, we examine whether there are consistent relationships among bottle incubation methods, focusing on ^{13}C and ^{14}C versus ^{18}O incubations.

2.3 Background

For this study, both in situ and in vitro methods were utilized. In situ methods rely on natural chemical distributions that reflect productivity rates, gases within the mixed layer for example. The in situ methods we use here produce single, depth-integrated rates at each station. In vitro methods involve removing the water from the ocean, adding an isotopic tracer, and incubating the amended sample over some time period, assuming conditions during incubations are the same as the in situ conditions. In vitro samples are taken at multiple light depths and integrated to be comparable to in situ methods. The theoretical basis of each method is described in sections 2.3.1 to 2.3.3, with the analytical details described in section 2.4.

We measured several different fractions of production. Gross primary production (GPP) is the production of fixed carbon by autotrophs. Net primary production (NPP) is GPP minus respiration by those autotrophs. Net community production (NCP) is GPP minus respiration by both autotrophs and heterotrophs. NCP is equivalent to the carbon available for export. Primary production (PP) as measured by ^{13}C or ^{14}C incubations falls

somewhere between GPP and NPP, depending on factors such as time of integration, nutrient concentration, and respiration.

2.3.1 Estimating carbon export

2.3.1.1 Net Community Production from Oxygen / Argon Ratios (O_2/Ar-NCP)

A mass balance accounting for the ratio of dissolved oxygen to argon (O_2/Ar) can be used to estimate net community production (O_2/Ar-NCP) in situ in the mixed layer (e.g. Craig and Hayward, 1987; Emerson et al., 1995). Oxygen and argon have similar physical properties (e.g. solubility), but argon is biologically inert. By normalizing oxygen to argon, the impact of sea level pressure is removed, while physical contributions, such as bubbles and temperature changes, are minimized in the mass balance. Photosynthesis and respiration, diffusive gas exchange, and vertical or lateral mixing and advection are the main processes that affect the O_2/Ar ratio. Where mixing and advection are negligible, in regions that are less dynamic, the only loss of biological oxygen from the mixed layer is by air-sea gas exchange, which can be estimated based on a wind speed parameterization. By appropriately accounting for the recent history of past wind speeds (Reuer et al., 2007; Teeter et al., 2018), the loss of biological oxygen from the mixed layer is calculated and is equal to the exponentially weighted average of past NCP rates over the residence time of gases in the mixed layer (approximately 2 weeks). O_2/Ar-NCP obtained in this way is an estimate of carbon export and should be equivalent to new production (see next section; Reuer et al., 2007; Falkowski, 2003; Platt et al., 1989), except that O_2/Ar-NCP includes both the dissolved and particulate export from the mixed layer (Quay et al., 2010). In the open ocean, the main uncertainties in this method are parameterization of air-sea gas exchange and vertical mixing where a depth gradient

in O_2/Ar occurs below the mixed layer. In the coastal areas, advection is also an important uncertainty.

2.3.1.2 New Production from $^{15}NO_3^-$ bottle incubations (^{15}N-new)

Nitrate uptake in bottle incubations using ^{15}N labeled nitrate is an in vitro method that measures new production (^{15}N-new) at individual depths within the euphotic zone. New production assumes that export of organic nitrogen is bounded by the amount of nitrogen introduced into the system (Dugdale and Goering, 1967). In other words, at steady state the amount of new nitrogen-based nutrients input into the euphotic zone has to balance the export of organic nitrogen out of the euphotic zone. ^{15}N-new further assumes that the only source of new nitrogen to the euphotic zone comes from nitrate transported from below, so measuring how much production is supported by nitrate should yield an estimate of carbon export over sufficient temporal and spatial scales (Dugdale and Goering, 1967). To quantify ^{15}N-new, samples are spiked with ^{15}N-labeled nitrate and incubated as close to in situ conditions as possible. At the end of the incubation, the sample is filtered, and the ^{15}N enrichment of the particles is measured. Since only particles are measured, this method does not include the dissolved carbon export (Legendre, 1989; Reuer et al., 2007). Dissolved organic carbon is exported by vertical mixing and could account up to 20% of the biological pump in the North Atlantic (Hansell et al., 2009). Other possible sources of new nitrogen from nitrogen fixation, atmospheric deposition, and coastal runoff are not considered, unless those sources directly add nitrate, which would then be included in ^{15}N-new. Nitrate produced by nitrification (oxidation of ammonium to nitrate) would bias this method too high, because nitrification represents a nitrate source from recycled sources not new sources.

Nitrification is traditionally thought to be negligible in the euphotic zone because nitrification is photoinhibited (Horrigan et al. 1981) but that is not always the case (Dore and Karl 1996; Grundle et al., 2013). If nitrification in the euphotic zone is more important than previous assumed, ^{15}N-new would be an overestimate.

2.3.2 Estimating gross primary production

2.3.2.1 Gross Primary Production from Triple Oxygen Isotope ($^{17}\Delta$-GPP)

A mass balance of the three isotopes of oxygen in the mixed layer can be used to estimate gross primary production ($^{17}\Delta$-GPP) in this in situ method. The method hinges on determining the origin of dissolved oxygen from either air-sea gas exchange or photosynthesis (Luz et al., 1999; Luz and Barkan, 2000). In the stratosphere, photochemical reactions involving oxygen, carbon dioxide, and ozone fractionate the three stable oxygen isotopes (^{16}O, ^{17}O, ^{18}O) in a mass independent way, such that atmospheric oxygen is depleted in ^{17}O relative to ^{18}O (Thiemens et al., 1995). On the other hand, oxygen produced during photosynthesis has an isotopic composition close to that of the water it is formed from and is distinct from the ^{17}O depleted atmospheric oxygen (Luz and Barkan, 2000; Luz and Barkan, 2011). A parameter that distinguishes between the two sources of oxygen in the surface waters is $^{17}\Delta=\ln(\delta^{17}O/1000+1) - 0.5179\ln(\delta^{18}O/1000+1)$. This parameter is not affected by respiration, because an oxygen molecule with ^{17}O is discriminated against during respiration at about half the rate (0.5179) compared with oxygen molecules with ^{18}O. In contrast, oxygen produced by photosynthesis has a $^{17}\Delta$ near 250 per meg while atmospheric oxygen has a $^{17}\Delta$ of 0 per meg. Surface water dissolved oxygen has a $^{17}\Delta$ that is a mixture of oxygen from air-sea gas exchange and photosynthesis depending on which process dominates (Luz and Barkan, 2000; Cassar et al., 2015). Like O_2/Ar-NCP, uncertainties in air sea gas exchange

parameterizations and in vertical mixing can also affect this method. In particular, a subsurface maximum in $^{17}\Delta$ often forms below the mixed layer, where oxygen has been produced through photosynthesis but cannot escape via gas exchange. Any mixing or entrainment with this high $^{17}\Delta$ water can bias the $^{17}\Delta$-GPP method high and needs to be corrected (Nicholson et al., 2014). Although the $^{17}\Delta$ parameter is a useful way to think about the theoretical underpinnings of this method, however, the actual gross primary production rates are calculated directly from isotopic ratios (Kaiser 2011; Prokopenko et al. 2011).

2.3.2.2 Gross Primary Production from $H_2{}^{18}O$ bottle incubations (^{18}O-GPP)

Oxygen production in bottle incubations using ^{18}O labeled water (^{18}O-GPP) is an in vitro method that estimates gross primary production at individual depths within the euphotic zone. This method is based on the way that water is split to form oxygen gas during photosynthesis. As a result, the dissolved oxygen produced has nearly the same isotopic composition as the water (Guy et al., 1993; Luz and Barkan, 2011). After spiking the sample water with ^{18}O-labeled water, the subsequent ^{18}O enrichment of the dissolved oxygen pool can be measured to determine gross primary production. Because the dissolved oxygen (O_2) pool is much larger than the particulate organic carbon pool, respiration is less likely to consume some of the labeled product, so that this method is much less sensitive to respiration than other in vitro methods. One issue with this method is determining what ratio to use to convert from oxygen units to carbon units with inherent assumptions of the amount of decoupling between oxygen production and carbon fixation. In this chapter, we use a photosynthetic quotient of 1.4 O_2/C but this could be impacted by factors such as decoupling between splitting of water and carbon

fixation. Another assumption that could bias this method is that it assumes there is no intracellular recycling of ^{18}O (other in vitro also have the same issue with ^{13}C, ^{14}C or ^{15}N), which would cause the methods to underestimate gross primary production (Juranek and Quay, 2005).

2.3.3 Estimating primary production from carbon uptake incubations (^{13}C-PP and ^{14}C-PP)

Carbon uptake in bottle incubations using ^{13}C and ^{14}C labeled inorganic carbon are in vitro methods to measure primary production at individual depths within the euphotic zone, utilizing stable isotope and radioisotope methods, respectively. After spiking the sample water with isotopically enriched inorganic carbon, the carbon isotopes are used to track phytoplankton uptake during photosynthesis by measuring carbon enrichment of the particulate carbon (Slawyk et al., 1977; Nielsen, 1952). For ^{14}C, assimilation is determined by measuring the beta-radiation from the particulates, whereas, for ^{13}C, assimilation is determined by measuring both the ^{13}C excess in the particulates and the particulate carbon concentration (including phytoplankton, detritus, and other particulate matter). Although the label uses the same element, the measurement fundamentals are different. These methods are thought to measure somewhere between net primary production and gross primary production (Marra, 2009). ^{13}C incubations (^{13}C-PP) and ^{14}C incubations (^{14}C-PP) should measure the same fraction of productivity (Hama et al., 1983). It should be noted that ^{12}C is preferentially used over other carbon isotopes during photosynthesis but by a small fraction (Nier and Gulbransen, 1939).

2.4 Methods

2.4.1 Study area

This study was part of the Canadian contribution to the international GEOTRACES program in the Arctic. The cruise on the CCGS Amundsen departed Quebec City on 10 July 2015 and arrived in Kugluktuk on 20 August 2015. A total of 10 stations were

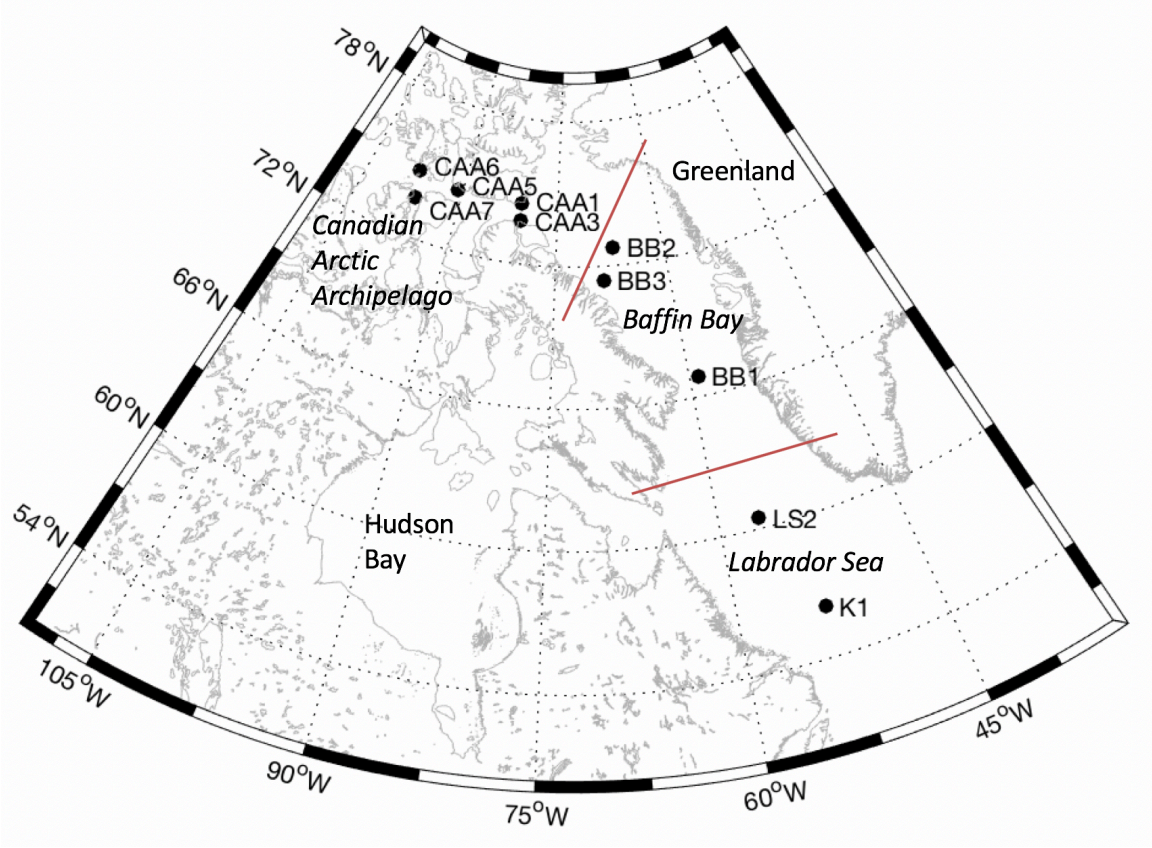

Figure 2.1. Station locations in the Labrador Sea (K1, LS2), Baffin Bay (BB1, BB2, BB3), and the Canadian Arctic Archipelago (CAA1, CAA3, CAA5, CAA6, CAA7). We also refer to K1 and LS2 as LabSea-S and LabSea-N, respectively; the three Baffin Bay stations (BB1, BB2, BB3) as Baffin-S, Baffin-central, and Baffin-W, respectively. CAA1 (Lancaster-N) and CAA3 (Lancaster-S) are located in Lancaster Sound. CAA5 (CAA-central) is central in the archipelago. CAA6 (Resolute-N) and CAA7 (Resolute-S) are near Resolute Bay. L1, LS2, BB1, BB2, BB3, CAA1, CAA3, CAA5, CAA6, and CAA7 were sampled on 14July, 17July, 3Aug, 8Aug, 6Aug, 10Aug, 11Aug, 13Aug, 15Aug, and 16Aug, respectively.

sampled for productivity rates (Figure 2.1): two in the *Labrador Sea*, three in *Baffin Bay* and five in the *Canadian Arctic Archipelago* (CAA). Two of the CAA stations were located at the entrance to the archipelago in *Lancaster Sound* (CAA1 and CAA3), and two stations were located in the western part of the archipelago at *Resolute Bay* (CAA6 and CAA7). All stations were ice free except the southern Baffin Bay station (BB1) and southern Resolute Bay station (CAA7). The northern Resolute Bay station (CAA6) was at the ice edge. Daily ice coverage was determined from IFREMER's CERSAT SSM/I ice coverage 2.0 product (ftp://ftp.ifremer.fr/ifremer/cersat/products/gridded/psi-concentration/data/arctic). Advection and mixing is particularly important and making the oceanography complicated in this region. Primary production is generally limited by nitrogen.

2.4.2 CTD and PAR

Water samples were collected from Niskin bottles on a rosette equipped with a Sea-Bird Scientific SBE 9 CTD, Seapoint fluorometer, and a SBE 43 for dissolved oxygen. Mixed layer depth was determined using a criterion of 0.1 kg m^{-3} change in potential density from the shallowest measurement. For Labrador Sea and Baffin Bay stations, incubations and gas ratios came from different casts, while both were collected from the same cast at the CAA stations. The mixed layer depth from the cast where the sample was collected was used for all calculations. Mixed layer depths were determined based on a 0.1 kg m^{-3} difference from surface density.

A Li-COR sensor mounted on the ship measured PAR every 10 minutes. However, the sensor malfunctioned starting 2 Aug and caused PAR values to sometimes appear to be

negative, so values will only be considered as relative to each other and not as absolute values.

2.4.3 Size fractionated chlorophyll a

Chlorophyll a was size fractionated into 3 size classes: 0.7 – 5 μm, 5 – 20 μm, and >20 μm, using 20 μm silk mesh, 5 μm Nuclepore polycarbonate membrane, and uncombusted glass fiber filters (GF/F; nominal pore size of 0.7 μm). The volume of water filtered varied between 0.1 L and 1 L. Standard chlorophyll a protocols were used (Parsons et al., 1984).

2.4.4 In situ methods

2.4.4.1 Net community production from O_2/Ar (O_2/Ar-NCP)

For net community production from O_2/Ar, duplicate samples were collected at two depths within the mixed layer. Samples were analyzed following Emerson et al. (1999). In short, water was siphoned from Niskin bottles through CO_2-flushed tubing into pre-evacuated $HgCl_2$ poisoned flasks until half-full (~90 mL). Back on shore, flasks were weighed (to determine mass of water sample), equilibrated in a water bath at a known temperature for 12 hours (to determine how much of the gas is in the water versus the headspace), and then the vast majority of the water removed leaving the headspace gas behind. Water and CO_2 were cryogenically removed from gas sample and frozen into a steel tube using liquid He. The O_2/Ar ratio of the gases was then determined on a Thermo MAT 253 isotope ratio mass spectrometer at the University of Victoria and against standards of similar composition (Giesbrecht et al., 2012). A small correction was made for the differences in ionization of sample and standard gases when they contained different proportions of oxygen.

NCP, equivalent to carbon export, was calculated as:

$$O_2/Ar\text{-}NCP = k\,[O_2]_{eq}\left(\frac{\left(\frac{O_2}{Ar}\right)_{ml}}{\left(\frac{O_2}{Ar}\right)_{eq}} - 1\right)\rho$$

Where k is the gas transfer velocity (m d^{-1}), $[O_2]_{eq}$ is the equilibrium oxygen concentration (µmol kg^{-1}), (O_2/Ar) is the O_2/Ar ratio either in the mixed layer (denoted ml) or at equilibrium (denoted eq), and ρ is the mixed layer density (kg m^{-3}). The solubility of oxygen was calculated based on Garcia and Gordon (1992). A photosynthetic quotient (PQ) of 1.4 O_2/C was used to convert from units of oxygen to carbon (e.g. Cassar et al., 2005). The gas transfer velocity was estimated from wind speed based on Ho et al. (2006), and converted to oxygen using a Schmidt number based on Ferrell and Himmelblau (1967) and Sharqawy et al. (2010). Gas transfer velocities were then weighted following Reuer et al. (2007) as modified by Teeter et al. (2018), such that the most recent velocity is most heavily weighted and decreases moving back in time depending on mixed layer depth and wind speed. The original Reuer et al. (2007) formulation weights over 60 days assuming a constant mixed layer depth. Because of the shallow mixed layer depths observed and the dynamic nature of the environment, the surface water is likely replaced on shorter timescales, so we weighted for 30 days following Teeter et al. (2018).

Several wind products were used to evaluate the uncertainty in winds: global deterministic prediction system reforecasts (CGRF), ERA-Interim, National Centers for Environmental Protection (NCEP), North American Regional Reanalysis (NARR), and Cross-Calibrated Multi-Platform (CCMP) version 2.0. The CGRF is from the Canadian Meteorological Centre on a 33 km grid every hour (http://data.ec.gc.ca/data/weather/products/global-deterministic-prediction-system/). ERA-Interim is a reanalysis produced by the Royal Meteorological Society with a grid of

45 km every 3 hours (https://www.ecmwf.int/en/forecasts/datasets/reanalysis-datasets/era-interim). NCEP is a reanalysis from NOAA on a grid of 2.5 degrees every 6 hours (https://www.ncep.noaa.gov/). NARR is a reanalysis from NOAA with a 32 km resolution every 3 hours (https://www.ncdc.noaa.gov/data-access/model-data/model-datasets/north-american-regional-reanalysis-narr). CCMP from Remote Sensing Systems is gridded every 0.25 degrees for every 6 hours (https://podaac.jpl.nasa.gov/dataset/CCMP_MEASURES_ATLAS_L4_OW_L3_0_WIND_VECTORS_FLK).

2.4.4.2 Gross primary production from triple oxygen isotope ($^{17}\Delta$ - GPP)

For gross primary production from the triple oxygen isotope method ($^{17}\Delta$ - GPP), duplicate samples were collected from one depth within the mixed layer and one below. Samples were processed and analyzed at the University of Washington in a similar way to O_2/Ar samples, except that N_2 was removed prior to analysis. Samples were analyzed for oxygen isotopes, and sample volumes were larger (~250mL) and were equilibrated for 24 hours following Palevsky et al. (2016). In addition to oxygen isotopes, O_2/Ar (and thus NCP) was also measured on the same samples. Oxygen isotope samples from the central Baffin Bay station (BB2) and southern Lancaster Sound station (CAA3) were lost. In addition, duplicate samples at K1, LS2, CAA1, and CAA5 were also lost resulting in only single samples in the surface water. GPP was calculated from the triple oxygen isotope data following Hamme et al. (2012) that takes into account kinetic fractionation during gas exchange. Because this method relies on a mass balance of gases in the mixed layer (Section 2.2.1), weighted air-sea gas exchange rates must also be estimated in the same way as for O_2/Ar-NCP. A photosynthetic quotient (PQ) of 1.4 was used to convert

from units of oxygen to carbon. Corrections were made for the ^{18}O of the ambient water following Manning et al. (2017) and for the volume of water sample collected. ^{18}O of ambient water were collected in 13 mL plastic test tubes at standard depths and analyzed at the GEOTOP-UQAM stable isotope laboratory using a Micromass Isoprime universal triple collector IRMS. For this study, ^{18}O-water measurements were interpolated to in vitro sample depths. Duplicate discrete oxygen samples, used for the vertical flux calculation, were collected from the same two depths and analyzed with an automatic amperometric endpoint detection using Winkler methods (Carpenter, 1965). Oxygen data was intercalibrated with samples taken in the Labrador Sea by Fisheries and Oceans Canada through the Bedford Institute of Oceanography in May 2015.

A potential correction for vertical mixing was calculated based on Nicholson et al. (2014), using the difference in isotopic composition between the mixed layer and the sample from below the mixed layer at either the oxygen maximum or about 20 m below the bottom of the mixed layer and a vertical eddy diffusivity (Kz) of 10^{-5} m^2 s^{-1}. We calculated what Kz value would be necessary to make the in situ GPP and NCP methods equal to the in vitro methods at each station (see section 5.1.4).

2.4.5 In vitro methods

Samples were taken from 6 light level depths (100%, 50%, 30%, 15%, 1%, 0.1%), determined using a secchi disk and a PNF-300 probe. Although this is an older method for determining euphotic depth, other groups still use it as well, such as the California Cooperative Oceanic Fisheries Investigations (CalCOFI). All incubation samples were collected from the same cast and depths but sometimes multiple Niskins were fired at the same depth due to volume constraints. ^{13}C-PP, ^{15}N-new, ^{18}O-GPP incubations were all

placed in the same incubator while ^{14}C-PP was placed in a separate one. Both incubators were on deck with continuously flowing surface seawater to best represent the in situ temperature. Different light levels matching the sampled levels were achieved using blue and neutral density photographic film. All incubations were conducted for 24 hours starting around dawn, immediately after sampling. The chlorophyll maximum was sampled if it was close to one of the light levels.

Trapezoidal integration was used to calculate integrated rates for the mixed layer and the euphotic zone. Depths were interpolated to obtain the rate at the base of the mixed layer. For incubations integrated to the mixed layer and the euphotic zone depth, a ML or eu subscript is added to the method name, respectively. If no subscript is indicated, integration was not applied and the value is on a volumetric basis. The standard deviation of the integrated rates was calculated from Krause et al. (2011).

2.4.5.1 Primary production from ^{13}C incubations (^{13}C-PP)

Sample collection and analysis for ^{13}C-PP were based on Slawyk et al. (1977). In short, samples were collected into polycarbonate bottles with a volume of 570 mL at all depths except for the 50% light level where the volume was 1183 mL. Samples were spiked with an enriched sodium bicarbonate ($NaH^{13}CO_3$; 97 atom % ^{13}C from Ambridge Isotope Laboratories) solution to a level that was less than 11% of the total ambient DIC. Single samples were taken at all depths except at the 100% light level, where triplicate samples were taken to assess variability. An initial (T0 with spike) and a dark sample were also collected at the 100% light level. At the end of the 24-hr incubation, samples were filtered onto combusted GFF filters and frozen until they could be dried in an oven at 60 °C. Filters were not acidified for this method. Samples were analyzed for carbon isotopes

and POC concentrations at University of California Davis Stable Isotope Facility using an elemental analyzer and isotope ratio mass spectrometer (see https://stableisotopefacility.ucdavis.edu/ for more information). Then primary production was calculated based on Hama et al. (1983). DIC samples were collected and analyzed onboard using a VINDTA 3C following Dickson et al. (2007) and were used in the production calculation.

2.4.5.2 Primary production from ^{14}C incubations (^{14}C-PP)

Duplicate samples for ^{14}C-PP incubations were collected into 500-mL polycarbonate bottles and inoculated with 10 μCi of $NaH^{14}CO_3$. Immediately, 50 μL of three random samples were subsampled to determine the exact amount of radioisotope in the samples. Incubations were terminated by filtering 250 mL onto uncombusted GF/F filters and acidifying in scintillation vials with 0.2 mL of 0.5N HCl. To remove unincorporated ^{14}C, samples were left to evaporate overnight (Lean and Burnison, 1979), and then the sample radioactivity was counted on a Packard Tri-Carb 2900 TR liquid scintillation counter. ^{14}C-PP was calculated according to Parsons et al. (1984).

2.4.5.3 New production from ^{15}N incubations (^{15}N-new)

Incubations for ^{15}N-new were performed on the same water samples as ^{13}C-PP (Dugdale and Goering, 1967; Dugdale and Wilkerson, 1986) by also adding isotopically labeled potassium nitrate ($K^{15}NO_3$; 97 atom % ^{15}N from Cambridge Isotope Laboratories) to a concentration of 0.1 μM. The ambient surface concentration ranged from 0 to 1.51 μM, resulting in overspiking at a few stations. Nitrogen isotopes on the particulates and PON concentrations were also measured at University of California Davis. NO_3^- concentrations were analyzed onboard. Nitrogen units were converted to carbon units

based on the C:N ratio of individual samples, which had an average of 8.6±1.7, which includes autotrophs, heterotrophs, and detritus.

2.4.5.4 Gross primary production from ^{18}O incubations (^{18}O-GPP)

Three samples for ^{18}O-GPP determinations were collected from each depth into ~135 mL borosilicate glass flasks (pyrex iodine determination flask), following the methods of Juranek and Quay (2005). Each sample was spiked with 400 μL of $H_2{}^{18}O$ (Cambridge Isotope Laboratories, Inc. with an isotopic purity of ≥98%) that had been distilled in a trace metal clean laboratory to purify the spike. One sample was processed immediately instead of incubating following the methods done at the end of the incubation as an initial point. Following the incubation, ~35 mL were siphoned through CO_2-flushed tubing into $HgCl_2$ poisoned pre-evacuated flasks. Care was taken to ensure siphoned water came from the bottom of the flask away from contact with the atmosphere. Gas samples within the flasks were analyzed in the same way as O_2/Ar samples but for the isotopic composition of O_2. Calculations of GPP from these measurements were made following Juranek and Quay (2005), correcting for the ambient ^{18}O isotopic composition of the water (Section 2.4.4.2). Oxygen concentrations (Section 2.4.4.2) were used in calculations for this method as well.

2.5 Results

2.5.1 Carbon export

Two methods for estimating carbon export (O_2/Ar-NCP, ^{15}N-new) were measured at 10 stations across the Labrador Sea, Baffin Bay, and the Canadian Arctic Archipelago. O_2/Ar-NCP and $^{15}N\text{-new}_{ML}$ do not have the same trends across the transect; however, neither is consistently biased high or low (Figure 2.2a), with roughly half of the samples having one method higher than the other. The highest rates for $^{15}N\text{-new}_{ML}$ were measured

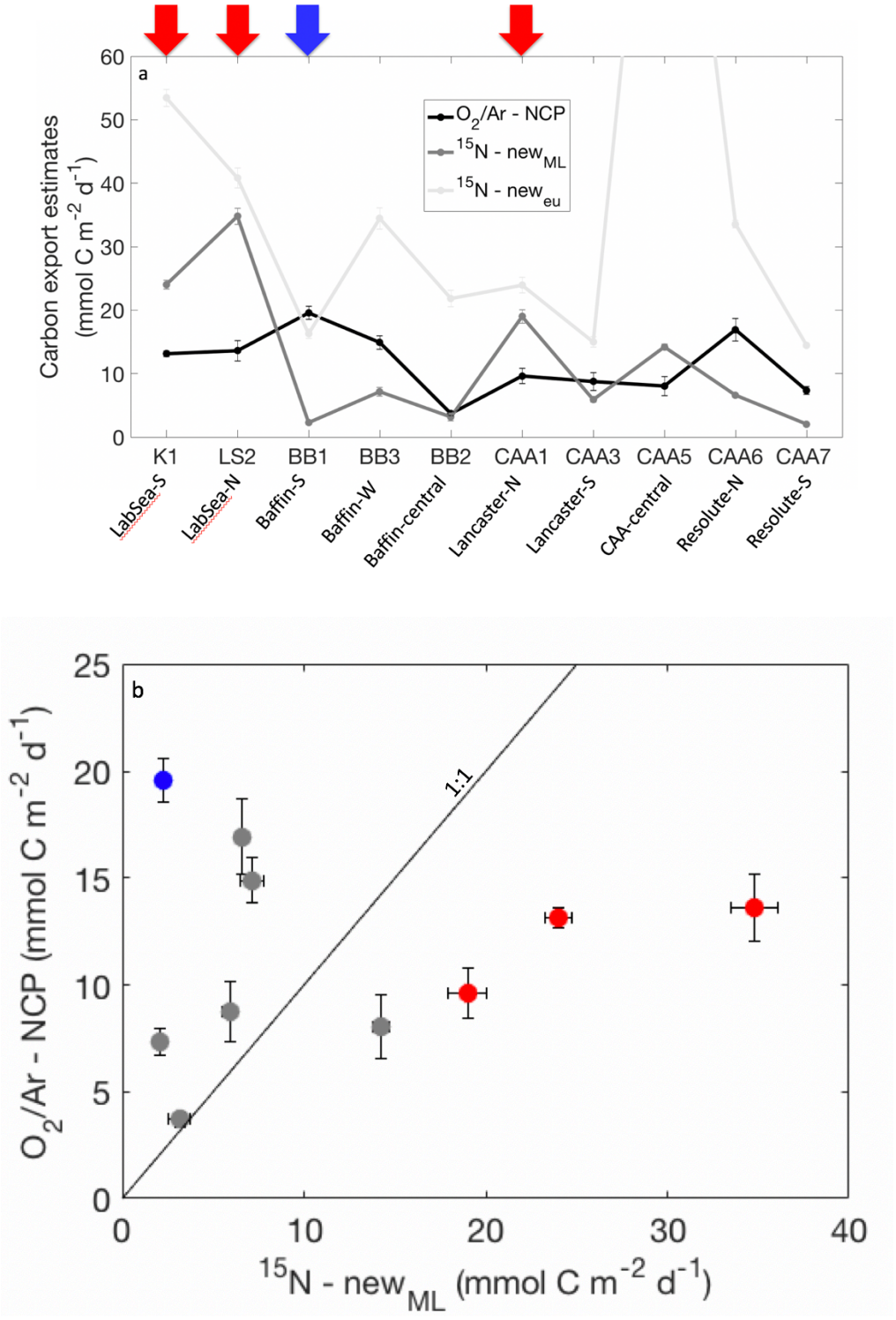

Figure 2.2 (a) Carbon export rates (mmol C m^{-2} d^{-1}) estimated from O_2/Ar-NCP, ^{15}N-new$_{ML}$, and ^{15}N-new$_{eu}$ along the cruise track. Red arrows indicate where ^{15}N-new$_{ML}$ is at least 1.8 times greater than O_2/Ar-NCP and blue indicates where ^{15}N-new$_{ML}$ is at least 8 times less than O_2/Ar-NCP. (b) Comparison of O_2/Ar-NCP vs. ^{15}N-new$_{ML}$. Black line is the 1:1. Red and blue points in

panel b indicate particular outliers highlighted in panel a. O_2/Ar-NCP error bars are based only on the standard deviation of duplicate samples, and do not include uncertainty in gas exchange of about 15% (Juranek and Quay, 2010). ^{15}N-new error bars are based on triplicate surface samples and assumed to apply to all incubation depths integrated using Krause et al. (2011). Both error bars are conservative compared to the likely true error for each method.

in the Labrador Sea, whereas the highest rates for O_2/Ar-NCP show no clear geographic trend. Baffin Bay had the lowest rates for ^{15}N-new$_{ML}$ but some highs for O_2/Ar-NCP. Canadian Arctic Archipelago samples had variable, moderate rates for both methods. O_2/Ar-NCP vs. ^{15}N-new$_{ML}$ fall close to the 1:1 line (Figure 2.2b), with several outliers. Three stations had anomalously higher ^{15}N-new$_{ML}$ rates than O_2/Ar-NCP in the Labrador Sea and Northern Lancaster Sound (CAA1). In contrast, O_2/Ar-NCP in southern Baffin Bay (BB1) was about 7.5 times higher than ^{15}N-new$_{ML}$. Central CAA stands out as having the highest ^{15}N-new$_{eu}$ rate in this study, driven by one depth (15% light level) with an extremely high value (6.57 μmol C L^{-1} d^{-1}). Since the euphotic zone is deeper than the mixed layer depth, ^{15}N-new$_{eu}$ is always greater than ^{15}N-new$_{ML}$ (Figure 2.2a).

2.5.2 Chlorophyll a

Mixed layer chlorophyll *a* concentrations were dominated by the smallest size fraction (0.7 to 5 μm) in the Labrador Sea and Baffin Bay (Figure 2.3a). In the CAA, the importance of the smallest size fraction to total chlorophyll *a* was variable. In northern Lancaster Sound (CAA1) and Baffin-S (BB1), the smallest size fraction made up 29% and 90% of the total chlorophyll *a*, respectively. In northern Resolute Bay, the largest size fraction of chlorophyll a was most important. In northern Lancaster Sound, all three size fractions of chlorophyll a had similar concentrations. The two stations with the highest average total chlorophyll a concentrations in the mixed layer occurred when the

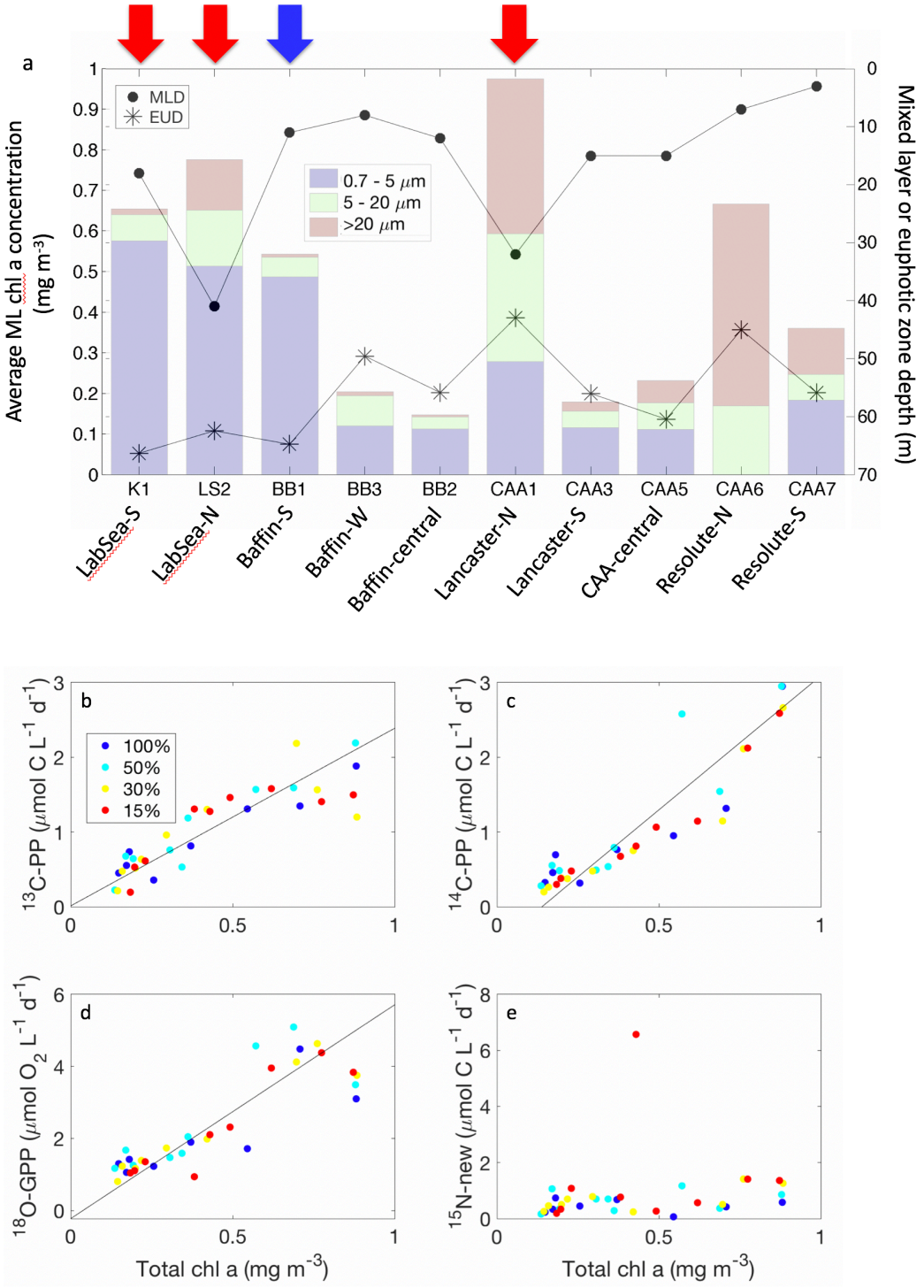

Figure 2.3 (a) Bars represent the average chlorophyll a concentration within the mixed layer along the cruise track for the following three size fractions: 0.7 – 5 µm, 5 – 20 µm and > 20 µm. Average chlorophyll a concentrations were calculated by dividing the trapezoidal integration by the mixed layer depth. Black points and grey stars are the mixed layer depth and euphotic zone

depth, respectively. Red arrows indicate where ^{15}N-new$_{ML}$ is much higher than O_2/Ar-NCP and blue where ^{15}N-new$_{ML}$ is much less than O_2/Ar-NCP as in Figure 2.2. Comparison between the total chlorophyll a concentration in the mixed layer (mg m^{-3}) and (b) ^{13}C-PP, (c) ^{14}C-PP, (d) ^{18}O-GPP and (e) ^{15}N-new volumetric rates. Lines show the best linear fit.

mixed layer depth was deepest (Figure 2.3a). These also correspond to the stations where ^{15}N-new$_{ML}$ uptake was higher than O_2/Ar-NCP (red arrows).

Total chlorophyll *a* concentration is strongly related to volumetric ^{13}C-PP (R^2=0.77), ^{14}C-PP (R^2=0.84), and ^{18}O-GPP (R^2=0.76) rates (Figure 2.3b, c, d), but not to ^{15}N-new (Figure 2.3e). Even with the high ^{15}N-new outlier removed, there is still no relationship between chlorophyll and ^{15}N-new, which could imply significant regenerated production.

2.5.3 Gross primary production and primary production

^{18}O-GPP$_{ML}$ rates were high in the Labrador Sea and in northern Lancaster Sound, but much lower in Baffin Bay and the rest of the archipelago (Figure 2.4). $^{17}\Delta$-GPP rates had different trends, being high in the Labrador Sea, southern Baffin Bay, central archipelago, and Resolute Bay stations. In general, $^{17}\Delta$-GPP tended to be higher than ^{18}O-GPP$_{ML}$. However, ^{18}O-GPP$_{ML}$ was similar in magnitude or higher than $^{17}\Delta$-GPP when the mixed layer was deep, also corresponding to where ^{15}N-new$_{ML}$ is higher than O_2/Ar-NCP (red arrows).

There is scatter when comparing ^{13}C-PP and ^{14}C-PP rates either on a depth-by-depth basis (Figure 2.5a) or integrated over the euphotic zone (not shown). Most data lie below the 1:1 line, indicating higher ^{13}C-PP rates than ^{14}C-PP. However, ^{14}C-PP rates were greater than ^{13}C-PP rates at two Baffin Bay stations and in southern Lancaster Sound. Since ^{13}C-PP was generally higher than ^{14}C-PP, when comparing ^{18}O-GPP to primary

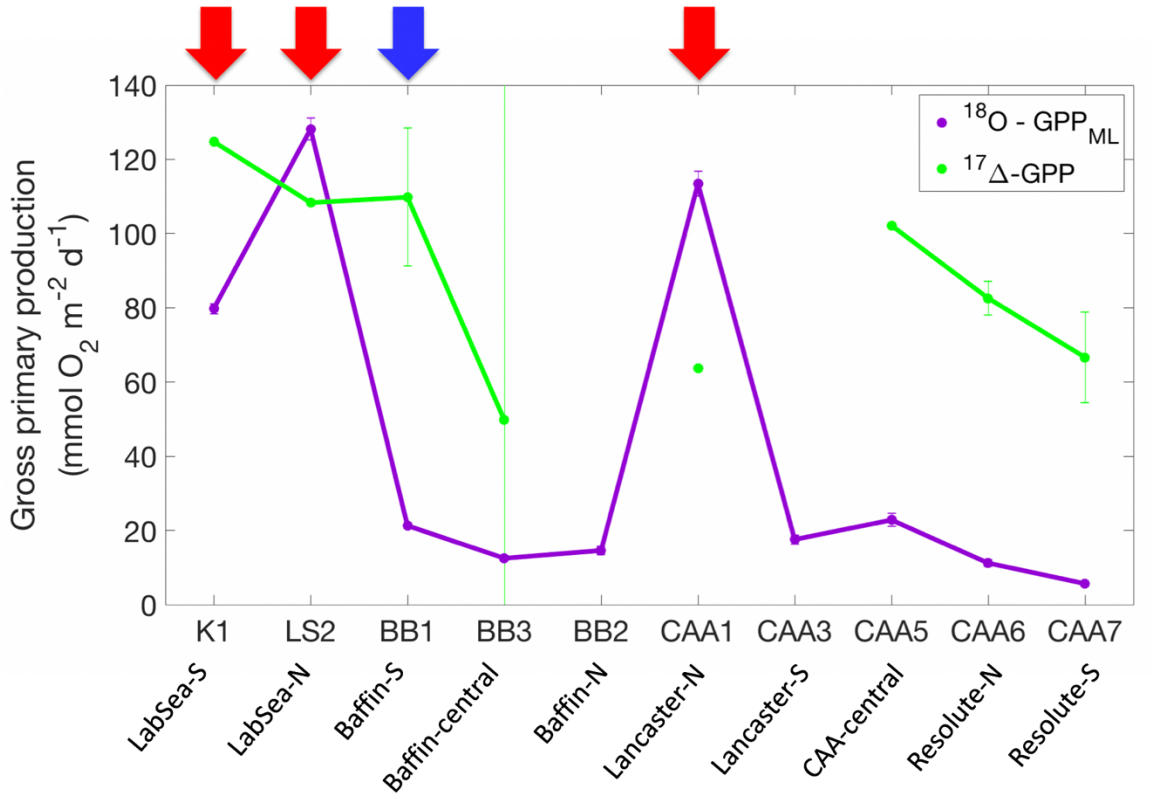

Figure 2.4 Gross primary production rates (mmol O_2 m^{-2} d^{-1}) estimated from $^{18}O\text{-}GPP_{ML}$ and $^{17}\Delta$-GPP along the cruise track. Red and blue arrows indicate the same stations as in Figure 2.2.Error bars were based on duplicate samples. Standard deviation for $^{18}O\text{-}GPP_{ML}$ is based on duplicate samples at each depth and the integrated standard deviation for the error bars was calculated based on Krause et al. (2011). Error bars for $^{17}\Delta$-GPP are for duplicate samples at BB1, BB3, CAA6, and CAA7. For the other stations, $^{17}\Delta$-GPP were based on single samples and are an underestimate of the actual confidence in estimating GPP.

production yields a slightly steeper slope for ^{13}C-PP (slope=2.5 and R^2=0.79), closer to the JGOFS ratio of 2.7, compared to ^{14}C-PP (slope=1.85 and R^2=0.71; Figure 2.5b). ^{13}C-PP and ^{18}O-GPP are also slightly better correlated than ^{14}C-PP.

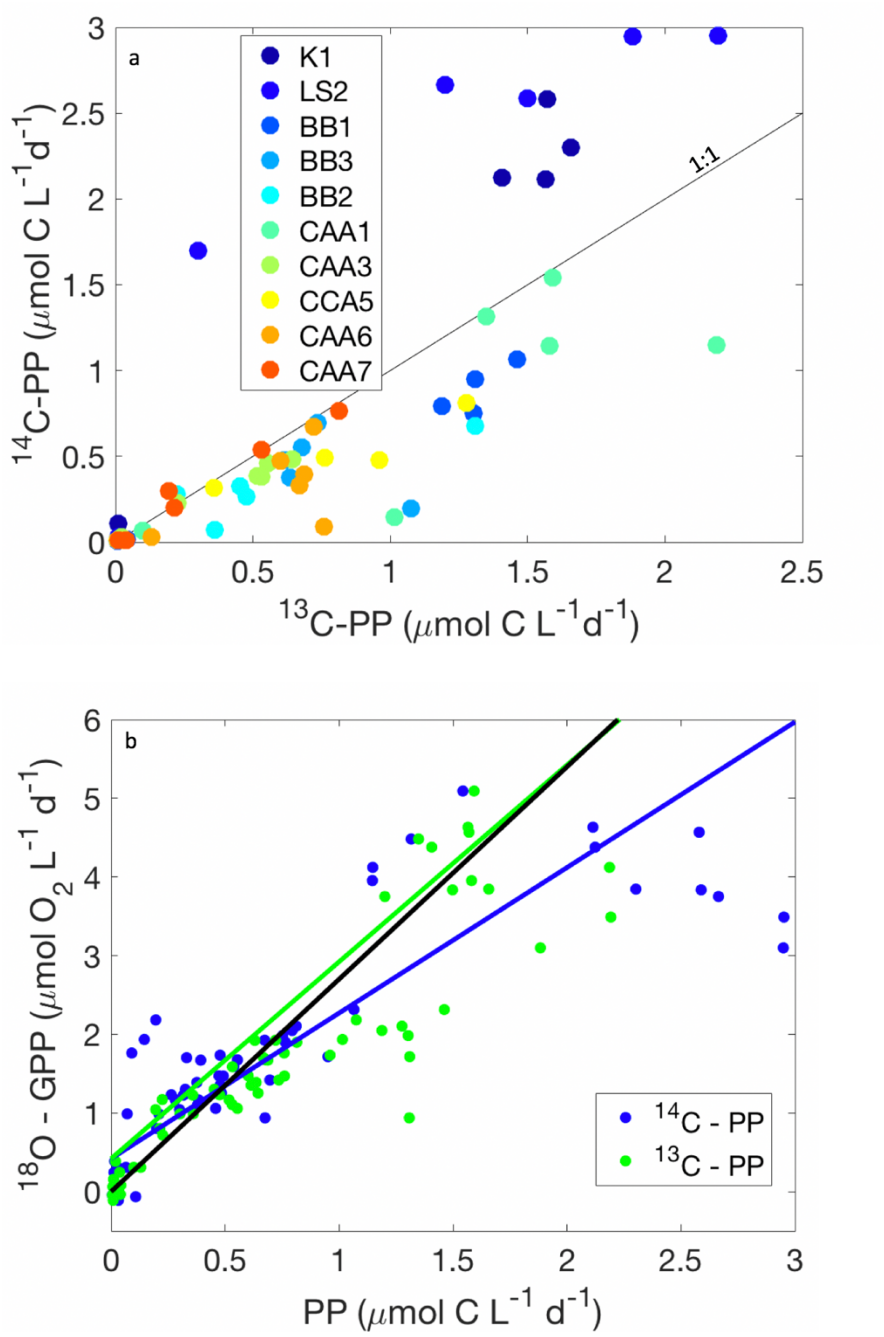

Figure 2.5 (a) Comparison of volumetric ^{14}C-PP vs. ^{13}C-PP at individual depths for each station, where the point color indicates the station. Black line is the 1:1 line. (b) ^{18}O-GPP rates versus ^{13}C-PP (green) and ^{14}C-PP (blue) rates. Best fit lines are colored while the JGOFS slope of 2.7 (derived from ^{18}O and ^{14}C data) is black.

2.6 Discussion

2.6.1 In situ versus in vitro

No single reason can explain the differences between in situ and in vitro methods, which is not surprising given how different and dynamic our study region is. We suggest five factors that help explain method differences in the North Atlantic and the Arctic. In situ and in vitro methods integrate over different time and depth scales. A recently shoaled mixed layer mainly bias in vitro methods. Mixing at the base of the mixed layer can bias in situ methods but not in vitro methods. Lastly, specific methodological issues for each method can introduce biases.

2.6.1.1 Hypothesis 1: Time of integration

One major assumption when comparing methods is that productivity rates are constant, such that methods will measure the same value regardless of their different integration times. However, productivity rates are often dynamic, making time of integration stand out as a likely difference between methods. Productivity is known to be dynamic in the CAA (e.g. Rao and Platt 1984; Sakshaug, 2004) and North Atlantic (e.g. Harrison et al., 1982; Sakshaug, 2004). The in vitro methods integrate over the length of the incubation, 24 hours in this study. We started all incubations around dawn so that the tracer was taken up first and then available within the organism to be released again by net respiration at night. When incubations begin at night, the period of net respiration occurs before the tracer is taken up by phytoplankton, resulting in an overestimate of the productivity rate. The in situ gas ratio methods (O_2/Ar-NCP, $^{17}\Delta$-GPP) estimate rates averaged over approximately the residence time of oxygen in the mixed layer, but exponentially weighted toward the sampling time (Teeter et al., 2018). Estimating residence time as the mixed layer depth divided by the weighted gas transfer velocity

shows that the gas ratio methods had integration times ranging from 3.2 days to 33 days (Table 2.1). If there is a dynamically changing mixed layer depth, in situ methods could be overestimated or underestimated depending on whether there is more production or less production below the mixed layer, respectively. Since in vitro methods integrate over much shorter times

than in situ methods, incubations are more likely to miss episodic events that in situ

Table 2.1. An average of the 30-d weighted gas transfer velocity (k weight) derived from five wind products (m d^{-1}), residence time of O_2 in the mixed layer (days), eddy diffusivity (Kz; m^2 s^{-1}) that would make $^{17}\Delta$-GPP equal to ^{18}O-GPP_{ML}, and Kz that would make O_2/Ar-NCP equal to ^{15}N-new_{ML}. A vertical mixing correction was tested based on the isotopic composition of oxygen within and below the mixed layer (Nicholson et al. 2012), varying Kz by trial and error until the in situ and in vitro methods gave the same result. The same was done for the export methods using the O_2/Ar within and below the mixed layer. NaNs in the Kz column indicate locations where it was not possible to find a Kz that would make the methods equal, because the gradient at the base of the mixed layer was in the wrong direction for increased mixing to make the methods more similar.

	K1	LS2	BB1	BB3	BB2	CAA1	CAA3	CAA5	CAA6	CAA7
k weight 30 days	2.98 ±0.36	3.05 ±0.27	0.60 ±0.23	0.75 ±0.32	0.84 ±0.26	0.90 ±0.39	1.20 ±0.47	1.01 ±0.44	0.74 ±0.21	0.76 ±0.29
Res time of O_2 in the ML	8.0	11.7	6.8	13.5	12.6	33.3	14.0	13.5	7.3	3.2
Kz to match GPP	$8.22*10^{-5}$	NaN	NaN	$1.62*10^{-5}$	$3.9*10^{-5}$	NaN	NaN	$6.68*10^{-4}$	$7.61*10^{-5}$	$4.73*10^{-5}$
Kz to match NCP	$2.25*10^{-3}$	$1.58*10^{-4}$	NaN	NaN	NaN	$3.02*10^{-5}$	NaN	NaN	$2.28*10^{-5}$	$4.30*10^{-5}$

methods capture, which may explain differences between methods. For the in situ gas ratio methods, southern Resolute Bay (CAA7) had the shortest integration time, suggesting that O_2/Ar-NCP should most comparable to ^{15}N-new_{ML}; however, the in situ and in vitro methods are not the same at this station (Figure 2.2a). Southern Labrador Sea

(K1), southern Baffin Bay (BB1), and northern Resolute Bay (CAA6) had similar integration times of around 7 days. The rest of the stations were longer than 10 days, and northern Lancaster Sound (CAA1) had the longest integration time. Although integration time is an important factor, it cannot explain all the variability between methods. For example, in southern Resolute Bay (CAA7), where integration times are most similar, GPP methods do not agree well. Other factors also need to be considered to help explain differences between methods.

A phytoplankton bloom (episodic event) may drive rapidly changing productivity rates. Episodic events influence only in situ methods if they happened a while ago or influence in vitro methods more if they are happening at the time of sampling. One mechanism could be that recent upwelling (advection) causes ambient nutrient concentrations to increase and stimulate a phytoplankton bloom. However, ambient nutrient concentrations did not correlate with method disagreement. We would expect high nutrient concentrations to correlate with higher in vitro measurements and low nutrient concentrations to correlate with in situ being higher; however, that is not what is observed. At low average ambient nitrate concentrations within the mixed layer (<0.05 μM), two stations had ^{15}N-new that was higher than O_2/Ar-NCP and five where O_2/Ar-NCP was higher. At the station with the highest average ambient nitrate concentrations within the mixed layer, O_2/Ar-NCP was higher. We can also use chlorophyll as an indicator of a recent bloom. In our study, high chlorophyll was observed at stations where ^{15}N-new$_{ML}$ incubations tended to exceed the in situ O_2/Ar-NCP method (Figure 2.2b and 2.3a). During a bloom, production rates are higher than in the recent past. Averaged over time for the in situ method, recently increased productivity will cause the in situ rates to

be lower than what the incubations measure (Figure 2.6). GPP methods follow this trend, indicating that time of integration and bloom dynamics are important in this method comparison.

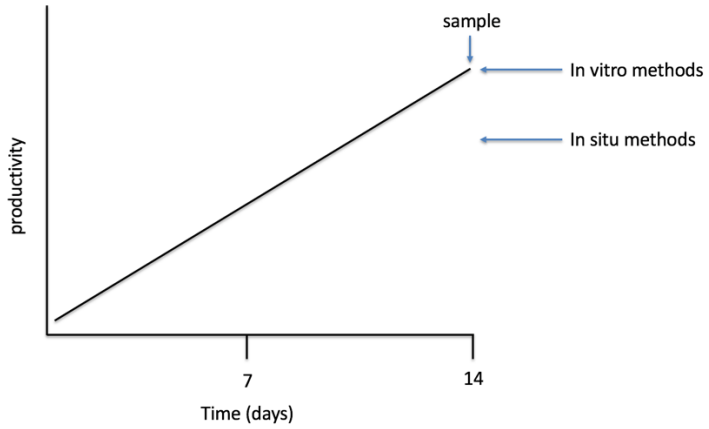

Figure 2.6. Cartoon of how phytoplankton bloom dynamics affect in situ vs. in vitro method comparison. During a phytoplankton bloom, a hypothetical instantaneous productivity measurement would increase leading to the time of sampling. Since in vitro methods integrate over 24 hours, the measurement would be close to the productivity at the time of sampling. On the other hand, in situ methods integrate over the residence time of oxygen in the mixed layer. As a result, in situ observations include previous productivity (exponentially weighted to the sampling time) and would be lower than in vitro methods. This example could also apply to an end of bloom, where productivity would be decreasing and in vitro methods would be lower than in situ.

2.6.1.2 Hypothesis 2: Depth of Integration

In situ and in vitro methods can integrate productivity rates over different depths. Our in situ methods are based on a mixed layer mass balance, yielding one value that naturally integrates over the mixed layer. Our in vitro methods measure volumetric rates (per L) at discrete depths, and can be integrated to any depth shallower or equal to the euphotic zone depth. In this paper, we specifically calculate in vitro values integrated to

the mixed layer depth (always shallower than the euphotic zone depth at these stations) for clearer comparison with our in situ methods.

One example of how the depth of integration affects methods is by comparing the in situ and in vitro methods that are measuring the same fraction of production. In this study, there is the potential for significant productivity under the mixed layer since the mixed layer was always shallower than the euphotic zone depth. When there is no productivity under the mixed layer, integrating to the mixed layer or euphotic depth would not matter. ^{15}N-new$_{ML}$ and O_2/Ar-NCP had a similar magnitudes with four outliers (Figure 2.2b). At three stations (K1, LS2 and CAA1), ^{15}N-new$_{ML}$ was higher than O_2/Ar-NCP, and at one station (BB1) O_2/Ar-NCP was higher than ^{15}N-new. Similarly, ^{18}O-GPP and $^{17}\Delta$-GPP measure the same fraction of production but are a factor of 4 different. Northern Labrador Sea (LS2) had the most similar GPP estimates, whereas Baffin-central (BB2) has the most similar carbon export estimates. GPP from the two methods might also have been similar at BB2, however the $^{17}\Delta$-GPP samples were lost so are unable to examine this. Interestingly, at Baffin-W (BB3) in situ methods were higher than in vitro for both carbon export and GPP estimates. To make in vitro methods comparable to in situ methods in terms of depth of integration, in vitro methods were integrated to the base of the mixed layer. In this case, depth of integration should not affect the comparison between in situ and in vitro methods, so other factors must be important at those stations (Figure 2.2 and 2.4).

Another issue with the depth of integration is that the in vitro methods are conducted at discrete depths so if there is a particular depth with higher productivity that is not sampled, we miss sampling it due to too much difference between light depths at

predetermined levels of 100, 50, 30, 15, 1 and 0.1%. The vertical sampling resolution might not be sufficient enough to capture a potential chlorophyll maximum, causing the incubations to be an underestimate when integrating to the euphotic zone depth.

2.6.1.3 Hypothesis 3: Recently shoaled mixed layer

A mechanism for method differences that combines time and depth of integration issues is recent shoaling of the mixed layer. For example, if two water masses of different densities converge at the surface, the less dense water mass will move over top of the more dense water mass, and the resultant mixed layer will be shallower (Figure 2.7). Calmer winds could also cause the mixed layer in a single water mass to shoal. In vitro methods are very sensitive to changing mixed layer depths. For example, suppose that the deeper mixed layer (before shoaling) encompassed three light level depths, but only one

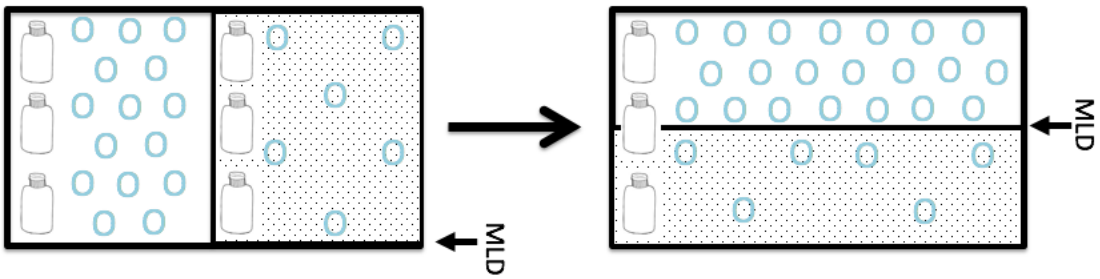

Figure 2.7 Conceptual cartoon of how two water masses with different densities can affect in situ and in vitro methods when they meet and stratify. The y-axis is water depth. The more dense water mass has black dots and less oxygen. The O symbols represent the amount of oxygen in each water mass. Bottles represent incubation depths at specific light levels. The mixed layer depth (MLD) is denoted in the figure.

light level after the stratification event. When applying trapezoidal integration to the base of the mixed layer, the depth of the mixed layer can have a large impact on the calculation. In situ methods are less sensitive to changing mixed layer depths on short

timescales. Changing the mixed layer depth would initially have no impact on the concentration of gas in the surface water. Over time, gas exchange would remove the old higher integrated productivity signal coming from the deeper mixed layer, reducing O_2/Ar to a lower value that reflected the new lower mixed layer productivity.

One example of where the mixed layer may have changed depth radically is the northern Labrador Sea (LS2) where samples were collected on two different casts. Incubation samples were taken when the mixed layer was deeper (~35 m) while gas ratio samples were collected about 15 hours later when the mixed layer was shallow (~15 m), indicating a dynamic mixed layer. To estimate how the two different mixed layers had an effect on both methods, GPP was calculated by only changing the mixed layer depth in the calculations. If the mixed layer depth increases by 21 m and $^{18}O\text{-}GPP_{ML}$ and $^{17}\Delta$-GPP are recalculated, $^{18}O\text{-}GPP_{ML}$ increases by 49 mmol m^{-2} d^{-1} and $^{17}\Delta$-GPP decreases by 17.1 mmol m^{-2} d^{-1}. Mixed layer depth plays a role in determining the weighted gas transfer velocity (k), so a changing mixed layer could bias the in situ gas ratio results in either direction. In this particular case, k decreased. For this station, it happens that incubations were taken from the deeper mixed layer cast and the gases from the shallower making the estimates for GPP similar. If both methods were sampled on either the first or second cast, there would be an even larger difference between the two methods. So collecting at different casts has an impact if the mixed layer is changing depths. For the Labrador Sea and southern and western Baffin Bay stations, incubations and gas ratios were not taken from the same cast. Some stations had in situ and in vitro methods collected on different casts. Although it does not appear to affect all stations, it could have been a factor for BB1. It is possible that during the time between sampling the two casts, that different

water mass were sampled. This mechanism will also cause differences between in situ and in vitro methods even when the samples are taken from the same cast, affecting both GPP and NCP vs new production comparisons. It would be ideal to have a history of mixed layer depths at each station to determine how representative the sample cast is compared to the average, perhaps derived from a nearby profiling float. The Arctic may be particularly problematic because dissimilar water masses frequently converge in this region (Hughes et al. 2018).

We tested whether decreasing wind speeds prior to the sampling date would have been expected to cause a shoaling mixed layer through surface warming. There was no correlation between wind speed trends prior to sampling compared to sampling day for the outlier stations where methods did not agree (Figure A1). The only stations with decreasing winds were K1 and LS2, both of which had relatively deep mixed layers. Based on this result, we conclude changing wind speeds did not cause a shoaling mixed layer within our dataset.

2.6.1.4 Hypothesis 4: Mixing at base of mixed layer

Another mechanism that can cause differences between in situ and in vitro methods is vertical mixing at the base of the mixed layer. Where a gradient exists for $^{17}\Delta$ and $\Delta O_2/Ar$ below the mixed layer, mixing at the base of the mixed layer introduces another flux into the surface mass balance that is not typically accounted for. A subsurface oxygen maximum can form under the mixed layer when oxygen production by photosynthesis cannot be removed by gas exchange. In this case, gas-based in situ productivity rates would be overestimated compared to what is measured in the mixed layer by in vitro methods integrated to the base of the mixed layer. In our dataset, higher oxygen was

observed below the mixed layer at all stations except LS2, sometimes roughly coincident with the depth of the chlorophyll maximum. In contrast, oxygen could decrease at the base of the mixed layer if deeper layers are not as productive, which would cause gas-based in situ methods to underestimate production. At locations such as Hawaii, mixing with higher O_2/Ar below the mixed layer could create as much as a third of the productivity signal from O_2/Ar-NCP leading to an overestimate of mixed layer productivity (Hamme and Emerson 2006).

At LS2, oxygen decreases under the mixed layer. This is the only station where this occurs. If vertical mixing is significant, then O_2/Ar-NCP should be biased low relative to $^{15}N\text{-new}_{ML}$, which is indeed what we observe. So vertical mixing could be important in explaining in situ and in vitro differences. Nicholson et al. (2014) formulated a method to correct $^{17}\Delta$-GPP for vertical mixing by using the gradient and a rate of mixing (Kz: eddy diffusivity) to estimate the vertical flux, which could also be applied to O_2/Ar-NCP. At LS2, the vertical mixing correction reduces $^{17}\Delta$-GPP. Even though oxygen concentration decreases under the mixed layer, $^{17}\Delta$-GPP depends on the isotopic composition of oxygen and $^{17}\Delta$ is increased by mixing in this case. For the calculations in Figure 2.4 and Table 2.1, we employed a constant low value for Kz of 10^{-5} m^2 s^{-1} (Yang et al., 2018). If we instead vary Kz to force the mixing corrected $^{17}\Delta$-GPP to match $^{18}O\text{-GPP}_{ML}$, necessary Kz values would range from 1.62 x 10^{-5} to 6.68 x10^{-4} m^2 s^{-1}, where the higher values might not be reasonable based on values used in other studies (e.g. Yang et al. 2018; Palevsky et al., 2016). Besides vertical mixing, fall entrainment can also be important (Nicholson et al., 2012) especially in coastal areas where the mixed layer changes rapidly, but likely did not affect our summer dataset.

We also considered whether shallower bottom depths could drive more mixing. If the bottom depth was shallow, interaction with the topography may cause nutrient rich deep water to be mixed into surface waters. However, there was no correlation between bottom depth and any of the method comparisons. Hill et al. (2013) predicts that changes in primary production, due to climate change, could occur around bathymetric features due to enhanced mixing, inputting nutrients to surface waters. The LS stations are deeper than 3000 m. BB stations are deeper than 1000 m. CAA1 and CAA3 have bottom depths around 650 m and the other CAA stations less than 300 m. One of the deepest stations had some of the highest productivity rates.

2.6.1.5 Hypothesis 5: Methodological issues

Lastly, specific biases inherent in each of the rate measurements could cause discrepancies. Without an absolute standard for flux measurements, method accuracy is not easily assessed (Ulfsbo et al., 2014).

The two methods that estimate carbon export measure different fractions of export. O_2/Ar-NCP represents both the dissolved and particulate carbon export, because it depends on a mass balance of O_2 for the entire mixed layer. ^{15}N-new only represents particulate carbon export. This would make ^{15}N-new lower relative to O_2/Ar-NCP, and that is the case for only half of the stations. So DOC export may be less important at some Arctic stations or other factors may dominate the method comparison. Dissolved organic material can make up 50% to more than 90% of the total organic material (Wheeler et al. 1997). However, this does not necessarily point to proportionately high export. In the Canada Basin, up to 65% of primary production ends up in the DOC pool

(Gosselin et al. 1997) but very little of the DOC is thought to be exported deeper (Anderson 2002).

Both our in situ methods rely on a mixed layer mass balance where uncertainty in the air-sea gas exchange rate can be important. Different wind products yield different wind speed estimates, and no wind stations exist close to our Arctic stations to assess wind product accuracy. We used an average of multiple wind products with an average standard deviation in the wind of 0.33 m s^{-1}. The average k weight for each station based on five wind products was highest in the Labrador Sea (Figure A1). Different wind products give an average uncertainty of ±0.32 m^2 d^{-1} in k. The number of days for wind speed data used in the weighting scheme (30 vs. 60 d) made very little difference (Table A1).

Uncertainty in factors used to convert from the native units of some measurements to carbon fluxes may also impact comparisons. Thinking in terms of carbon units is more useful, however some of the methods measure in oxygen or nitrogen units and have to be converted. O_2/Ar-NCP, $^{17}\Delta$-GPP, ^{18}O-GPP are all natively measured in oxygen units. We used a PQ of 1.4 from the literature to convert; however, the conversion can vary due to decoupling of oxygen production and carbon fixation. For example, under conditions of too much sunlight, to protect the cell from damage, light energy may be used to split water without carbon fixation. Cassar et al. (2015) convert NCP from O_2 to C using a 1.4 O_2:C ratio. Laws (1991) suggest that a O_2:C ratio of 1.25 should be used when NH_4 was the source and between 1.5 to 1.8 should be used when NO_3 is the source. Anderson (1995) suggests a lower value for nitrate growth ranging from 1.35 to 1.49. To convert N to C, we used the C:N ratio from the samples and not Redfield. The average C:N ratio for

this study is 8.6±1.7 compared to Redfield of 6.625; however, our POC ratio measurements apply to the total particulate pool rather than phytoplankton only. Only the export comparison (^{15}N-new vs. O_2/Ar-NCP) will be affected by this caveat.

We investigated if the time of day that gases were sampled could have biased the O_2/Ar-NCP method. Hamme et al. (2012) showed from underway sampling that ΔO_2/Ar increases during the day to a maximum at sunset and decreases at night to minimum at sunrise. Although time of day could have affected our results, it cannot be the dominant factor. The station where O_2/Ar-NCP exceeded ^{15}N-new was not sampled at sunset nor were the stations where ^{15}N-new exceeded O_2/Ar-NCP more likely to have been sampled at dawn.

For ^{15}N-new, one of assumptions is that there are no recycled sources of nitrate from nitrification and no new sources of nitrogen from nitrogen fixation. It has long been thought that nitrification is inhibited by light, but this is currently under debate because ammonia-oxidizing archaea are present and active in the surface waters. Still, there is mounting evidence that nitrification is not important in surface waters. DiFiore et al. (2009) show that nitrification is not important in the Ross Sea. Manning et al. (2017) show that nitrification is not important in Monterey Bay. Smith et al. (2014) found that, when there is high competition for NH_4 by phytoplankton, nitrification was inhibited more by NH_4 availability rather than light. Yool et al. (2017) found nitrification is important in stratified oligotrophic systems. However, our study stations were not oligotrophic, and we conclude that nitrification is unlikely to have been a major factor in our study. Many other assumptions affect the ^{15}N method. For example, too much production compared to the spike concentration could cause the ^{15}N substrate to be

exhausted, causing an underestimate. Second, excretion of ^{14}N into the dissolved pool (recycling) will cause the isotope to be diluted, creating an underestimate. Finally, bottle effects could inhibit incubations where they do not adequately simulate in situ conditions.

2.6.2 In vitro comparisons

2.6.2.1 ^{14}C-PP and ^{13}C-PP

The ^{14}C-PP method has been widely used in the oceanography community; however, in the mid 1980s, the ^{13}C-PP method started to gain traction as investigators transitioned away from using radioisotopes. If these are equivalent, then the two methods are interchangeable. Historical data generally show that ^{13}C-PP and ^{14}C-PP agree well, and neither tends to be higher than the other. One of the first comparisons of ^{13}C-PP and ^{14}C-PP rates was done using batch cultures including a range of incubation times (4-24 hours), light levels, and species, resulting in better agreement at lower rates (Slawyk et al., 1977). However, Regaudie-de-Gioux et al. (2014) found the opposite, with methods agreeing better at higher rates using field data but ^{13}C-PP exceeding ^{14}C-PP at lower rates. Mousseau et al. (1995) found that ^{14}C-PP rates were higher than ^{13}C-PP close to the base of the euphotic zone. Hama et al. (1983) concluded that ^{13}C-PP and ^{14}C-PP are close enough they can substitute each other.

Our data show that ^{13}C-PP is usually higher than ^{14}C-PP (Figure 2.5a). The GFF filters used at the end of the incubations were precombusted for the ^{13}C-PP method but were not for the ^{14}C-PP method. Nayar et al. (2003) show that muffling decreases pore size in GFF filters, so that ^{13}C-PP would have collected smaller phytoplankton and thus would have higher rates. However, muffling only decreases the pore size from 0.7 µm to 0.4 µm. There are likely very few phytoplankton in the 0.4-0.7 µm size class, so this change in filter pore size is not likely the main reason for the discrepancy. What caused K1, LS2,

and CAA3 to have ^{14}C-PP rates higher than ^{13}C-PP is unclear. The particulate carbon collected on the combusted filters versus the particulate organic carbon samples do not stand out as particularly different for these three stations (K1, LS2, CAA3). Also, blanks generally did not seem unusual at these stations. Instead we hypothesize that not all conditions were exactly the same for each method. For this study, ^{13}C-PP and ^{14}C-PP were also carried out in different incubators, so they could have experienced slightly different light fields. Dring and Jewson (1982) show different light intensities can change ^{13}C-PP rates, but the difference is not significant until incubation times are on the order of 40 hours. Our incubations were 24 hours, so differences in light intensities are unlikely to have had a significant effect on our measurements. It is possible that inherent differences between the methods caused the methods to not agree. For example, both ^{13}C enrichment and particulate carbon need to be measured for ^{13}C-PP but only beta counts are needed for ^{14}C-PP. Measurement of particulate carbon (PC) is required for the ^{13}C-PP calculation, which includes all particulate carbon, not only phytoplankton. It is possible that problems in the PC measurement could bias with the ^{13}C-PP method.

2.6.2.2 ^{14}C-PP and ^{13}C-PP versus ^{18}O-GPP

The JGOFS research effort compared ^{18}O-GPP to ^{14}C-PP finding a ratio of ^{18}O-GPP (in units of oxygen) to ^{14}C-PP (in units of carbon) of 2.7 (Juranek and Quay 2013). Robinson et al. (2009) observed a ^{18}O-GPP to ^{14}C-PP ratio of 4.5 and a slope of 5.25 in the Celtic Sea. At station ALOHA, the ratio is 2.2 when corrected from 12 to 24 hour ^{14}C-PP (Quay et al., 2010). Our study has a slope of 1.35 and 2.05 for ^{18}O-GPP vs. ^{14}C-PP and ^{13}C-PP, respectively (Figure 2.5b). The ratios for ^{18}O-GOP:^{14}C-PP and ^{18}O-GOP:^{13}C-PP are 4.39±5.37 and 2.50±4.01, respectively. We prefer the slope as less likely biased by

outliers, but also report ratios for ease of comparison to other studies. The ^{18}O-GPP to ^{13}C-PP ratio is closer to the JGOFS ratio. It is surprising how different the ratio is compared to the best fit slope. Deviation from this ratio cannot be explained by most of the hypotheses in section 2.6.1 because both of these are in vitro methods. So deviations must be explained by either methodological biases or decoupling of O_2 production from carbon fixation (Juranek and Quay, 2013). The Mehler reaction, chlororespiration, and photorespiration are all mechanisms that produce O_2 but do not create organic carbon (e.g. Quay et al., 2010). Juranek and Quay (2013) suggest that lower ratios could indicate more electron flow going to carbon fixation and higher ratios could indicate more alternative electron flow.

2.6.3 Comparison to other Arctic studies

Our carbon export estimates agree well with other studies in the Arctic. The average ^{15}N-new$_{ML}$, ^{15}N-new$_{eu}$, and O_2/Ar-NCP is 11.9±11.0 mmol C m^{-2} d^{-1}, 37.9±33.2 mmol C m^{-2} d^{-1}, and 11.6±4.9 mmol C m^{-2} d^{-1}, respectively. Other studies found average carbon export estimates for the upper 100 m east of Greenland of 14.38±19.9 mmol C m^{-2} d^{-1} using Th disequilibrium methods (Le Moigne et al., 2015). Interestingly, their lowest rate was in ice and the highest was on the ice edge. Similarly, Resolute-N (CAA6) was along the ice edge (about 20 km away from 60+% ice coverage) during this study and corresponded to the highest O_2/Ar-NCP but modest ^{15}N-new$_{ML}$ and increased ^{15}N-new$_{eu}$ compared to other stations in the CAA. Varela et al. (2013) grouped values based on geographical area. Their average ^{15}N-new$_{eu}$ had similar rates in both the Canadian archipelago (26.2±9.6 mmol C m^{-2} d^{-1}) and in Labrador Sea and Baffin Bay (24.4±7.0 mmol C m^{-2} d^{-1}) when assuming Redfield ratio. This study had an average of 33.4±14.9

and 42.4±47.0 mmol C m^{-2} d^{-1}, for LS-BB and CAA, respectively, of similar magnitude to Varela et al. (2013). The high standard deviation for CAA is driven by the central CAA station (CAA5), where $^{13}C\text{-}PP_{eu}$ was very high at one depth, but it is unclear why. Varela et al. (2013) calculated new production by multiplying the f-ratio (^{15}N-new divided by production fueled by other nitrogen sources) and ^{13}C-PP. When using that method for this study, the two regions had lower rates for new production, averaging 20.3±16.5 mmol C m^{-2} d^{-1} and 21.8±11.8 mmol C m^{-2} d^{-1} for CAA and LS-BB, respectively. Varela et al. (2013) found urea fueled a significant portion of primary production. This study measured ammonium uptake but did not measure urea uptake rate. Adding urea would have decreased new production calculated from the f-ratio method even farther. The f-ratio for our study was above 0.6 at LS2, BB3, CAA1, and CAA5, but the average for the rest of the stations (not including K1 due to no measurement for ammonium uptake) was 0.4.

C-PP, both integrated and for surface waters alone, agreed with previous studies from across the Arctic. East of Greenland was characterized by an average $^{14}C\text{-}PP_{eu}$ of 36.8±17.6 mmol C m^{-2} d^{-1} (Le Moigne et al., 2015). Varela et al. (2013) found an average $^{13}C\text{-}PP_{eu}$ in LS-BB of 84.3±21.1 mmol C m^{-2} d^{-1}. This study determined an average $^{13}C\text{-}PP_{eu}$ and $^{14}C\text{-}PP_{eu}$ in LS-BB of 48.5±14.9 and 46.6±40.5 mmol C m^{-2} d^{-1}, respectively. Varela et al. (2013) measured an average $^{13}C\text{-}PP_{eu}$ in the CAA of 56.5±16.3 mmol C m^{-2} d^{-1} compared to 29.5±16.4 mmol C m^{-2} d^{-1} in this study. Matrai et al. (2013) collated ^{14}C-PP data from 1953 to 2007 for surface waters in the pan-Arctic finding a summer average of 3.9±0.2 mmol C m^{-3} d^{-1} compared to this study's average surface ^{14}C-PP of 1.8±1.0 mmol C m^{-3} d^{-1}.

Very few studies measured GPP in the Arctic. Average GOP from triple oxygen isotopes in the Canada Basin was 27±4 mmol O_2 m^{-2} d^{-1} (Stanley et al., 2015), much lower than our study with an average of 84.4±34.4 mmol O_2 m^{-2} d^{-1}. To our knowledge, ^{18}O-GPP has not been measured in the Arctic. Average ^{18}O-GPP_{eu} and ^{18}O-GPP_{ML} were 88.7±50.8 mmol O_2 m^{-2} d^{-1} and 42.7±46.2 mmol O_2 m^{-2} d^{-1}, respectively.

Chlorophyll concentration could also be a controlling factor for production rates. Hill et al. (2013) found a strong relationship between ^{14}C-PP and chlorophyll a concentrations from Arctic data spanning 1954 to 2007, with an R^2 value of 0.66 when comparing values at each depth excluding light depths deeper than 5 %. Our study also demonstrates a strong relationship between ^{13}C-PP, ^{14}C-PP, and ^{18}O-GPP versus chlorophyll a concentrations with an R^2 value of 0.77, 0.84, and 0.76, respectively (Figure 2.3b-d). In contrast, no relationship exists between chlorophyll and ^{15}N-new, even when the outlier is removed.

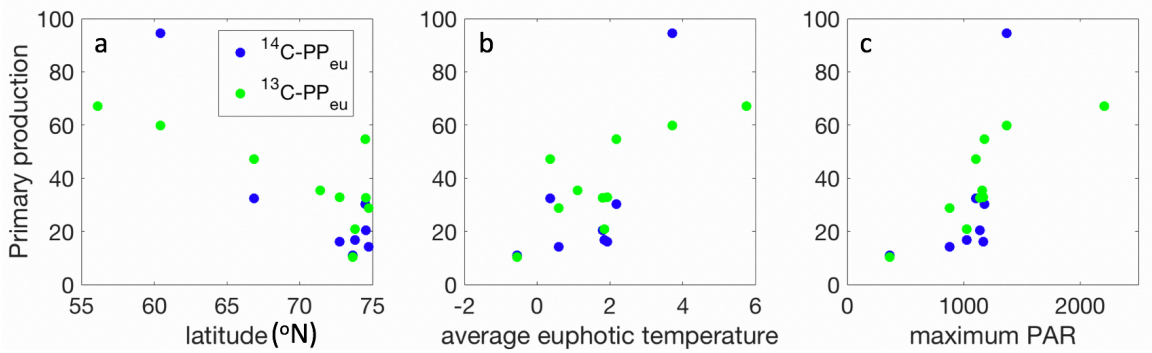

Figure 2.8 PP_{eu} versus (a) latitude (b) average euphotic temperature and (c) maximum PAR (µmol m^2 s^{-1}).

Our study finds a latitudinal trend in primary productivity (carbon uptake) rates, including all factors that could affect this relationship. For example, the timing of the

spring bloom, upwelling and mixing rates, stratification, and nutrient limitation are all changing for the different latitudes and likely contributing to the latitudinal trend observed in the this study. Not all studies have found such a geographical difference. Matrai et al. (2013) find "no indication of geographical distribution or change over time" due to "highly irregular and scarce regional sampling" when subdividing the Arctic into 13 regions. Other studies agree with our results; for example, Harrison et al. (1982) observed a higher ^{14}C-PP$_{eu}$ at 45°N that decreased going northward to 70°N in the Labrador Sea and Baffin Bay. Our study also finds a linear relationship between latitude and ^{13}C-PP integrated to the euphotic zone depth, with higher rates at lower latitudes (Figure 2.8a). Such a trend is intuitive since increasing latitude is associated with decreasing daily solar radiation and thus lower euphotic zone temperatures. Temperature and latitude were well correlated in our dataset. We find a positive relationship between the average euphotic zone temperature and euphotic zone integrated PP (Figure 2.8b). Interestingly, we find no relationship between temperature and ^{13}C-PP when comparing on a depth by depth basis (Figure not shown), probably because light levels have a greater influence on the deep samples than temperature. Temperature is better correlated with latitude than maximum PAR is correlated with latitude. However, this study suggests a slight positive relationship between ^{13}C-PP$_{eu}$ and maximum PAR recorded at each station during the incubation (Figure 2.8c).

2.7 Conclusion

This paper compared seven methods for quantifying productivity rates on a 2015 Arctic GEOTRACES cruise. We compared both in vitro and in situ methods, which should theoretically measure the same fraction of production. However, we found strong method

disagreement at some stations and hypothesize five main reasons for disagreement: time of integration, depth of integration, a recently shoaled mixed layer, mixing at the base of the mixed layer, and methodological issues. Because of the dynamic nature of this biogeochemical province, no single mechanism dominated the method comparisons. However, episodic events that affect the different time of integration of the methods and a recently shoaled mixed layer could be the more important mechanisms during this study.

Multiple in vitro methods were also conducted during the cruise. Interestingly, ^{13}C-PP and ^{14}C-PP were not equivalent, where ^{13}C-PP was mainly higher than ^{14}C-PP, but ^{14}C-PP was higher than ^{13}C-PP at three stations. ^{18}O-GOP to ^{13}C-PP ratios were closer to the global average from JGOFS compared to ^{14}C-PP. We observed chlorophyll-*a* was strongly linearly correlated to many of the production methods, possibly indicating it as a controlling factor. We also observed a latitudinal trend in primary production, even with the many factors that affect production. Quantifying productivity rates and what controls them in the largely undersampled Arctic will improve understanding of the carbon cycle.

2.8 Acknowledgements

We thank Jennifer Reeve, Lianna Teeter, and Hollie Johnson for their expertise in sample analysis. We appreciate the support of ArcticNet scientists and technicians especially Gabrièle Deslongchamps, Jonathan Gagnon, Pascal Guillot, Isabelle Courchesne, and Martine Lizotte. Thank you to Paul Quay, Johnny Stutsman and Mark Haught for help with the triple oxygen isotope analysis. Thank you to Alfonso Mucci for analyzing d^{18}O of water samples. Thank you to Jacoba Moi for analyzing DIC samples. Thanks to the captain and crew of the CCGS Amundsen. We also thank Clark Pennelly

for his help with wind data. Wind data came from Global deterministic prediction system reforecasts (CGRF), ERA-Interim, National Centers for Environmental Protection (NCEP), North American Regional Reanalysis (NARR). CCMP Version-2.0 analyses are produced by Remote Sensing Systems and sponsored by NASA Earth Science funding. Data are available at www.remss.com/measurements/ccmp. Daily ice coverage was determined from IFREMER's CERSAT SSM/I ice coverage 2.0 product. This work was supported by NSERC DG 329290-2012 to R. Hamme, and NSERC CCARs 433848-2012 to Roger Francois and 433898-2012 to Paul Myers.

Chapter 3. Phytoplankton response and upwelling cause productivity rate methods in the NE subarctic Pacific to disagree

Key points

1. When rates are low, strong correlations exist among different productivity rate methods
2. Methods disagreements occur at locations with high chlorophyll a
3. Three processes tend to cause methods to disagree: dissolved organic matter release, bloom dynamics, and upwelling.
4. Satellite net primary production is consistently different from carbon uptake in the NE subarctic Pacific

3.1 Abstract

Phytoplankton photosynthesize in surface waters, exporting organic carbon to depth through the biological pump. Quantifying productivity and the export of carbon is important to understanding the global carbon cycle and predicting its future changes. During this study we measured productivity by six methods in the NE subarctic Pacific: ^{13}C, $^{15}NO_3$, $^{15}NH_4$, and ^{18}O uptake rates through incubations as well as oxygen to argon ratio and triple oxygen isotope mass balance approaches. We specifically compare in situ and in vitro methods to identify what causes differences. We present evidence that dissolved organic matter release, upwelling effects on vertical transport, and the interaction between bloom dynamics and a method's inherent time of integration are the most important reasons for method disagreement. We further show one particular instance where end-of-bloom dynamics caused by a relaxation in upwelling created an extreme example of method disagreement. By identifying consistent trends and what causes disagreement, we facilitate future comparison of methods across studies.

3.2 Introduction

The biological pump is an important mechanism for sequestering carbon from the surface ocean to the deep sea, lowering atmospheric carbon dioxide levels and thus keeping the planet cooler. Both the solubility pump and the sinking of organic carbon create a vertical carbon gradient with higher carbon in the deep ocean, moving carbon away from contact with the atmosphere. About 75% of that gradient is driven by the biological pump (Volk and Hoffert, 1985). Understanding what controls productivity rates is necessary to provide insight into possible climate change scenarios (Munro et al. 2013). For example, the Fifth Assessment Report of the Intergovernmental Panel on Climate Change (IPCC) says the biological pump is too poorly understood to determine whether the sign or magnitude will change in the future (Portner et al., 2014). If the strength and efficiency of the biological pump do change, it would affect how carbon is vertically distributed in the ocean and impact the ocean's uptake of atmospheric carbon (Passow and Carlson, 2012).

Multiple methods need to be employed to better constrain production rates in spite of measurement biases. Because different biases affect different methods, comparison creates an opportunity to uncover those biases. Moreover, since there can be no 'standard' for rate measurements, multiple measures are needed to ensure consensus. The majority of studies use only one method to estimate primary production and carbon export, which can be problematic when comparing different studies. As different methods measure different fractions of primary production, there is a need to determine conversion factors so that results can be compared. For example, Regaudie-de-Gioux et al. (2014) compiled many studies and found methods could differ by orders of magnitude.

There are two main types of productivity measurement methods: in vitro and in situ. In vitro methods involve removing water from the environment, adding a labeled tracer, and incubating for a specific length of time. The amount of change measured with the tracer over time is used to quantify some portion of production, depending on the tracer. In vitro methods integrate to any depth where measurements have been taken. To facilitate comparisons, we focus on integration to the mixed layer depth in this paper. In vitro methods also integrate only over the time-frame of the incubations themselves (typically 24 hours), which can potentially miss episodic events (Falkowski and Woodhead, 2013). Rates measured during incubations are assumed to represent in situ rates; however, bottle effects can bias this method type. For example, phytoplankton in bottles are not exposed to the natural turbulence they would experience in the ocean (Gocke and Lenz, 2004). Incubation bottles made of polycarbonate, borosilicate, or Pyrex may change the light spectrum during incubations (Hama et al., 1993; Garcia-Corral et al., 2014; Helbling et al., 1992). Evidence on whether bottle size affects productivity incubations is unclear (Gieskes et al., 1979; Laws et al., 1987). Metal contamination of incubation water could result in either an under- or over-estimation depending on the metal and concentration (Fitzwater et al., 1982). Finally, food web interactions are perturbed when isolated in bottles (Quay et al., 2010).

In situ methods depend on the natural distribution of chemical tracers in the environment and do not require incubation. The methods in this study involve a mass balance of oxygen or its isotopes in the mixed layer. They integrate to the mixed layer depth and over roughly the residence time of oxygen in the surface water (Cassar et al., 2014; Teeter et al., 2018), about two weeks. Because of the longer integration, these in

situ methods are less likely to miss episodic events (Munro et al., 2013), though more recent time periods still affect them more strongly (Teeter et al., 2018). Typical calculations assume mixing is negligible, but this is not always the case and can cause biases. For example, modelling shows that mixing can underestimate seasonal O_2/Ar-based in situ rates by 21 to 36% in the Southern Ocean (Jonsson et al., 2013). In the offshore subarctic northeast Pacific, Giesbrecht et al. (2012) found diapycnal mixing causes the O_2/Ar method to be significantly biased low during winter, such that the method could not be reliably used in that season. In coastal regions, upwelling may also bias in situ methods (Izett et al., 2018; Haskell et al., 2016). The effect of mixing on in situ methods can be estimated based on a vertical eddy diffusivity rate and the gradient from within the mixed layer to below (Nicholson et al., 2014).

Methods also often measure different fractions of production, complicating comparison. Gross oxygen production (GOP) quantifies production by autotrophs. When GOP is converted from oxygen to carbon units, it is termed gross primary production (GPP) in this paper. Net primary production (NPP) is defined as GPP minus respiration by autotrophs, while net community production (NCP) is defined as GPP minus respiration by autotrophs and heterotrophs.

The majority of method comparison studies have focused on subtropical gyres (e.g. Luz and Barkan, 2000; Corno et al., 2005; Luz and Barkan, 2009), the North Atlantic (e.g. Chipman et al., 1993; Robinson et al., 2009), and Southern Ocean (e.g. Hamme et al., 2012; Cassar et al., 2015). At the Hawaii Ocean Time-series, in the North Pacific subtropical gyre, in vitro methods detected lower average annual carbon export rates than in situ methods (Juranek and Quay, 2005). However, the subtropical gyre is oligotrophic,

so results from it may not be applicable to the high nutrient low chlorophyll subarctic NE Pacific. Some projects explored method comparison in the subarctic NE Pacific such as the Joint Global Ocean Flux Study (JGOFS), where carbon export methods varied by two orders of magnitude (Berelson, 2001). Besides JGOFS, the only other method comparisons conducted in the NE Pacific were the Subarctic Pacific Ecosystems Research (SUPER) program (Emerson et al., 1993; Welschmeyer et al., 1993) and Giesbrecht et al. (2012).

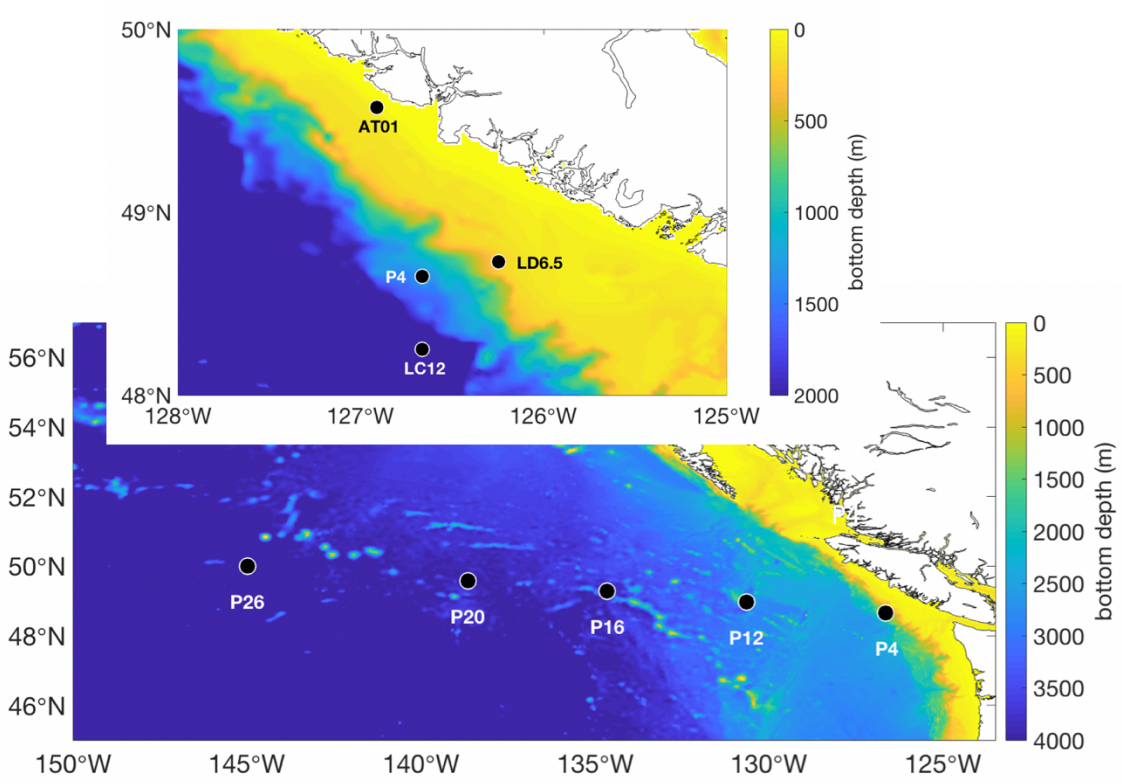

Figure 3.1 Map of stations sampled including major stations along Line P (P4, P12, P16, P20, P26) and three La Perouse cruise stations (inset shows their relation to P4). Background color is bathymetry from NOAA's National Centers for Environmental Information (Amante and Eakins, 2009). Nearshore bottom depths are 64 m at AT01 (on shelf), 178 m at LD6.5 (shelf break), 2543 m at LC12, and 1300 m at P4.

Line P, located in the subarctic NE Pacific, is an ideal setting for method comparison because of the varied environments encountered along the 1500 km transect (Figure 3.1). An iron gradient exists with high concentrations onshore decreasing to limiting concentrations offshore (e.g. Martin et al., 1989; Boyd et al., 1996; La Roche et al., 1996). Macronutrients have the opposite trend, and the offshore region is characterized by high nutrient-low chlorophyll (HNLC) conditions (Miller et al., 1991; Boyd et al. 1996). Upwelling affects the coastal station (P4), suppling nutrients in the spring and summer during upwelling favorable wind conditions, feeding productive phytoplankton that draw down nutrients (Freeland 1982). In addition to the local upwelling, remote upwelling from Oregon and California (Freeland, 1982) via coastal-trapped waves (Engida et al., 2016) can also influence the coastal area. Transition stations are not directly influenced by upwelling but also have sufficient iron that macronutrients become limiting in the summer (Figure 3.1; Whitney et al., 1998) and in an extreme case, extended to P21 in August 2014. There is no consistent subsurface chlorophyll maximum across the transect (Peña and Varela, 2007).

In this paper, we compare productivity rate methods at stations along the Line P transect and at three additional stations targeting the shelf. We focus first on comparing in situ and in vitro carbon export and gross primary production methods. These methods, in theory, measure the same fraction of production, so we explore what drives the methods to disagree. Next, we compare an in vitro method (^{13}C uptake) against the other methods. Finally, we examine how chlorophyll a relates to productivity.

3.3 Methods

Samples were collected at the five major Line P stations (P4, P12, P16, P20 and P26) in June and August beginning in August 2014 and ending in June 2017 (Figure 3.1). Additional coastal samples were collected on a British Columbia coastal time series cruise (called La Perouse; Mackas et al., 1992) in May 2016. The three coastal stations AT01, LD6.5, and LC12 had bottom depths of 64m, 178 m, and 2543 m, respectively, targeting on-shelf, shelf-break but still on-shelf, and offshore. All samples were collected from the same rosette cast, with pressure, conductivity and temperature measured using a SBE 911plus and fluorescence using a SeaPoint fluorometer.

3.3.1 In situ

The first in situ method we used measures dissolved oxygen in the mixed layer to estimate the net production and consumption of oxygen. However, oxygen concentrations are also influenced by physical factors such as temperature change and bubble injection from breaking waves (Craig and Hayward, 1987). To account for these factors, we actually measure the oxygen to argon ratio, because argon has similar physical properties to oxygen but is inert, so the oxygen/argon ratio is not affected by temperature change or bubbles (Craig and Hayward, 1987). Where vertical and horizontal mixing are negligible, the major source of biologically derived oxygen to the mixed layer is through photosynthesis and the main sinks are through respiration and air-sea gas exchange. If the air-sea flux can be estimated, this mass balance method then yields an estimate of net community production (abbreviated O_2/Ar-NCP). Vertical mixing and diapycnal mixing typically bias the O_2/Ar mass balance low. This O_2/Ar-NCP is an estimate of the potential amount of carbon that is available for export (Juranek et al., 2012). A photosynthetic quotient (PQ) of 1.4 O_2/C was applied to convert from oxygen to carbon units.

Duplicate O_2/Ar samples for this study were collected at two depths within the mixed layer and processed/analyzed following Emerson et al. (1999). In short, samples were collected into pre-evacuated $HgCl_2$-poisoned ~180mL flasks until about half full. Tubing was flushed with carbon dioxide before sampling to prevent air from entering the flask. On land, flasks were weighed and placed overnight in a temperature controlled water bath to equilibrate the water and headspace in the flask. Then the water was removed, leaving behind the gases, which were then purified through a liquid nitrogen trap to remove water and carbon dioxide and subsequently frozen into a metal tube using liquid helium. Gases in the tube were analyzed against standards of similar gas composition on a Thermo MAT 253 isotope ratio mass spectrometer at the University of Victoria. Chemical slope corrections were applied, based on the standards with known O_2/Ar ratios, to account for differences in gas ionization efficiencies when the sample did not have identical oxygen concentrations to the standard (Emerson et al., 1999; Hamme, 2003). Error bars represent the standard deviation of the four samples collected within the mixed layer and are a very conservative estimate of precision only.

The second in situ method we used is known as the triple oxygen isotope method, which measures gross oxygen production (abbreviated $^{17}\Delta$-GOP; Luz et al., 1999; Luz and Barkan, 2000). The method is based on the principle that O_2 from air-sea gas exchange and O_2 produced during photosynthesis have different isotopic signatures among oxygen's three isotopes (Luz and Barkan, 2000). In the stratosphere, photochemical (mass independent) processes deplete ^{17}O relative to ^{18}O (Thiemens et al., 1995). Oxygen split during photosynthesis has a similar isotopic composition as the water, which is quite different from the stratospheric O_2 (Luz and Barkan, 2000; Luz and

Barkan, 2011). The oxygen in the mixed layer is a mass balance, where the inputs are either from the atmosphere or photosynthesis. We can then track the balance between the end members to estimate GOP. This method is largely insensitive to respiration (Luz and Barkan, 2005).

Duplicate samples for $^{17}\Delta$-GOP were collected at one depth in the mixed layer and one depth either in the oxygen maximum or about 20 m below the mixed layer depth in June and August 2015. Sampling was similar to O_2/Ar-NCP (Emerson et al., 1999), except the pre-evacuated flasks were larger (500 mL) collecting about 250 mL of water. Flasks were equilibrated for 24-hr in a temperature controlled water bath so the gases distributed between the headspace and the water (Palevsky et al. 2016), and then the water was removed. The remaining gas was purified on a vacuum line using liquid nitrogen to remove carbon dioxide, water vapor and a gas chromatograph column to remove N_2 (Barkan and Luz, 2003). The remaining gas was frozen into a metal finger and analyzed at University of Washington on a Thermo Finnigan IRMS to measure the oxygen isotopic composition and the O_2/Ar ratio, which were further corrected for the sample volume. From these measurements, $^{17}\Delta$-GOP was calculated according to Hamme et al. (2012). Error bars conservatively represent only the standard deviation of the duplicate samples within the mixed layer.

Both in situ methods are mass balances that rely on an estimate of air-sea exchange based on a gas transfer velocity. For example, the O_2/Ar-NCP method equates NCP to the diffusive gas exchange of biological oxygen. Gas transfer velocities were calculated from scatterometry-derived winds from the 6-hr Cross-Calibrated Multi-Platform (CCMPv2) dataset at the nearest grid point using the Ho et al. (2006) gas transfer velocity

parameterization. Error bars shown do not include the uncertainty in the gas transfer velocity parameterization. We weighted and averaged the gas transfer velocities over the previous 30 days following Reuer et al. (2007) as modified by Teeter et al. (2018), which heavily emphasizes the more recent time period.

3.3.2 In vitro

Four types of incubations were conducted using the following isotopes: ^{13}C, $^{15}NO_3$, $^{15}NH_4$, and ^{18}O. Water samples for incubations were collected at five light levels (100, 50, 30, 15, and 1% of surface irradiance), determined by photosynthetically active radiation (PAR, QSP 400) at the previous noon cast, which was sometimes at a different station. Samples were spiked with isotopes and then incubated for 24 hours starting around dawn in an on-deck incubator inside tubes wrapped in blue and neutral density photographic film. When sample water had to be collected significantly before dawn, samples were put into a container with flow through surface water in the dark and spiked just before dawn except for ^{18}O incubations, which had to be spiked at collection. The incubator was placed on the helideck with continuously flowing seawater, drawn from about 4.5 m. This results in deeper samples being exposed to warmer temperatures, possibly changing productivity rates, but would only affect samples collected below the mixed layer, which are not included in our integrated estimates. To reduce external temperature influences, white insulated tubing with the shortest possible length was used for the seawater water input. All samples were collected from the same CTD cast except for dissolved inorganic carbon (DIC). Standard deviation of the integrated estimates was calculated based on trapezoidal integration according to Krause et al. (2011).

Carbon uptake (abbreviated ^{13}C-PP) is a measure of primary production. Like ^{14}C incubations, this is likely a measure somewhere between net primary production and gross primary production (Marra, 2009, Hama et al., 1983; Slawyk et al., 1977). Samples (1200 mL acid washed polycarbonate bottles) were spiked with ^{13}C labelled bicarbonate to ~10% of the climatological DIC concentration. Triplicate samples, an initial (T0 with spike) and a dark sample were collected at 100% light and single samples were collected at all other depths. Because ^{13}C-PP was done as a dual tracer, there were actually two sets for a total of 6 samples, 2 blank and 2 dark at 100% and duplicates at all other depths. At the end of the incubation, water was filtered onto precombusted GF/F filters (Hama et al., 1983). Filters were analyzed for atom % ^{13}C, atom % ^{15}N, particulate carbon and nitrogen by the Stable Isotope Laboratory at the University of California Davis. DIC samples were collected at the same station but not from the same cast. The August 2014 and La Perouse cruise (May 2016) were the only cruises where DIC samples were not taken or not analyzed yet, so an empirical equation based on hydrographic and DIC samples collected in coastal waters (DIC = 46.362609062 * sigma_theta + 0.765762453966 * AOU + 852.908307996) was used instead, where sigma_theta is density (kg m^{-3}) and AOU is apparent oxygen utilization (μmol kg^{-1}; Personal communication - D. Ianson). Since two sets of ^{13}C-PP were collected because of the dual tracer, error bars represent the standard deviation calculated from six samples in the surface waters and duplicates at all other depths.

New production (abbreviated ^{15}N-new) is considered to be an estimate of carbon export. At steady state, new sources of bioavailable nitrogen into surface waters have to balance organic nitrogen exported with its associated carbon. This method assumes that

nitrate is the only source of new nitrogen into the system (i.e. other new sources of nitrogen like nitrogen fixation are not significant) and that all nitrate comes from locations external to the local euphotic zone (i.e. nitrate cannot be significantly regenerated in the surface waters through processes such as nitrification). Incubations for ^{15}N-new were performed in the same bottles as the ^{13}C-PP incubations as dual tracers (Dugdale and Goering, 1967; Slawyk et al., 1977), and therefore processed in the same way as the ^{13}C-PP samples. Triplicate samples, a blank and a dark sample were collected at 100% light and single samples were collected at all other depths. Our goal was to spike samples with ^{15}N labelled nitrate to a concentration of 10% of ambient or less as suggested by Dugdale and Goering (1967). During the first cruise (August 2014), we used climatological nitrate concentrations to determine the amount of spike added; however, actual nitrate concentrations were much lower than expected leading to overspiking for most of the offshore stations (by more than 50%). This situation was partially due to the anomalously warm water situated offshore that year causing less nutrient inputs during the previous winter ("The Blob"; Freeland and Whitney, 2014; Bond et al., 2015; Whitney, 2015; Di Lorenzo and Mantua, 2016). After that cruise, to avoid stimulating production by overspiking, samples were spiked with 0.1 μM of ^{15}N labeled nitrate. which was about 2% to 5% of ambient at the lowest range. Many stations had 0 μM of nitrate, so spiking at the detection limit was the best choice that could be made but could have potentially stimulated productivity. Error bars represent the standard deviation calculated from triplicate samples collected at 100% and was assumed to be the same throughout the water column. Rates were calculated based on Dugdale and Wilkerson (1986) and corrected using blank samples. Dark samples were also incubated

and checked to ensure values were low. It is theoretically possible to have small amounts of ^{15}N uptake at night if the phytoplankton were storing in the cell for utilization once there is sufficient sunlight. However, I expect this to be low and is confirmed by the dark samples, where rates were low.

There are two ways to calculate new production. The first, which we abbreviate ^{15}N-new, is to convert the nitrate uptake to carbon using the carbon to nitrogen ratio from each sample, which was also measured at University of California Davis. The second is to multiply ^{13}C-PP by the f-ratio, where the f-ratio is calculated as the nitrate uptake rate divided by the sum of nitrate uptake and ammonium uptake rates. Each method has respective assumptions so we compare both to identify important biases and provide insight into which is most appropriate in this region (Appendix B-1).

Recycled production (^{15}N-recy) is an estimate of the recycled production through ammonium uptake, assuming ammonium is the only source of recycled nitrogen. However, urea uptake, which we did not measure, has also been shown to be important in this region (Varela and Harrison 1999). ^{15}N-recy incubations were also performed as a dual tracer with ^{13}C-PP, meaning both spikes were placed in the same bottle (Dugdale and Goering, 1967; Slawyk et al., 1977). A 0.1 μM addition of ^{15}N labelled ammonium was added and is the detection limit for this method. Ambient ammonium concentrations are regularly 0 μM in the surface waters. Triplicate samples, a blank, and a dark sample were collected at 100% and single samples were collected at all other depths. Error bars were calculated in the same way as ^{15}N-new.

Gross oxygen production can be estimated from ^{18}O incubations because, during photosynthesis, water is split in photosystem II to produce oxygen. By spiking the

incubation sample with ^{18}O labeled water and measuring the amount of ^{18}O enrichment in the dissolved oxygen pool, gross oxygen production can be estimated (abbreviated ^{18}O-GOP; Bender et al., 1987; Grande et al., 1989; Bender et al., 1999). ^{18}O incubation samples were only collected during four cruises in 2015-2016. Sample collection and analysis largely followed Juranek and Quay (2005). In short, samples (with a natural ^{18}O abundance of 0.200%) were spiked with 400 µL of ^{18}O labeled water (^{18}O abundance of 97% from Medical isotopes) in an ~140 mL pyrex glass bottle with ground glass stopper. The ^{18}O spike was distilled prior to use in a trace metal clean laboratory to remove potential contamination from the spike. At the end of the incubation, samples were siphoned into pre-evacuated, $HgCl_2$-poisoned flasks and processed in the same manner as O_2/Ar samples, except analyzed for $\delta^{18}O$ of the dissolved O_2. At each depth, three samples were collected; two were incubated and the third was ended immediately to serve as an initial value. GOP was calculated based on equation 1 from Juranek and Quay (2005). Error bars represent the standard deviation of the duplicate samples at each depth.

3.3.3 Ancillary data and processing

Single chlorophyll a samples were collected at the same depths as the incubation light levels. 304 mL were filtered onto GF/F filters and analyzed following Holm-Hansen et al. (1965). Dissolved oxygen samples were collected at the same depths as the $^{17}\Delta$-GOP, O_2/Ar-NCP, and ^{18}O-GOP samples and analyzed by Winkler titration using a visual endpoint and a dry WAKO-brand potassium iodate standard (Carpenter, 1965; Emerson et al., 1999). Nutrient samples were collected at all in vitro light levels, frozen at -20°C, and analyzed on an Astoria analyzer following Barwell-Clarke and Whitney (1996).

Ammonium samples were kept in the dark and cold before spiking with working reagent and then incubated at room temperature and analyzed following Holmes et al. (1999). Blanks and standards were ideally made with seawater collected from offshore at 2005 m in the water column. However, sometimes onshore stations had to be used from 250 m, following Fisheries and Oceans Canada's Institute of Ocean Sciences protocol.

CTD Niskin bottles were modified with the intention of decreasing trace metal contamination before the June 2016 cruise. All equipment used in collection of incubation samples was acid washed including incubation bottles, sample tubing, pipette tips, spike bottles, and the distillation rig. Care was taken not to touch anything that came into contact with the incubation water. Black rubber O-rings were replaced with viton O-rings and the Niskin closure mechanisms were changed from a mixture of springs and tubing to silicon tubing. A comparison shows no statistical difference between the modified and unmodified Niskins based on the Wilcoxon statistic (Appendix B-2). Even if iron was inadvertently added, biological effects would not be measured during the short 24-hour incubations (e.g. Boyd et al., 1996).

Net primary production was estimated using the Carbon-based Production Model (CbPM) algorithm (Westberry et al., 2008) based on Visible Infrared Imaging Radiometer Suite (VIIRS) satellite observations and the (Garver-Siegel-Maritorena) GSM algorithm for chlorophyll (Maritorena et al., 2002). We used an 8-day average incorporating the sampling date for each station. Spatial resolution was 1/6 of a degree, so data was chosen from the grid point closest to the stations for comparison. All data was downloaded from the Ocean Productivity site at http://orca.science.oregonstate.edu/1080.by.2160.8day.hdf.cbpm2.v.php.

One way to assess local upwelling strength is through NOAA's Pacific Fisheries Environmental Laboratory upwelling index calculated based on Ekman's theory of wind stress driven mass transport (where positive values indicate upwelling). Data was downloaded from https://www.pfeg.noaa.gov/products/PFEL/modeled/indices/upwelling/NA/upwell_menu_NA.html.

All regression fit equations were calculated as a neutral regression according to Marsden (1999). Neutral regression assumes errors may exist in both the x and y parameters such that both axes are dependent variables. We fit both a slope and intercept except when the error in the intercept includes 0 and the error in the slope when fit through 0 is within the confidence interval of the slope when the intercept is included. This exception, when only a slope is fit forcing the intercept through 0, applies to the following relationships: ^{13}C-PP with O_2/Ar-NCP and ^{13}C-PP with ^{15}N-new.

3.4 Results and discussion

We compare productivity methods to determine if there are consistent differences and to identify what factors causes methods to disagree. We contrast in situ with in vitro methods and compare methods to primary production.

3.4.1 Estimates of carbon export integrated to the mixed layer depth

The two methods for quantifying carbon export (O_2/Ar-NCP and ^{15}N-new) do not produce equivalent rates; however, trends emerge in the comparison. At lower production rates, O_2/Ar-NCP tends to be higher than ^{15}N-new (22 out of 26 stations; Figure 3.2a). When rates are lower than 30 mmol C m^{-2} d^{-1}, our results suggest a rough conversion

between the two estimates of O_2/Ar-NCP = 2.6*^{15}N-new – 4.4, but the relationship is not a tight correlation, having an R^2 of only 0.34. At higher primary production rates, there is no consistent trend between ^{15}N-new and O_2/Ar-NCP. Higher rates were generally observed at coastal stations with high surface chlorophyll (Figure 3.2b). Several of the higher points also fall above the 1:1 line but still close to the slope defined by the lower productivity values.

This O_2/Ar-NCP vs. ^{15}N-new relationship is similar to other studies. Giesbrecht et al. 2012 found a similar trend at lower production rates along Line P in 2007-2009, although their study is not directly comparable because not all incubations started at dawn. In the Southern Ocean, O_2/Ar-NCP also tended to be higher than ^{15}N-New when O_2/Ar-NCP rates were positive (Hamme et al., 2012). Interestingly, in the Arctic there are four locations (Labrador Sea and Canadian Archipelago) where ^{15}N-new is higher than O_2/Ar-NCP at lower rates (Chapter 2). However, the Arctic is a quite different biogeochemical region, with dynamic physical circulation that introduces other mechanisms for method disagreement.

We suggest four mechanisms that could cause methodological differences. First, phytoplankton can excrete some of the ^{15}N label as dissolved organic nitrogen (DON; Bronk and Ward 2000), causing ^{15}N-new to be underestimated because we did not measure DO^{15}N at the end of the incubation. Giesbrecht et al. (2012) suggest that offshore stations might have increased DON release due to suboptimal growth and point specifically to iron stress. It is possible the DON could be recycled and could stimulate more growth but did not appear to be important. With ^{15}N-new consistently lower than O_2/Ar-NCP (Figure 3.2), except for a few outliers, it might be possible that DON release

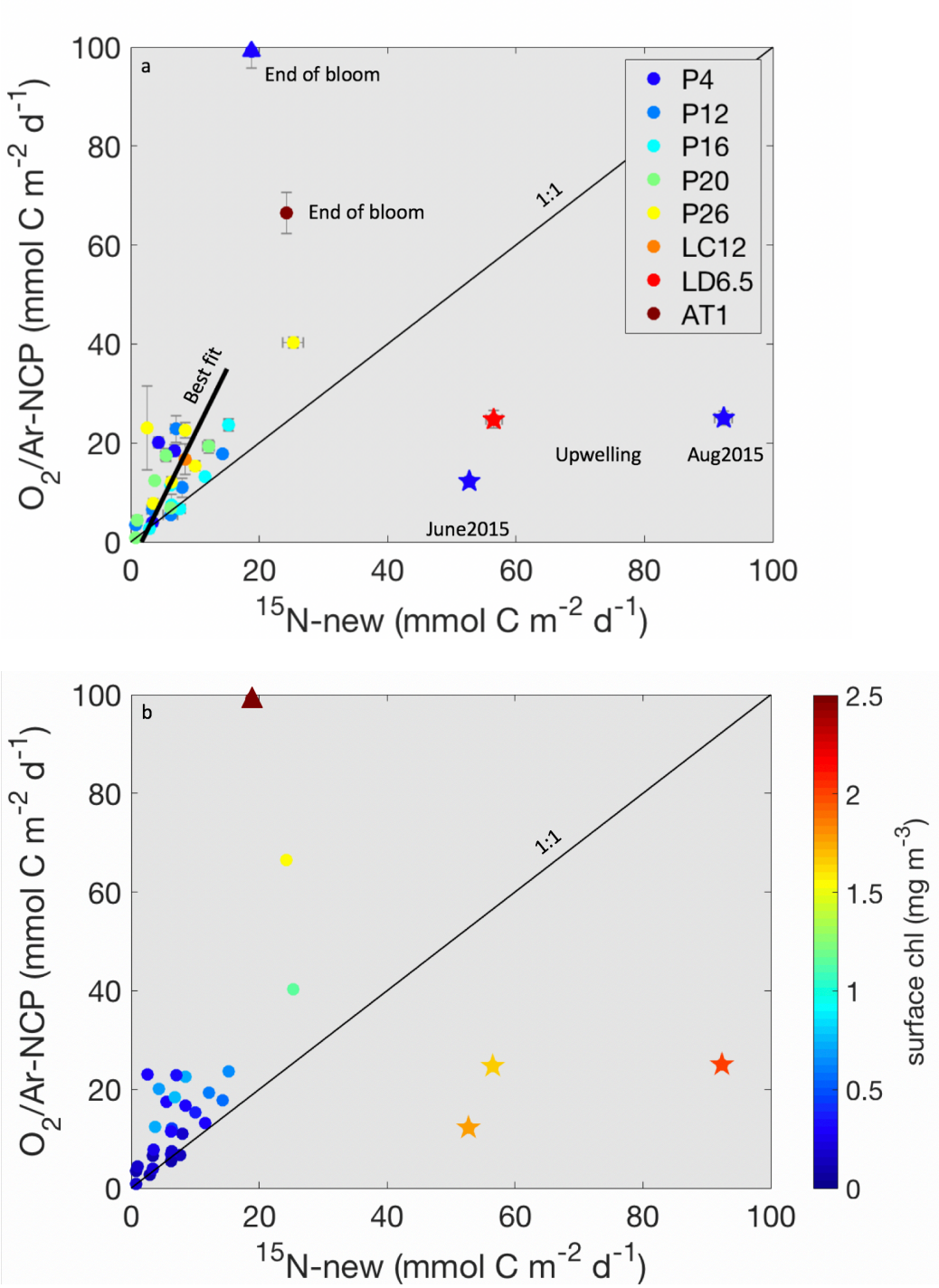

Figure 3.2 (a) All 2014-2017 O_2/Ar-NCP vs. ^{15}N-new data, where color indicates station number. Both rates are integrated to the base of the mixed layer. Thick line is the linear best fit of the data, and the thin line is the 1:1. P4 from August 2016 is indicated by a triangle. Stations likely influenced by recent upwelling are indicated by stars. (b) O_2/Ar-NCP versus ^{15}N-new where the color indicates surface chlorophyll a concentration.

is not limited to offshore stations. Dissolved organic matter excretion does not affect the O_2/Ar-NCP method, because all O_2/Ar exists in the dissolved pool where we measure it. This excretion mechanism potentially dominates most of the low rates and would explain why O_2/Ar-NCP is higher than ^{15}N-new except when upwelling affects the station. Second, upwelling will bias the O_2/Ar-NCP mass balance approach too low (stars in Figure 3.2). Typically, this method assumes that the only source of oxygen to the mixed layer is net biological production and the only sink is air-sea gas exchange. Upwelling brings low oxygen water into the mixed layer, violating this assumption. Some methods exist to correct the O_2/Ar-NCP method for vertical exchange (Cassar et al., 2014; Izett et al., 2018; Haskell et al., 2016), but without those corrections, our O_2/Ar-NCP will be underestimated during upwelling (Teeter et al., 2018). O_2/Ar-NCP can be so biased that it actually appears to be negative (Ianson et al., 2009; Tortell et al., 2012; Izett et al., 2018). For the three samples where ^{15}N-new is greater than O_2/Ar-NCP (stars in Figure 3.2a), the upwelling index reached a maximum one to two days before sampling, suggesting that these stations were particularly influenced by recent upwelling. The La Perouse station (LD6.5) was on the shelf and had a positive upwelling index for 14 days prior to sampling. P4 is further off the shelf and upwelled water likely would have been at the surface longer before reaching P4. The upwelling index was positive (upwelling favorable) for 35 days and 11 days before P4 sampling during June 2015 and August 2015 cruises, respectively. Third, discrepancies can be caused by each method's time of integration. ^{15}N-new measures productivity over 24 hours (the incubation time itself) while O_2/Ar-NCP is influenced by past productivity rates over the last two weeks or so. This time issue could also affect the upwelling regions because upwelling brings nutrients

to the surface causing a phytoplankton bloom. At the start of a bloom, ^{15}N-new would only capture higher productivity rates, while O_2/Ar-NCP would include the lower production before the bloom. This mechanism could be applicable to the stars in Figure 3.2. Alternatively, at the end of the bloom, ^{15}N-new would be lower than O_2/Ar-NCP because of the shorter integration time for ^{15}N-new. This end of bloom scenario may be applicable to both AT01 in May 2016 and P4 in August 2016 where ^{15}N-new < O_2/Ar-NCP, chlorophyll was elevated, but nitrate concentrations were low. P4 during August 2016 is a particularly interesting case, which we discuss further in section 3.4.5. Fourth, bottle effects can bias incubation methods. Fixing the light field in the incubations is not representative of what cells experience in the natural light field within the mixed layer (i.e. changing light as the cell moves). During this study, volumetric rates from the multiple ^{15}N-new light levels within the mixed layer were sometimes similar but generally showed decreased production at the surface compared to deeper in the mixed layer. Thus, bottle effects could have variable impact depending on in situ conditions.

Other methodological biases can occur for ^{15}N-new but do not appear to affect our study. ^{15}N-new could overestimate rates because GF/F filters can retain about 40% the bacterial biomass (Kirchman et al. 1989). Kirchman and Wheeler (1998) found that heterotrophic bacteria take up on average 32% of the total nitrate at P26 and another station closer to the center of the Alaska Gyre, but such an uptake in our study would have biased ^{15}N-new rates high. Varela and Harrison (1999) hypothesize that phytoplankton specific growth rates are likely higher than bacterial rates along Line P, so bacterial uptake is unlikely to be a significant mechanism for method disagreement here. Nitrification is a microbially mediated process that oxidizes ammonium to nitrate and

will cause ^{15}N-new to be overestimated as nitrification elevates the general uptake of nitrate relative to that from actually new nitrate sources (Johnson et al., 2006). Grundle et al. (2013) suggest that, when the mixed layer depth is shallower than the euphotic zone depth on Line P, nitrate accumulation from nitrification occurs below the mixed layer, so our mixed layer incubations are unlikely to be strongly affected.

3.4.2 Gross primary production

The two methods that quantify gross primary production ($^{17}\Delta$-GOP and ^{18}O-GOP) yielded similar rates (Figure 3.3). Neither method was biased consistently high or low

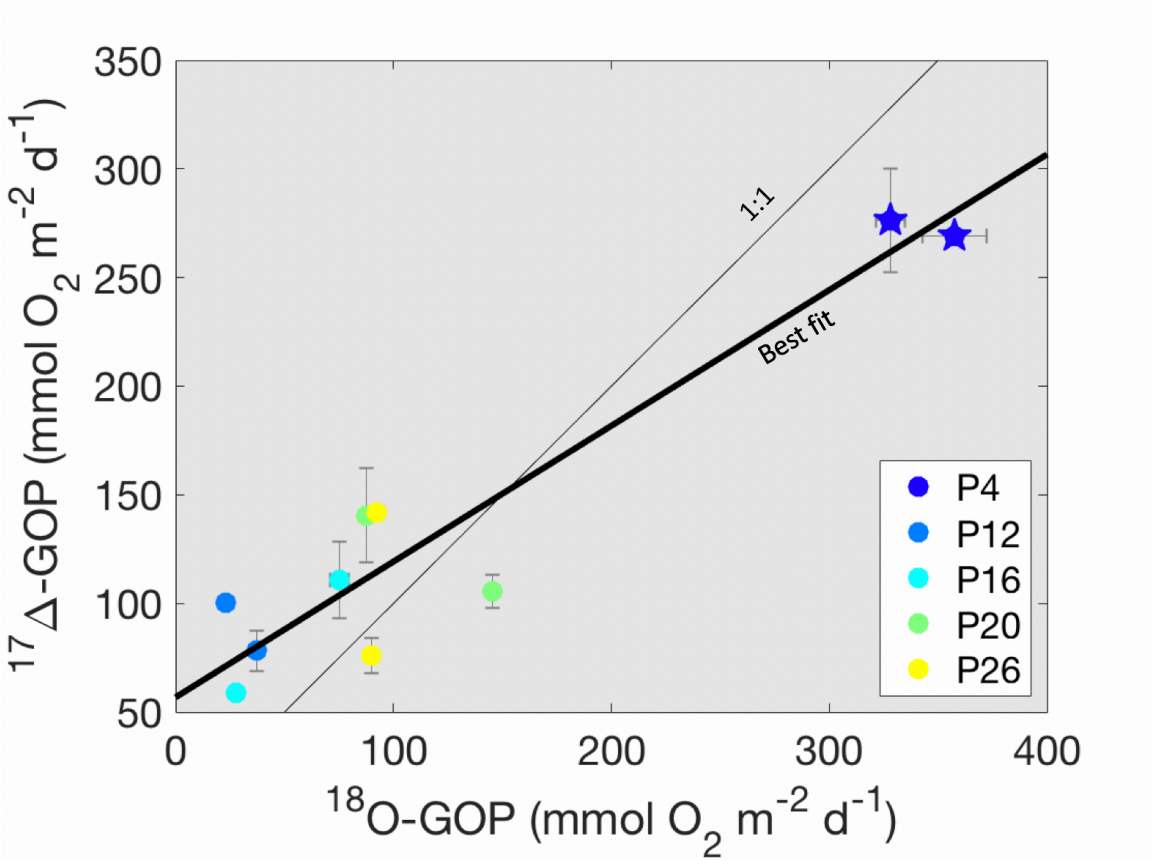

Figure 3.3 ^{18}O-GOP vs. $^{17}\Delta$-GOP, where color indicate station. Thick line is the linear best fit through all data, and the thin line is the 1:1. Stations likely influenced by recent upwelling are indicated by stars.

compared to the other, with a best-fit correlation of $^{17}\Delta$-GOP =0.62* ^{18}O-GOP$_{ML}$ + 56.8 when both are in units of oxygen (R^2 = 0.90). For this study, the $^{17}\Delta$-GOP to ^{18}O-GOP$_{ML}$ ratio is 1.63±1.09. Excluding P4, ^{18}O-GOP$_{ML}$ and $^{17}\Delta$-GOP had an average of 76.3±46 mmol O_2 m^{-2} d^{-1} and 101±30 mmol O_2 m^{-2} d^{-1}, respectively, showing gross production offshore is actually quite variable, similar to the conclusions in Chapter 4. Over the four spring/summer cruises, the standard deviation can vary by up to 50% offshore.

The comparison between GOP methods in this study is similar to those in other locations in the Pacific Ocean. At Hawaii Ocean Time-series (HOT), the $^{17}\Delta$-GOP to ^{18}O-GOP$_{ML}$ ratio has been measured at 1.9±0.9 in 2002-2003 (Juranek and Quay 2005) and at 1.2±0.7 in 2006 and 2008 (Quay et al. 2010). Off the coast of Japan, a lower ratio was observed (1.0±0.2; Sarama et al. 2005). Our study fits in the middle of these estimates. However, despite a mean $^{17}\Delta$-GOP to ^{18}O-GOP$_{ML}$ ratio greater than one, we find that neither method is consistently higher or lower than the other (no majority of points on either side of the 1:1 line). In contrast, at the Hawaii Ocean Time-series, $^{17}\Delta$-GOP was consistently higher than ^{18}O-GOP by 25-60% in 2006 and 2008 (Quay et al. 2010), and in 3 out of 4 sampling periods in 2002-2003 (Juranek and Quay 2005). Our average value was about half that of Juranek et al. (2012), who found an average $^{17}\Delta$-GOP for the subarctic (not Line P) of 193±16 mmol O_2 m^{-2} d^{-1}, but about twice that of Palevsky et al. (2016) who found an average $^{17}\Delta$-GOP south of Line P in June-August of 58±22 mmol O_2 m^{-2} d^{-1}.

There are several potential reasons for disagreement between in situ and in vitro GOP methods, although these biases must be small because our estimates lie close to the 1:1 line. First, vertical mixing could bias the $^{17}\Delta$-GOP method high or low, depending on the

isotopic composition of the water below the mixed layer. For our study, mixing would always cause $^{17}\Delta$-GOP to be overestimated, because of production occurring below the mixed layer but still within the euphotic zone (Nicholson et al. 2014). When a mixing correction based on the measured isotopic gradient and an eddy diffusivity of 10^{-5} m^2 s^{-1} value from Yang et al. (2018) is applied to our $^{17}\Delta$-GOP estimates (based on Nicholson et al. 2014), we find the maximum corrections of 2.47 mmol O_2 m^{-2} d^{-1} and 7.96 mmol O_2 m^{-2} d^{-1} for June and August 2015, respectively. Second, both these methods are also affected by the different times of integration. The two highest rates (stars in Figure 3.3), were identified in section 3.4.1 as being influenced by upwelling. Both have ^{18}O-GOP > $^{17}\Delta$-GOP, suggesting that upwelling stimulated increased production yielding high rates for the 24-hour ^{18}O-GOP incubations but influencing the longer integration $^{17}\Delta$-GOP method less. Third, Quay et al. (2010) point to bottle effects causing ^{18}O-GOP to be an underestimate. This could be most applicable to the lower rates offshore where $^{17}\Delta$-GOP is greater than ^{18}O-GOP. Bottle effects are likely to be most noticeable where rates are low creating a clear bias, but overwhelmed at higher rates. The strong similarity between the two GOP methods suggests that neither method was strongly biased by any of these mechanisms.

3.4.3 ^{13}C-PP compared to other methods

Consistent relationships between ^{13}C-PP and estimates of carbon export are emerging. There is a very strong linear relationship (R^2=0.91 with outliers denoted with stars removed) between ^{13}C-PP and O_2/Ar-NCP (Figure 3.4a) where the following conversion can be used: O_2/Ar-NCP = 0.62* ^{13}C-PP. The ratio of O_2/Ar-NCP to ^{13}C-PP is 0.69±0.38, higher than Giesbrecht et al. (2012) who observed a slope of 0.52 for a smaller dataset of

observations in the same region. A linear relationship exists between ^{13}C-PP and ^{15}N-new but with a lower R^2 value (0.64; Figure 3.4b), where ^{13}C-PP can be converted to ^{15}N-new using: ^{15}N-new = 0.37*^{13}C-PP. There are three notable outliers where ^{13}C-PP is much higher than O_2/Ar-NCP, but these same points are less of an anomaly when comparing

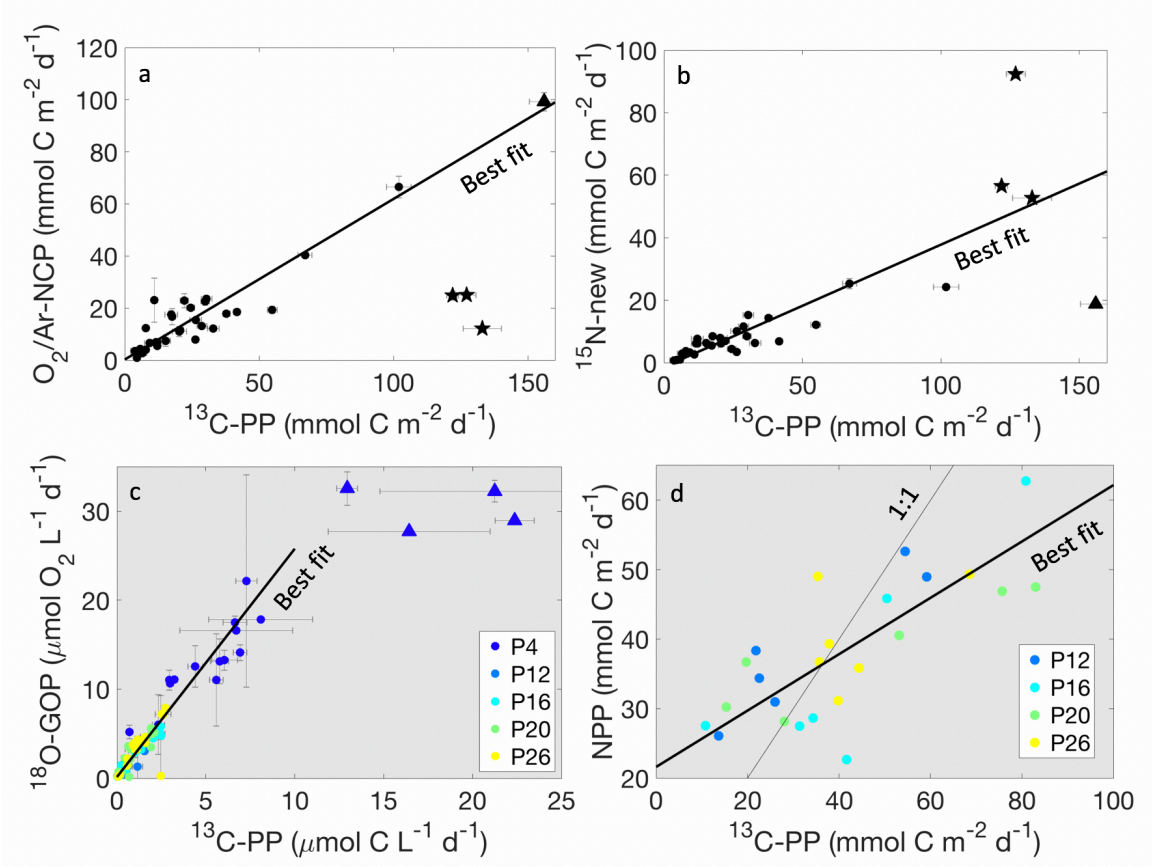

Figure 3.4 Each panel compares ^{13}C-PP to (a) O_2/Ar-NCP, (b) ^{15}N-new (converted to C using the C:N of each individual sample), (c) ^{18}O-GOP, and (d) NPP from the CbPM algorithm. Figure 3.4d only shows offshore data (excludes P4). Only Figure 3.4c is on a volumetric depth by depth basis, while the rest are depth integrated (a and b to the mixed layer depth and d to the euphotic zone depth). Stars in panels a, b represent upwelling influenced locations. Triangles in panels a, b, and c represent P4 from August 2016. Thick black lines in all figures are linear best fit to the data, while the thin line in panel d is the 1:1.

incubations ^{15}N-new vs. ^{13}C-PP (stars in Figure 3.4ab). These three outliers are the same outliers as in the O_2/Ar-NCP to ^{15}N-new comparison (Figure 3.2), where we showed that upwelling likely caused O_2/Ar-NCP to be biased low compared to ^{15}N-new because of a combination of upwelling suppling low oxygen water to the surface, perturbing the mass balance and differences in the integration time scale. We discuss the one point with high ^{13}C-PP but low ^{15}N-new (triangle in Figure 3.4a,b) in Section 3.4.5.

Comparing ^{13}C-PP to ^{18}O-GOP depth by depth on a volumetric basis, instead of integrated over the mixed layer, yields a high correlation with an R^2 of 0.88 (Figure 3.4c). The coastal station (P4) spans a much larger range in both rates than the other stations, and thus defines much of the trend. P4 from August 2016 again stands out as a particular outlier (triangles in Figure 3.4c) and will be discussed in Section 3.4.5 to illustrate a potential way methods can diverge from each other. If it is ignored, the R^2 improves further to 0.91, with a conversion equation of ^{18}O-GOP = 2.56 * ^{13}C-PP – 0.15. The ratio of ^{18}O-GOP to ^{13}C-PP on a depth by depth basis is 3.07±1.36 which is close to the JGOFS value of 2.7 (Hendricks et al. 2005; Marra 2002; Juranek and Quay 2013). Multiple studies have observed that ^{18}O exceeds ^{14}C in the upper euphotic zone but converges toward the same values at lower rates near the base of the euphotic zone (Juranek and Quay 2005; Quay et al., 2010). In contrast, we find in this study that the two methods maintain their relationship at lower rates (Appendix B-3).

Comparisons between ^{13}C-PP and ^{18}O-GOP will be influenced by several factors. The size of the organic pools affects what fraction of production is measured by each method. The dissolved oxygen pool is larger than the particulate organic carbon pool, making recycling / respiration of the labeled oxygen negligible compared with the labeled

particulate carbon (Juranek and Quay, 2005). However, if intracellular recycling of O_2 occurs, GOP would be underestimated (Bender et al., 1987; Juranek and Quay, 2005). A benefit of the ^{18}O-GOP method is that all the labeled ^{18}O that is split accumulates in the dissolved oxygen phase, whereas the ^{13}C and ^{15}N labels accumulate in both dissolved and particulate organic phases. Only the particulate organic phases of ^{13}C and ^{15}N are measured, causing ^{13}C-PP and ^{15}N-new to underestimate primary production and new production, respectively. A caveat of the ^{18}O-GOP method is that not all oxygen production is coupled to carbon fixation, with multiple pathways that produce O_2 but not organic carbon (alternative electron flow), including: the Mehler reaction, photorespiration, and chlororespiration (e.g. Bender et al., 1999). Halsey and Jones (2015) hypothesize that either phytoplankton need more photosynthetic energy to fix carbon or that energy is being lost (e.g. excretion) when the ^{18}O-GOP to ^{13}C-PP ratio is much higher than the average JGOFS ratio of 2.7. These potential biases affect this study at about the same rate as other studies, since our observed ratio is close to previous estimates.

We also compared algorithms for primary production based on satellite remotely sensed data to our discrete water column measurements at offshore stations. The CbPM algorithm for net primary production averaged over 8 days with a spatial resolution of 1/6 degree does not equal our ^{13}C-PP results when integrated to the euphotic zone (Figure 3.4d). Along Line P, the following can be used as a conversion: ^{13}C-PP=2.46*NPP – 53.24, with an R^2 value of 0.58. Using this conversion, ^{13}C-PP can be extrapolated over larger spatial and temporal scales from the satellite derived values. The satellite algorithm uses particulate backscatter and phytoplankton absorption coefficients, tuned to ^{14}C

measurements. Thus, the CbPM algorithm is meant to yield identical results to ^{13}C-PP. Given the consistent difference we find, scope may exist for the development of a regional algorithm that would better reproduce primary production incubation data.

3.4.4 Chlorophyll as a control

Chlorophyll and productivity rates were highly correlated. On a depth by depth comparison, both ^{13}C-PP and ^{18}O-GOP linearly increase with increasing chlorophyll a concentrations with R^2 values of 0.86 and 0.81, respectively (Figure 3.5a,b). The higher

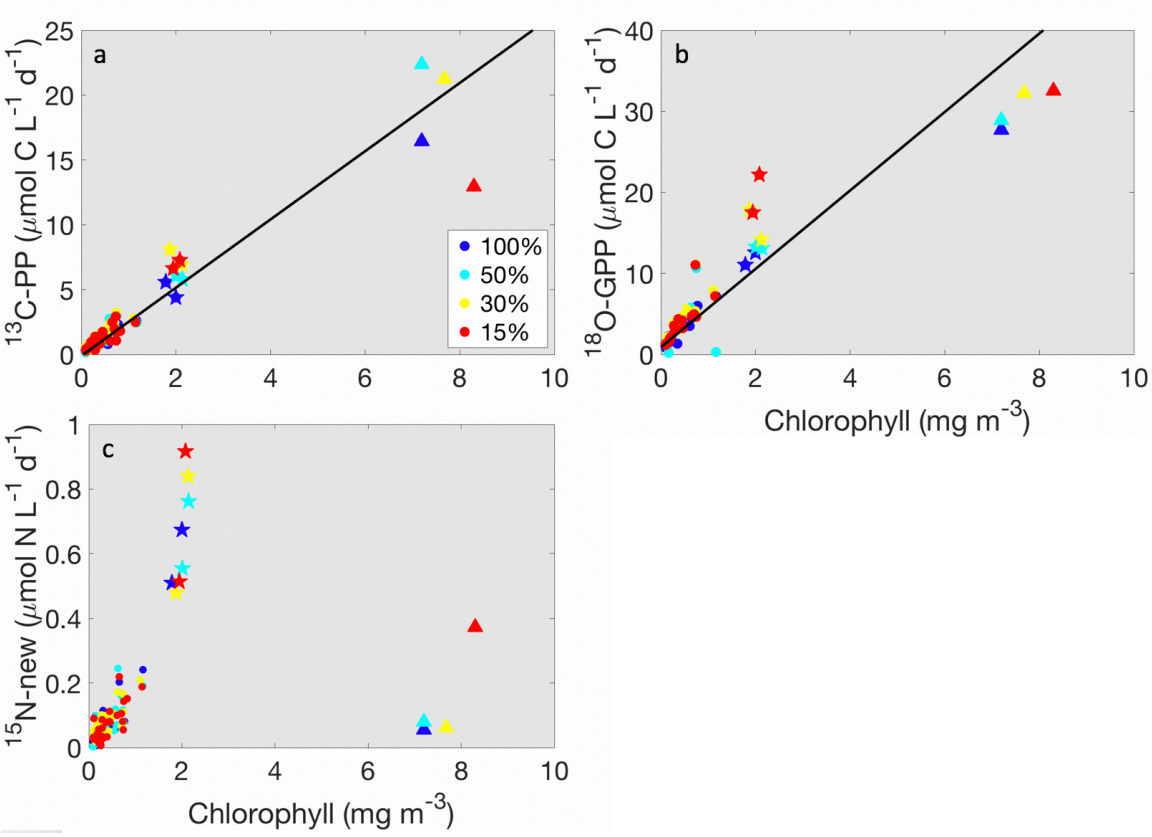

Figure 3.5 Each panel compares chlorophyll a concentration to (a) ^{13}C-PP, (b) ^{18}O-GOP, and (c) ^{15}N-new. All are on a volumetric depth by depth basis (instead of integrated) where colour indicates the light level at the sampling depth. Panels a and b display productivity rates in carbon units, while panel c uses N units. Stars are P4 from June and August 2015 (upwelling influenced stations) and triangles are P4 from August 2016.

productivity rates at station P4 in August 2016 largely define these relationships. ^{15}N-new and chlorophyll a are less closely related (Figure 3.5c). Instead, an apparent exponential relationship exists at high rates, largely driven by P4 in June and August of 2015, stations and times influenced by upwelling (Section 3.4.1). The data from P4 in August 2016 is again an exception to the linear trend (Section 3.4.5). Carbon to chlorophyll ratios can vary by an order of magnitude due to factors such as light and nutrient concentrations (Caron et al., 1995), meaning that just because there is increased chlorophyll there is not necessarily increased phytoplankton biomass. For example, on one La Perouse cruise in coastal B.C, carbon to chlorophyll ratios varied from 45 to 180 (Ianson et al., 2003). However, Burt et al. (2018) show that ratios are less variable (50-80) offshore in the NE subarctic Pacific. Because of this, chlorophyll is a reasonable proxy for phytoplankton biomass and productivity rates in this region, and when there is increased chlorophyll, productivity also increases.

3.4.5 Method Disagreement: August 2016 at P4

As a specific example when methods strongly disagree, we focus on what makes station P4 sampled 19August2016 unique (triangle in Figures 3.2a, 3.4a,b,c). At this station and time, we found very high rates of both O_2/Ar-NCP and ^{13}C-PP with a similar relationship to lower productivity stations, but ^{15}N-new was unusually low and ^{18}O-GOP was marginally low. We theorize that this station was sampled at the end of a phytoplankton bloom as upwelling relaxed, which caused our methods to disagree. There was a long term upwelling index high (>100 m^3 per 100 m of coastline) on 29/30July (19 days before sampling), which would have supplied high nutrients to the mixed layer. The next previous time when the upwelling index was above 100 m^3 per 100 m of coastline

was 7 May. Further south (36°N 122°W), the upwelling index had a maximum at 10 July, so remotely forced mechanisms could also be responsible for suppling higher nutrient water to P4 at this time. The addition of nutrients caused increased production, shown by increased chlorophyll and production rates (O_2/Ar-NCP, ^{13}C-PP, and ^{18}O-GOP). 42% of the phytoplankton were diatoms at P4, also indicating that nutrients were originally supplied by upwelling, and phytoplankton responded. Nitrate concentrations were low (0.04 μmol L^{-1}) indicating that phytoplankton had drawn down nitrate to limiting levels. ^{15}N-new and ammonium uptake were also very low compared to that expected given the high chlorophyll concentration, indicating no recent nitrate input. However, ^{13}C-PP and ^{18}O-GOP versus chlorophyll a do not stand out as outliers. That ^{13}C-PP and ^{18}O-GOP remained high implies that another nitrogen source, other than nitrate and ammonium, was fueling production. It is also a possibility that there was a decoupling of carbon fixation and nitrogen assimilation if nitrogen sources were exhausted. Alternatives include nitrite, urea, DON, and amino acids (Capone et al. 2008). Based on previous work, urea can support an average of 24% of production in this region (Varela and Harrison 1999), but it is unclear how important other nitrogen sources are. O_2/Ar-NCP was much higher than ^{15}N-new, again supporting the end of bloom hypothesis. At the end of a bloom, productivity rates would be sharply declining. Because of the different time of integration, ^{15}N-new would reflect recent lower rates compared to the longer integration time of O_2/Ar-NCP. Upwelled water makes O_2/Ar-NCP an underestimate; however, Teeter et al. (2018) show that the low oxygen water bias is quickly erased by high production on a similar timescale to the warming of cold upwelled water. So, we would not expect O_2/Ar-NCP to still be biased low at the end of an upwelling driven

bloom. The surface water temperature was within the typical summer range at 13.02°C for this location/time compared to typical upwelled water temperatures around 9°C (Asher et al., 2017), suggesting that upwelled water had been at the surface long enough to warm up and erase the O_2/Ar-NCP bias. The ^{13}C-PP versus O_2/Ar-NCP comparison was similar to most other stations and did not group with the upwelling influenced stations, again implying that upwelling no longer biased O_2/Ar-NCP.

Lastly, ^{18}O-GOP was somewhat lower than expected compared to ^{13}C-PP (points fall below the best fit line in Figure 3.4c). Perhaps there was less decoupling of water splitting and carbon fixation to cause ^{18}O-GOP to be lower than expected. At the end of a bloom, the phytoplankton community were likely dominated by diatoms. This is supported by Peña et al. (2018) where the nearby station of P5 had a diatom relative abundance of nearly 100%. Perhaps diatoms have different photosynthetic alternative electron flow than other phytoplankton species. It is possible, because of iron stress, alternative electron pathways are utilized. Only larger phytoplankton (like diatoms) are iron stressed, so they may be particularly affected. There is some evidence this is possible because the energy allocation for cyanobacteria and nitrogen fixers make up 4% and 75% of the gross photosynthetic energy (collated in annual review by Halsey and Jones, 2015).

3.5 Conclusion

Consistent differences between productivity methods are emerging in the NE subarctic Pacific. In the carbon export comparison, O_2/Ar-NCP (the in situ method) tends to be higher than ^{15}N-new (the in vitro method), likely from dissolved organic nitrogen excretion but perhaps also bottle effects. Time of integration and upwelling are major factors that causes method comparisons to disagree at specific locations and times.

Surprisingly, the two GOP methods agree well, so perhaps method biases do not strongly affect these two methods in this region. Satellite NPP (from the CbPM algorithm) is consistently different from ^{13}C-PP (integrated to the bottom of the euphotic zone). This implies that the algorithm may be able to be improved to better capture spatial and temporal PP rates in the offshore NE subarctic Pacific. We also find a high correlation between chlorophyll concentrations and many production methods. One main implication is that chlorophyll makes a good proxy for productivity rates, particular because it is easy to measure. Other factors can affect chlorophyll relationships such as varying carbon to chlorophyll ratios. However, our data here and in Chapter 4 shows that high chlorophyll corresponds to higher production rates in this region rather than changes in the carbon to chlorophyll ratio. This strong relationship between biomass and productivity rates implies that primary productivity in this biogeochemical region is mainly controlled by "bottom-up" factors such as trace metal availability rather than grazing pressure in June.

3.6 Acknowledgements

Thank you to Paul Quay, Johnny Stutsman and Mark Haught for their help with triple oxygen isotope sample analysis. CCMP Version-2.0 vector wind analyses are produced by Remote Sensing Systems. Data are available at www.remss.com. Estimates of NPP from the CbPM algorithm were downloaded from Oregon State University's Ocean Productivity website.

Chapter 4. Fronts potentially drive variability in phytoplankton productivity in the HNLC subarctic northeast Pacific

Key points

1. Challenging historical thought, HNLC chlorophyll a concentrations show mesoscale patchiness
2. Higher surface chlorophyll a is representative of increased productivity and carbon export rates
3. Higher surface chlorophyll a tends to occur in colder and saltier water, implying transport of water from below
4. Fronts as offshore iron input mechanisms can explain much of the chlorophyll a variability

4.1 Abstract

The canonical view of productivity in the iron-limited subarctic northeast Pacific is that it is low and constant throughout the spring and summer. Iron fertilization events that induce widespread blooms have been documented, standing in contrast to this steady picture, but are thought to be rare events. Here we show that offshore productivity in this region is quite variable on mesoscales (50–100 km). Because the main limitation in this area is iron supply, such productivity variability must be driven by small iron inputs. We hypothesize fronts as a mechanism for introducing iron into surface waters, causing higher chlorophyll *a* concentrations. In this region, we demonstrate that higher chlorophyll *a* indicates enhanced productivity, as shown by comparisons with estimates of marine productivity rates by several methods. We also show that higher chlorophyll *a* is associated with saltier and cooler surface water, which must come from below. Our study period spanned three years but we focus on June 2015 and 2016 where fronts, defined as 1°C change in temperature over a 1/3 degree distance, and cohesive mesoscale

features were present. Fronts in HNLC areas in the subarctic northeast Pacific need to be considered as a mechanism for iron supply in future studies.

4.2 Introduction

Marine production is important to the global carbon budget. Phytoplankton form the base of the oceanic food web and contribute about half of global primary production (Field et al., 1998). The biological pump exports organic carbon from the surface ocean via sinking particles, mixing of dissolved organic matter, and active transport by higher trophic levels (Emerson, 2014; Boyd et al., 2019; De La Rocha and Passow, 2007), where particle transport is the largest flux (Emerson, 2014). The deep ocean is a sink for carbon because carbon at depth is out of contact with the atmosphere for long time scales, hundreds of years at intermediate depths to hundreds of millions of years if makes it to the seafloor (Falkowski et al., 2003).

Spatial and temporal variability in offshore marine production has ramifications on local and global scales. Spatial variability in production ultimately affects the availability of food for higher trophic levels. For example, when prey is abundant, chinook salmon grow quicker and have better survival rates (Hertz et al., 2016). Failing to incorporate variability in regional estimates can create drastic uncertainty for the carbon cycle. One extreme example is the North Atlantic, a location with large pCO_2 fluctuations (up to ~30 μatm) on a spatial scale, compared to the situation on a global scale where an error of 1 μatm would result in a ~0.2 Gt C yr^{-1} error in carbon sink estimates (Watson et al., 1991). This highlights the importance during field campaign planning of defining what temporal and spatial scales should be used to take variability into account. Even in areas where

production is not as extreme, such as in High Nutrient Low Chlorophyll (HNLC) areas, effort should be taken to ensure regional estimates of production incorporate spatial and temporal variability to accurately represent the area.

Our study focuses on the HNLC subarctic northeast Pacific, which has three major currents. The North Pacific current flows west to east, splitting at the coast to form the California Current to the south and the Alaska Current (and the Alaska Gyre) to the north. The North Pacific Current can shift north and south over a total range of 15 degrees of latitude (Sydeman et al., 2011). On smaller spatial (a couple of degrees of latitude) and temporal (months) scales, the current will meander (Pelland et al., 2016; Pelland et al., 2018).

Line P is a unique repeat time series in the subarctic NE Pacific region. Line P extends 1500 km from Southern Vancouver Island into the Alaska Gyre and consists of five major stations (P4, P12, P16, P20, P26) and 22 minor stations (Figure 4.1). The station furthest west is P26 (also called Station P, Station Papa, or OSP) where hydrographic casts began in 1956 (Freeland, 2007).

Phytoplankton respond to the iron gradient along Line P. Iron is replete in coastal waters and becomes limiting offshore, creating a HNLC region within the gyre. In response to iron concentrations, there is also a gradient in phytoplankton iron stress, based on flavodoxin, a biochemical marker for iron stress (La Roche et al., 1996). Offshore P20 and P26 are iron limited year-round, while transition stations P12 and P16 can be controlled by either macronutrients or iron (Boyd et al., 1999). Transition stations have high macronutrients in the spring but experience nitrate depletion in the summer (Whitney et al., 1998). The onshore station (P4) is influenced by upwelling, one source of

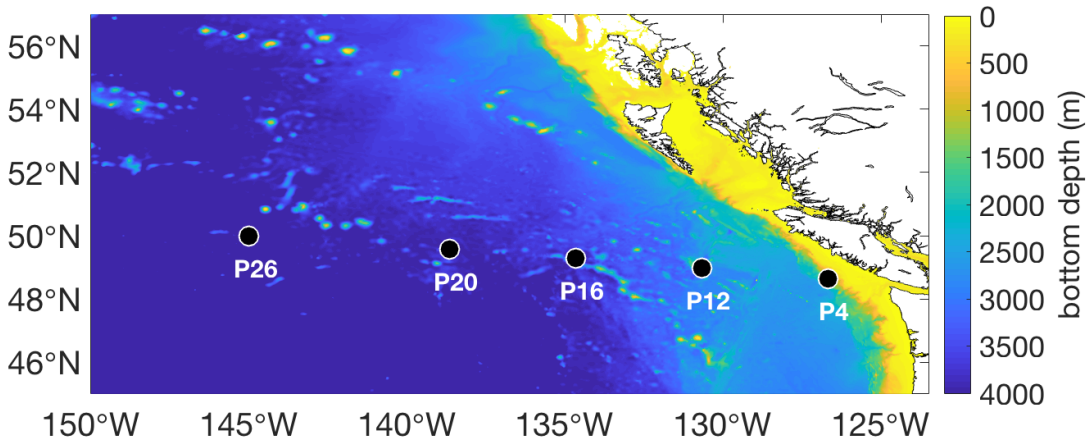

Figure 4.1 Map of subarctic northeast Pacific with bathymetry in color. Major stations along Line P P4, P12, P16, P20 and P26 are indicated by black dots. P4 is included in the map as a reference but is not the focus of this chapter. Bathymetry data came from NOAA's National Centers for Environmental Information (Amante and Eakins, 2009).

iron, in the spring and summer. The focus of this paper is on the HNLC region offshore, away from coastal upwelling influenced stations such as P4. See Chapter 3 for more information on spring and summer dynamics at P4 and how they affect productivity method comparisons.

Regional seasonal forcing affects the phytoplankton environment. In the winter, an Aleutian low is situated in the Alaska Gulf causing higher winds offshore, which together with cooling water in the fall and winter create deeper mixed layers (Harrison et al., 1999). However, mixed layers are still shallow compared to other regions at these latitudes because of the strong permanent pycnocline at 80-100 m driven by large salinity changes (Denman and Gargett, 1988; Bishop et al., 1999). Offshore storms in conjunction with deeper mixed layers in winter bring nutrients to the surface. Because of the low iron concentration and its limiting effect on phytoplankton production, the concentration of macronutrients remains high offshore during spring. During the summer, macronutrients

could be drawn down further offshore (transition stations) compared to spring. Chlorophyll a (chlorophyll) remains low at the offshore stations (~ 0.5 mg m^{-3}) with very little seasonality (Peña and Varela 2007). Many studies show low chlorophyll concentrations with low temporal variability in the area. Phytoplankton offshore are primarily small cells (Harrison et al., 1999), with flagellates making up 92 ± 2% of the total phytoplankton (Varela and Harrison, 1999).

Our goals in this paper are to identify the variability and structure in surface chlorophyll in the subarctic northeast Pacific and to understand what mechanisms could explain the patterns observed. We propose that fronts in the HNLC area can cause small scale iron inputs, driving chlorophyll variability in the area and corresponding primary production and carbon export. This study focuses on 2014-2017, but the implications extend to the past and future.

4.3 Methods

4.3.1 Satellite and model

For satellite chlorophyll, we used a merged gridded product based on SeaWiFS, MODIS, MERIS, OLCI-A, and VIIRS from GlobColour (Maritorena et al., 2010; Fanton d'Andon et al., 2009). The data is a weighted average based on sensor and product characterization (O'Reilly et al., 2000). To increase satellite spatial coverage (sometimes poor due to clouds), the following 8-day average periods were used focused on our field campaigns: 18-25 June 2015 and 9-16 June 2016.

Satellite chlorophyll and shipboard chlorophyll data were compared for June 2015 and June 2016 to validate the satellite data (Figure C1). All Line P stations west of 127°W (June 2015) or 126°W (June 2016) were included to increase the number of data points but to exclude coastal influences. The closest geographic satellite chlorophyll

concentration was compared to the shipboard chlorophyll concentrations. No comparison was made when there was no satellite data due to clouds. Overall, the satellite is neither biased high nor low compared to rosette data (Figure C1c).

Sea surface height anomalies (SSHa) used in this study are gridded data (interim version 1609) from the NASA Jet Propulsion Laboratory (Zlotnicki et al., 2016). The data product includes data from multiple satellites with a resolution of $1/6^{th}$ degree every five days. SSHa were averaged over each month to remove noise and to distinguish features.

Output from the Mercator model was used for sea surface temperature and geostrophic currents. Mercator is an assimilative reanalysis model that incorporates atmospheric forcing, satellite data, and in situ measurements with daily global coverage at a 0.083 x 0.083 degree resolution. All data was downloaded from the Copernicus website (https://www.mercator-ocean.fr). The model is a good estimate of sea surface temperature with R^2 of 0.97 and 0.96 for June 2015 and 2016, respectively (see Figure C2). To compare satellite chlorophyll and Mercator sea surface temperature, a polygon was used to isolate offshore data. For the June 2015 comparison, the following vertices were used for the polygon: 45°N 150°W, 55°N 150°W, 55°N 137°W, 45°N 127°W. The high chlorophyll coastal waters extended further in June 2016 so the third point of the polygon was modified to 55°N 140°W to remove coastal influences from the comparison. Fronts were identified as having a 1°C change in temperature over 1/3 degree distance, a definition which highlights features on the 50-100 km scale.

Three products were used to estimate aerosol concentration including dust or ash. The first is the aerosol index (AI) from the Ozone Measuring Instrument (OMI) that

specifically measures UV-absorbing aerosols (Pawan, 2012). OMI AI has a 1° resolution and daily AI were averaged over the month of June for 2015, 2016, and 2017. The second is aerosol optical depth (AOD) from MODIS Aqua at 550 nm with a resolution of 1° (Platnick et al., 2015). MODIS AOD also includes sea salt (Levy et al., 2013). Daily AOD was averaged over June for 2015, 2016, and 2017. Data for AI and AOD were downloaded from the Goddard Earth Sciences Data and Information Services Center through the Giovanni website (Acker and Leptoukh, 2007). The third method is the Japanese Reanalysis for Aerosol atlas (JRAreo V1.0) created by the Meteorological Research Institute of the Japan Meteorological Agency and the Research Institute for Applied Mechanics at Kyushu University. JRAero V1.0 was accessed from https://www.riam.kyushu-u.ac.jp/taikai/JRAero/atlas.html (Yumimoto et al., 2017). Daily, global aerosol optical thickness and dust deposition (dry and wet) from this product have a spatial resolution of 1.1°.

4.3.2 Shipboard data collection and sampling

Line P cruises occur three times a year (normally February, June and August). Our study focused only on spring and summer cruises from August 2014 through June 2017, though we also show some August 2017 chlorophyll data. At each station, all shipboard samples came from the same cast. P12-P26 sampling occurred 11-17 June 2015 and 9-14 June 2016. Although P4 was sampled as well, it is not included in this chapter. Chapter 3 more extensively details the productivity rate estimates, including P4.

4.3.2.1 Productivity rates

Water samples for incubations were collected at five light levels (100, 50, 30, 15, and 1% of surface irradiance) and were incubated (in on deck incubator) for 24 hours starting

around dawn. All incubations are integrated to the mixed layer depth. Carbon uptake (^{13}C-PP) was measured as an estimate of primary production, a rate that likely falls between net primary production and gross primary production, while nitrate uptake (^{15}N-new) was measured as an estimate of new production (Dugdale and Goering, 1967; Slawyk et al., 1977). Samples (1200 mL bottles) were spiked with ^{13}C labelled bicarbonate to 10% of the climatological dissolved inorganic carbon and with ^{15}N labelled nitrate to at least detection limits. At the end of the incubation, water was filtered onto muffled GF/F filters, which were analyzed for atom % ^{13}C, atom %^{15}N, particulate carbon and particulate nitrogen by the University of California Davis Stable Isotope Laboratory using an element analyzer and isotope ratio mass spectrometer. For more information on those methods see https://stableisotopefacility.ucdavis.edu/13cand15n.html. Dissolved inorganic carbon samples were collected at the same station but not from the same cast. Splitting of ^{18}O labeled water (^{18}O-GPP) was measured as an estimate of gross oxygen production (Bender et al., 1987; Juranek and Quay, 2005). Samples were spiked with 400 µL of ^{18}O labeled water in an ~140 mL glass bottle with ground glass stopper. At the end of the incubation, samples were siphoned into pre-evacuated, $HgCl_2$ poisoned flasks and analyzed for the $\delta^{18}O$ of the dissolved O_2 gas on a Thermo MAT 253 isotope ratio mass spectrometer at the University of Victoria.

Net community production was estimated from a mass balance of O_2/Ar in the mixed layer (O_2/Ar-NCP; Craig and Hayward 1987; Emerson et al., 1999). Samples were collected in duplicate from two depths within the mixed layer into pre-evacuated $HgCl_2$ poisoned flasks and analyzed for O_2/Ar ratios on the University of Victoria Thermo MAT

253. Outgassing of biological oxygen to the atmosphere was calculated using the Ho et al. (2006) gas transfer velocity parameterization from the Cross-Calibrated Multi-Platform (CCMPv2) wind dataset and weighted according to Reuer et al. (2007) as modified by Teeter et al. (2018). NCP is a weighted average of this air-sea flux, when vertical mixing fluxes are negligible. A PQ of 1.4 and 1.25 O_2/C was used to convert the O_2/Ar and ^{18}O based estimates to rates in carbon units, respectively.

4.3.2.2 Ancillary data

Nutrient samples were collected in plastic tubes and frozen (-20°C) in aluminum blocks. Samples were thawed just prior to analysis on an Astoria analyzer (Barwell-Clarke and Whitney 1996). Nitrate + nitrite was measured; however, since nitrite typically only comprises about 1-3% of the sum, we consider the sum to be equivalent to nitrate (following Varela and Harrison 1999). Nutrient drawdown was calculated by taking the surface nutrient data from the February Line P cruise minus the concentration measured during the June cruise to calculate seasonal nutrient drawdown. This assumes February nutrient concentrations are the highest during the year and that there are no further inputs over the course of the spring season.

Chlorophyll samples were collected from the rosette within the top 8 m. No underway samples (loop) were included in our analysis. 304 mL were filtered onto 25 mm GF/F filters and stored in glass scintillation vials at -80°C. Samples were extracted with 90% acetone at -20°C for 24 hours and analyzed on a Turner 10AU fluorometer with Sigma standards following the method described by Holm-Hansen et al. (1965).

Samples were collected for phytoplankton counts at 5 m during the June 2016 cruise at the major stations (P12, P16, P20, and P26) and were preserved with Lugol. Settling

columns (25 mL) were used, and 1 to 30 fields were counted for each sample using 40x magnification. Species were grouped by diatoms, dinoflagellates, flagellates, and others. Others includes unidentified Choanoflagellates, Telonema, and unidentified ciliates. Relative abundance was calculated using these four groups.

Zooplankton biomass was collected using a vertical bongo net with a 236 μm mesh size to a depth of 250 m. Zooplankton biomass anomalies were calculated using the average zooplankton biomass from 2000-2018. Note that many of the microzooplankton are not captured by such a net size, so the biomass estimates only larger zooplankton that are not necessarily grazing on phytoplankton but could be preying on smaller zooplankton.

4.4 Results and discussion

In our study, June 2015 and June 2016 had higher chlorophyll *a* (referred to as chlorophyll) in the HNLC region in cohesive features, so we focus our interpretation strongly on those cruises. We use these data to examine the prevalence of offshore chlorophyll variations and to demonstrate our hypothesis that fronts could cause this phytoplankton variability.

4.4.1 Higher chlorophyll is common offshore

The canonical view at P26 is that chlorophyll is low with low temporal variability (Parslow, 1981; Welschmeyer et al., 1993; Peña and Varela, 2007; Boyd and Harrison, 1999; Harrison et al., 1999); however, there is actually more variability than this view suggests. The offshore region may appear to be near constant in comparison to P4 or more coastal stations; however, significant variation still exists offshore. Wong et al. (1995) state an average chlorophyll of 0.4 mg m^{-3} for 1964-1991 with little temporal variability, and Banse and English (1999) of only 0.33 mg m^{-3} for 1980-1990. For 1988-

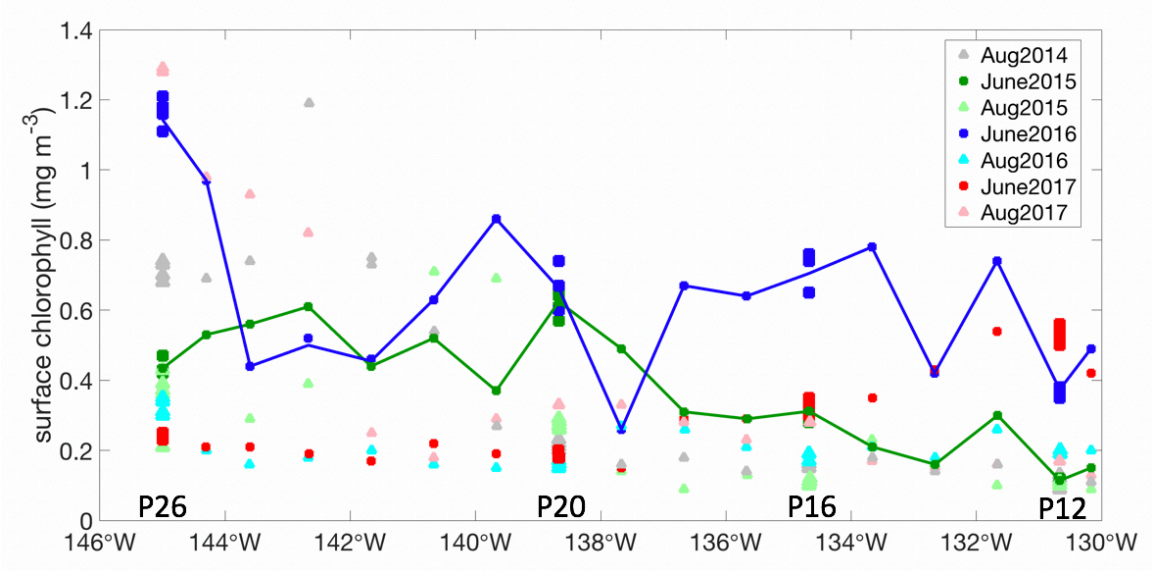

Figure 4.2 Surface chlorophyll (less than 8 m depth) measured on water samples along Line P for August 2014 to August 2017 vs. longitude. Major stations (P26, P20, P16 and P12) have slightly larger symbols and are labeled below. June 2015 and 2016 (green and blue lines, respectively) are explored in more detail in this chapter.

2005, chlorophyll ranged from 0.2 to 0.6 mg m^{-3} and only above 1 mg m^{-3} a handful of times (Peña and Varela 2007). During the Weathership years (1959-1970), where there was more frequent sampling, the majority of chlorophyll observations were 0.3-0.4 mg m^{-3} (Miller et al., 1991). However, the average and standard deviation of surface chlorophyll during the Weathership years was actually 0.43±0.32 mg m^{-3}; chlorophyll is more variable at P26 than what is historically acknowledged.

Compared to historical data, chlorophyll was higher than expected during this study. During the 11-year Weathership period, there were only 8 occasions when chlorophyll was higher than 1 mg m^{-3} (Miller et al., 1991). For this study, chlorophyll above 1 mg m^{-3} was measured three times within a three-year period offshore (Figure 4.2). Harrison et al., (1999) suggest that chlorophyll concentrations exceeding 1 mg m^{-3} likely imply iron

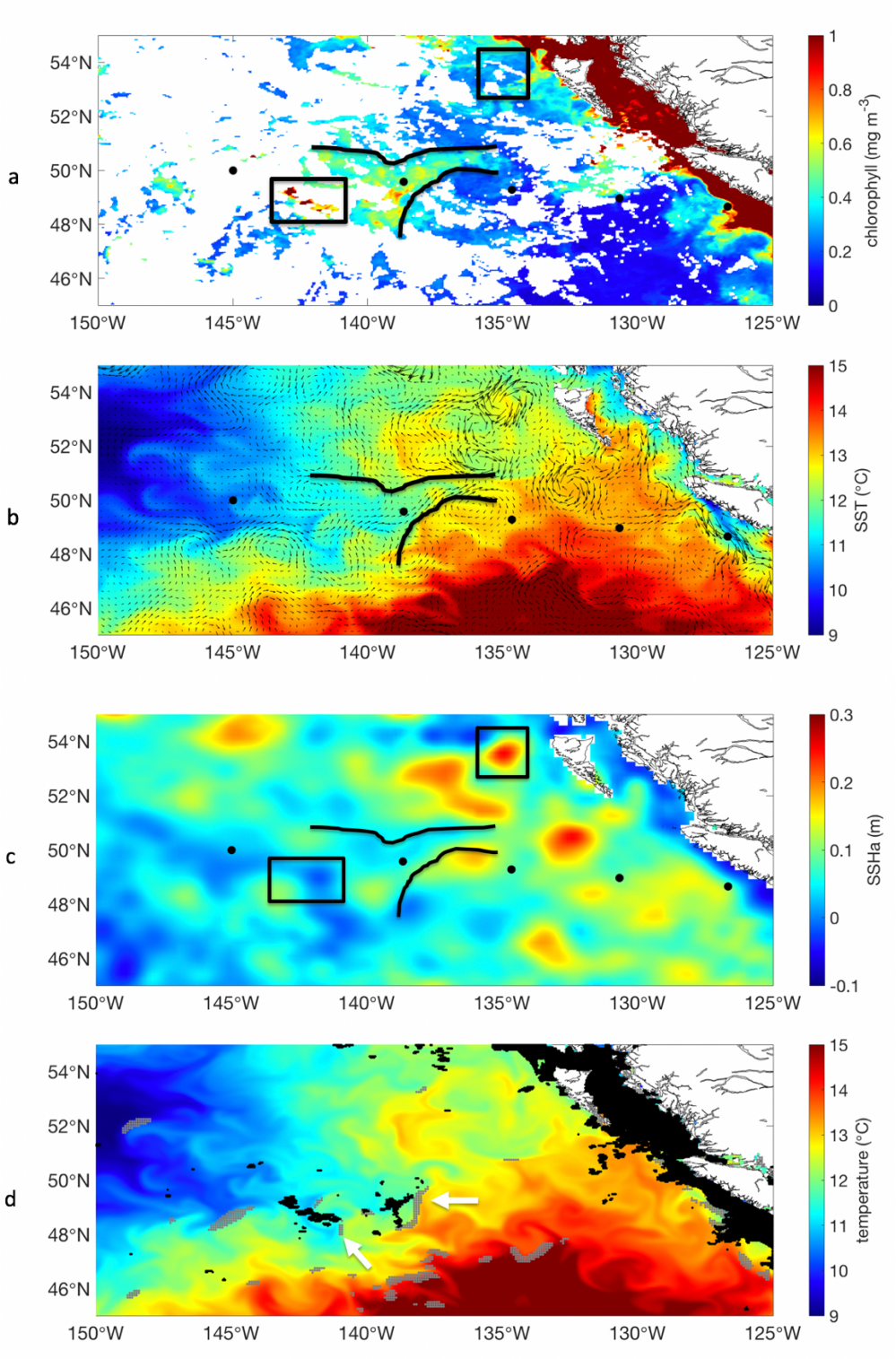

Figure 4.3 Property maps in June 2015. Several features of interest are highlighted by black lines and boxes in the same position on all figures. (a) 8-day average (18-25 June 2015) surface chlorophyll satellite data from GlobColour. (b) Colours show sea surface temperature and vectors

show geostrophic currents, both from the Mercator model. (c) Sea surface height anomalies (SSHa) from the JPL product. (d) Background colours are Mercator sea surface temperature. Black dots indicate surface chlorophyll above 0.6 mg m^{-3}. Grey dots indicate front locations based on a criterion of 1°C temperature change over 1/3 degree distance using Mercator sea surface temperature. White arrows indicate two fronts discussed in the text.

inputs. Although 1 mg m^{-3} is a somewhat arbitrary limit for a value above the average for the area, other papers appear to support this threshold. For example, Hamme et al. (2010) found iron supplied by volcanic ash in August 2008 fueled a bloom with surface chlorophyll between 1 and 2 mg m^{-3}.

We used satellite data to expand spatial coverage of chlorophyll in the subarctic northeast Pacific beyond what the Line P cruises can provide. Although clouds are widespread during the spring and summer season, satellites can still give insight into regional processes. Satellite chlorophyll data (averaged over 8 days) agrees well with the shipboard data (Section 4.3.1 and Figure C1) giving confidence in using it to expand the Line P data. June 2015 (Figure 4.3a) and June 2016 (Figure 4.4a) are of particular interest due to features identified in the satellite chlorophyll data. Chlorophyll was variable throughout the region and between these two periods.

During June 2015 there was a well-defined mesoscale tongue of higher chlorophyll water (outlined in black in Figure 4.3a), with areas above 0.8 mg m^{-3}. In this same region, station P20 had higher chlorophyll concentrations compared to the other stations (Figure 4.2). Satellite data also shows higher chlorophyll concentrations west of the tongue of water (black box in Figure 4.3a), where concentrations were above 1 mg m^{-3}; however, this region was not sampled along Line P.

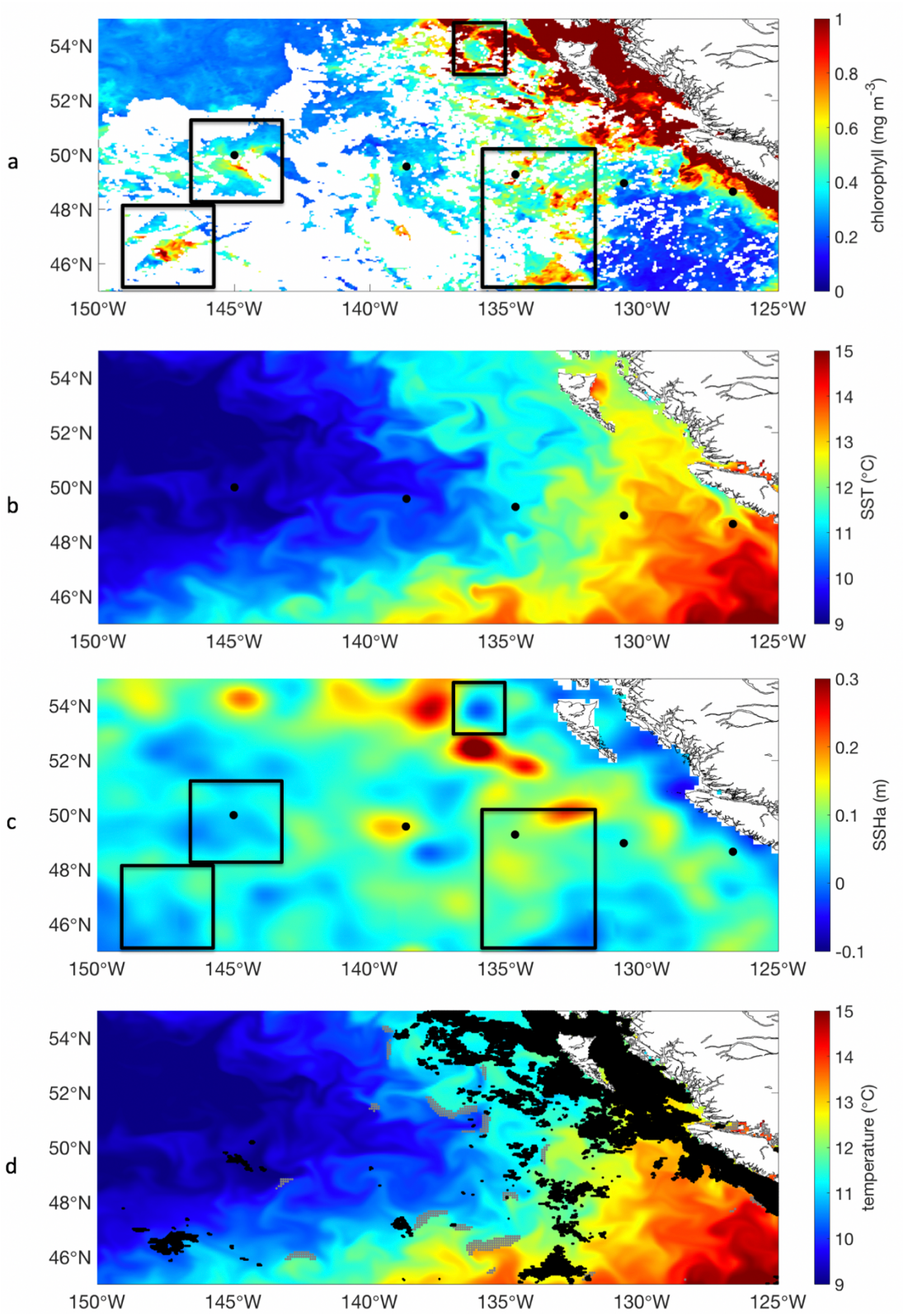

Figure 4.4 Same as Figure 4.3 except for June 2016. The 8-day average for surface chlorophyll satellite data is from 9-16 June 2016.

June 2016 had smaller productive areas but had higher overall chlorophyll in the region compared to June 2015 (Figure 4.4a). In the shipboard data, P26 had the highest chlorophyll concentrations, which decreased abruptly around 144°W and then steadily increased to around 0.7 mg m^{-3} until P12 where concentrations dropped back to historical values (Figure 4.2). The three offshore stations (P16, P20, P26) happened to sample high chlorophyll locations. The high chlorophyll in June 2016 is patchy with three main areas with higher chlorophyll (three southern black boxes in Figure 4.4a). These three areas had chlorophyll concentrations greater than 0.9 mg m^{-3} and the area furthest southwest had concentrations above 1 mg m^{-3}.

4.4.2 Higher chlorophyll is associated with higher productivity

Variations in satellite chlorophyll in our study region also correspond closely to variations in biomass and productivity rates, though this is not the case in other regions. Carbon to chlorophyll ratios can range by orders of magnitude and depend on many factors such as phytoplankton species, nutrients, and light levels. For example, photoacclimation causes phytoplankton to increase their chlorophyll when light levels decrease (decreases the C:chl ratio). Also, the carbon to chlorophyll ratio has been shown to increase with decreasing temperature for Skeletonema *costatum* (Yoder 1979). In our dataset, higher chlorophyll does corresponds to higher productivity. During the June 2015 cruise, the highest chlorophyll concentration measured was at P20 (Figure 4.5a). All four of our productivity estimates follow the same trend as chlorophyll (Figure 4.5a). The same is true for June 2016 (Figure 4.5b) and June 2017 (Figure 4.5c) for a range in chlorophyll and productivity rates, with one exception at P20 during June 2016. Here, ^{13}C-PP, ^{15}N-new, and O_2/Ar-NCP were lower than expected, and ^{18}O-GPP

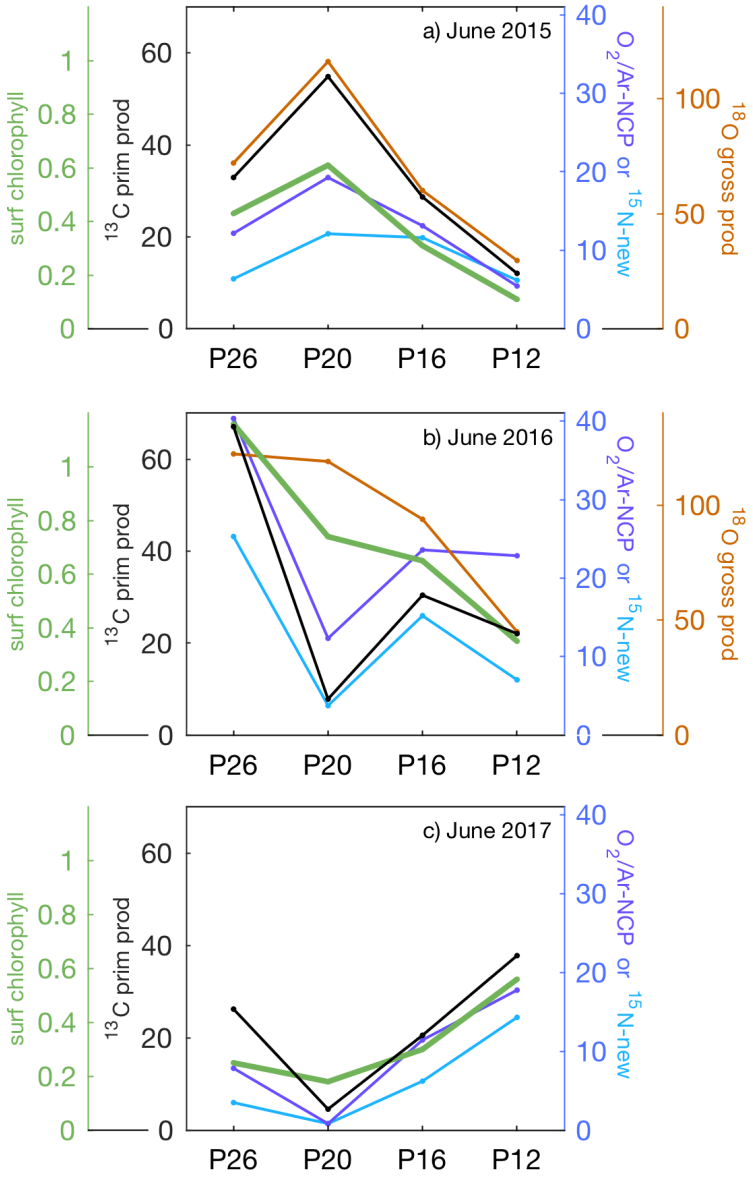

Figure 4.5 Surface chlorophyll, ^{13}C-PP, ^{18}O-GOP, ^{15}N-new, and O_2/Ar-NCP for (a) June 2015, (b) June 2016 and (c) June 2017. Surface chlorophyll is in mg m^{-3} and all the rate measurements are in mmol C m^{-2} d^{-1}. Measurements are made along Line P with station name on x axis. All incubations are integrated to the mixed layer depth.

was higher than expected based on chlorophyll at that one station (Figure 4.5b). Generally, production rate estimates have the same trend as the surface chlorophyll despite all measuring a different fraction of productivity or relying on different

approaches. See Chapter 2 (Arctic) and Chapter 3 (subarctic northeast Pacific) for a more in-depth look at method comparison.

4.4.3 Higher chlorophyll corresponds to colder and saltier water

On a point by point basis, chlorophyll and sea surface temperature have a complicated relationship. During June 2015, chlorophyll is more variable and reaches higher

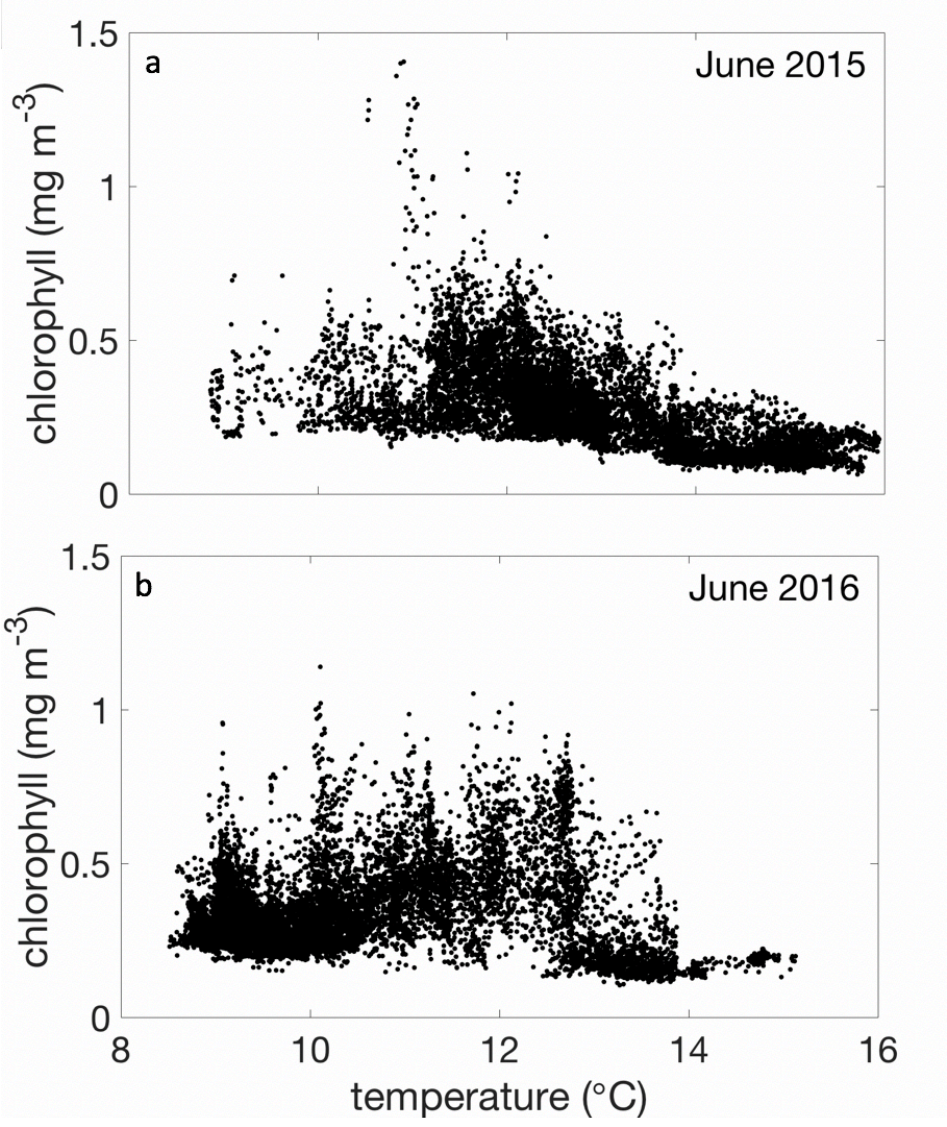

Figure 4.6 Satellite-derived chlorophyll concentrations vs. sea surface temperature from the Mercator model at the nearest locations for (a) June 2015 and (b) June 2016 in the offshore regions shown in Figures 4.3 and 4.4. See Section 4.3.1 for information on the polygon used to define the offshore region in this figure.

concentrations offshore in places where model sea surface temperatures are lower, with the highest chlorophyll concentrations are centered around 11°C (Figure 4.6a). This agrees with a visual comparison, where the coherent, mesoscale, higher chlorophyll

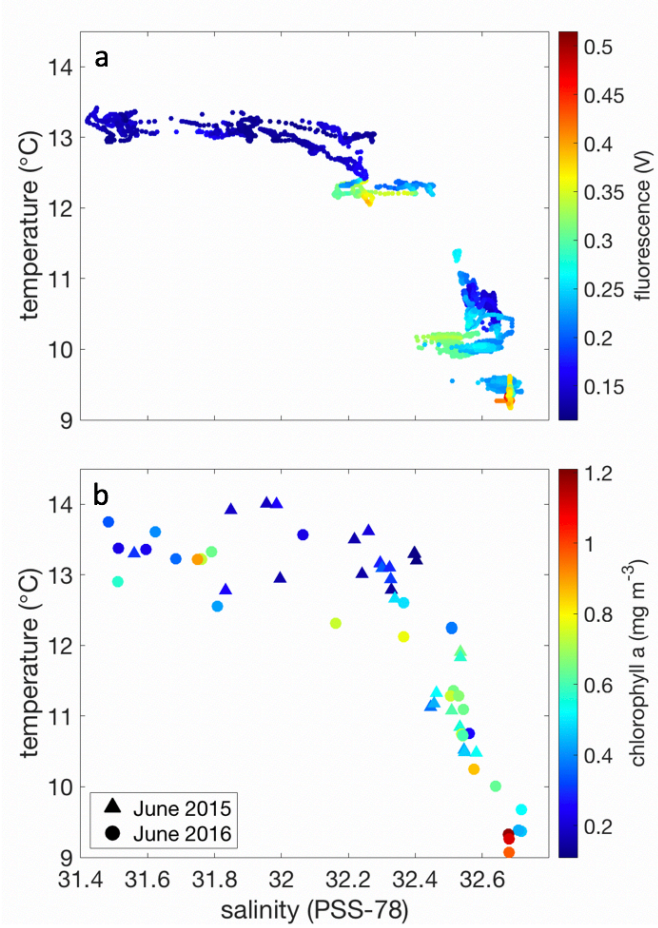

Figure 4.7 (a) Surface nighttime chlorophyll fluorescence (in raw volts) plotted as color on a temperature-salinity diagram for the 9-18 June 2016 Line P cruise. All data derived from the ship's underway system. Only nighttime data is included due to fluorescence quenching during the day. Only west of 131°W is included to highlight offshore conditions. (b) Similar to panel a but using offshore surface chlorophyll concentration, temperature, and salinity from rosette sampling in both June 2015 (triangle symbol; west of 127°W) and June 2016 (circle symbol; west of 126°W).

feature roughly corresponds to a cold water tongue (Figure 4.3a,b). Conversely, at higher sea surface temperatures, chlorophyll is low during June 2015. During June 2016, chlorophyll was low at temperatures around 14°C and higher, while chlorophyll is variable at lower temperatures with some high chlorophyll concentrations (Figure 4.6b).

The shipboard data also show a relationship between temperature/salinity and phytoplankton. Higher fluorescence is associated with lower temperature and higher salinity using the underway TSG from June 2016 (Figure 4.7a). Only night time fluorescence data was included to avoid the influence of fluorescence quenching (Kolber and Falkowski, 1993). Unfortunately, the June 2015 underway fluorescence data was highly biased and uncorrectable. However, surface rosette data from June 2015 and 2016 both show higher chlorophyll associated with the colder and saltier water (Figure 4.7b). Underway and rosette data are two independent methods that confirm that saltier and colder water was present in areas with higher chlorophyll.

4.4.4 Evidence for iron fertilization

We show next that iron additions are likely creating the increased chlorophyll observed. Iron measurements in the surface waters are sporadic along Line P but data generally support possible iron inputs. In June 2015, the dFe concentration at P20 was roughly double that found at P12 and nearly 10 times that at P26 (personal communication-Ben Twining and Peter Morton), supporting that increased chlorophyll concentrations were fueled by iron inputs. Iron samples from June 2016 show possible contamination, so we are unable to draw conclusions. In addition to the limited iron concentration data, inferences can be drawn based on previous studies.

A shift in phytoplankton species provides indirect evidence of iron fertilization, because larger phytoplankton are more severely iron limited (Marchetti et al., 2006). Diatoms made up at least 25% of the relative abundance of phytoplankton during June 2016 at P16 and P26 (Figure 4.8a). This is unusual for the region where diatoms normally make up 8 ±2% of the relative abundance (Varela and Harrison, 1999). Smaller

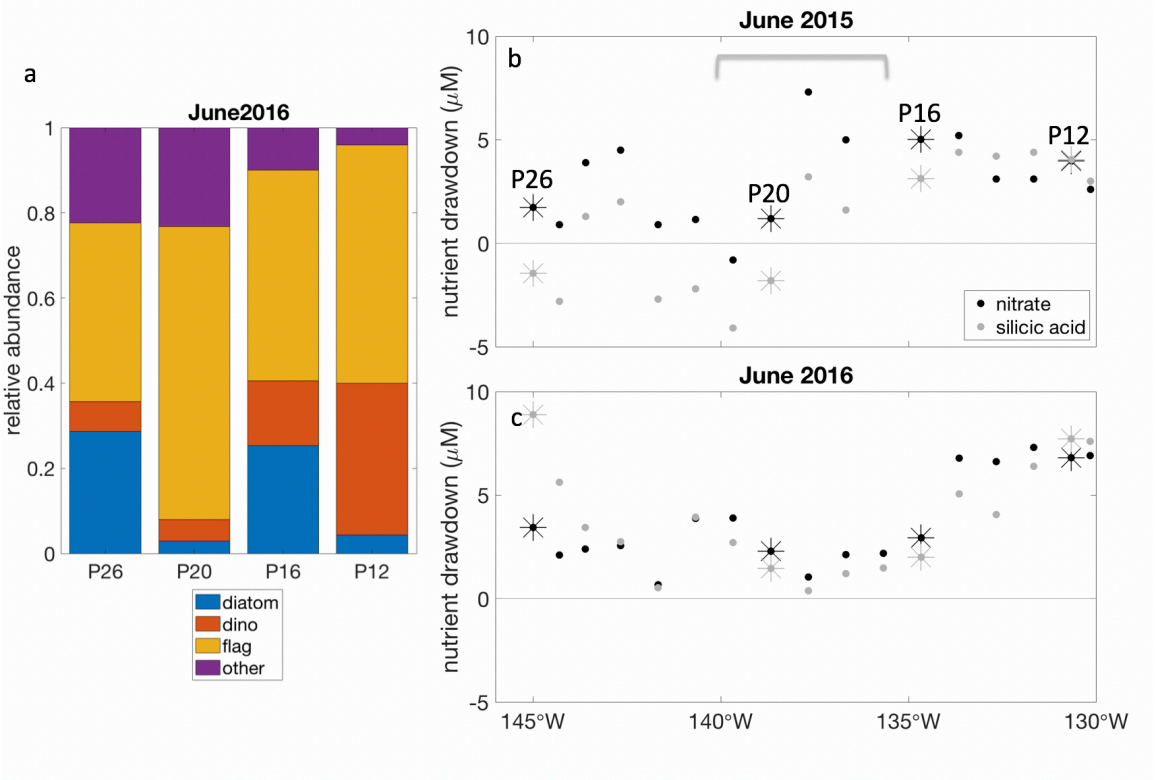

Figure 4.8 (a) Phytoplankton relative abundance at 4 major stations along Line P in June 2016 categorized as diatoms, dinoflagellates (dino), flagellates (flag), and other. Other includes unidentified Choanoflagellates, Telonema, and unidentified ciliates. Phytoplankton samples were not collected in June 2015. (b-c) Nutrient drawdown calculated as February minus June surface concentrations for both nitrate and silicic acid at all offshore stations along Line P in (b) 2015 and (c) 2016. The bracket in panel b indicates location where the cold water, higher chlorophyll tongue is located.

phytoplankton, mainly flagellates (from Crytophyceae, Prymnesiophyceae, and Prasinophyceae), are typically most abundant along Line P (Varela and Harrison, 1999).

Iron addition experiments show that the larger phytoplankton size class (>18 μm) increase on day 2 and exponentially increased by day 6 (Boyd et al., 1996). Zooplankton grazing is thought to control phytoplankton to some degree (Landry, 1993); however, zooplankton grazing was insufficient to prevent an iron-induced diatom bloom in this region, even when the number of zooplankton in the sample was doubled (Harrison et al., 1999). In addition to incubation experiments, an in situ iron fertilization Lagrangian study also showed a shift in species composition from nanophytoplankton to microphytoplankton including diatoms (Marchetti et al., 2006). These studies prove, specifically in this area, that diatoms dominate when iron is added. So the higher relative diatom abundance in June 2016 suggests there were iron inputs at P16 and P26 beginning more than 6 days prior to sampling.

Seasonal silicic acid drawdown provides indirect evidence of patchy iron additions in June 2015 and June 2016. All phytoplankton need nitrogen to grow; however, diatoms also require silicic acid to form their frustules. Since diatoms have increased relative abundance when iron is added, silicic acid drawdown can be used to imply seasonal diatom growth. The data from 2016 follows historical trends with all positive drawdowns (Figure 4.8c). Nitrate drawdown from the difference between winter (February) and summer (August), is on average 6.6 μM to 8.0 μM offshore (Peña and Varela 2007), within range of this study. Similarly, historic silicic acid drawdown ranged from 6.8 μM to 8.5 μM (Peña and Varela 2007) and agree with one exception. There was high silicic acid drawdown at P26 (8.9 μM), suggesting a diatom bloom occurred sometime between February and June 2016. Nitrate drawdown is generally of similar magnitude to silicic acid drawdown except at P26 where silicic acid drawdown was more than double the

nitrate drawdown. In contrast, 2015 was more extreme, where some of the offshore stations in 2015 had negative nutrient drawdowns, meaning there was higher silicic acid in June compared to February (Figure 4.8b). This implies macronutrients were added to the system either close to the sampling date or at higher concentrations compared to June 2016. These higher macronutrients may have come from deeper in the water column, which also has higher iron concentrations. If the nutrient additions were recent, there was not enough time before the cruise for phytoplankton to draw nutrients back down to February concentrations.

We hypothesize that the ecosystem in this region is predominantly controlled by phytoplankton dynamics at the base of the food chain rather than by grazers. As a proxy, we examine trends in zooplankton biomass anomalies to give insight into the importance of grazing. Total zooplankton biomass anomalies were positive in June 2016 but negative in June 2017 for station P16 and west (Personal communication- Moira Galbraith). We interpret this as more productive phytoplankton in June 2016 were able to support more zooplankton. Conversely, since phytoplankton were not very productive in June 2017, zooplankton anomalies were also low. If grazing was the most important control on phytoplankton, then there should be higher zooplankton anomalies when chlorophyll is low.

4.4.5 Mechanisms for iron supply and ecosystem response

We have presented indirect evidence that there were iron inputs offshore in the HNLC area in June 2015 and June 2016. Only small amounts of iron would be required to cause the mesoscale variability in chlorophyll. Macronutrients are plentiful in the HNLC area and mixed layer depths are shallow enough in summer that light is not limiting (i.e.

mixed layer depth<euphotic depth). Therefore, iron is the main limiting factor and must be supplied to create increased productivity. The amount of iron does not have to be large, because modest increases in chlorophyll only need modest iron inputs to drive the observed spatial and temporal variability offshore. Much less iron is needed in comparison to coastal waters with chlorophyll concentrations in excess of 40 mg m^{-3}, for example. There are three potential sources of iron input: above (atmospheric), horizontal, or vertical.

4.4.5.1 Iron supply from above

The atmosphere is a known source of iron for the HNLC areas of the ocean. Boyd et al. (1998) suggest that dust from Asia or Alaska could occasionally supply iron to the study region. In addition to dust, volcanic ash can also deliver iron to the ocean (Hamme et al., 2010). In this study, satellite data does not show consistent increased aerosols over the area to explain the patterns in this study (Figure C4, C5, C6). In June 2015, the aerosols do not look like they originated from Asian dust but are instead an isolated patch. No Aleutian volcanoes were erupting that could cause the isolated patch. During June 2016, increased aerosols are confined further west and do not reach into our study area except for one isolated patch around P16. Higher aerosol areas were detected in June 2017 but that was the year with low chlorophyll throughout the entire region. Aerosols from dust or volcanoes cannot explain the chlorophyll variability, and do not explain why higher chlorophyll is associated with colder and saltier water.

4.4.5.2 Horizontal iron supply

Iron could also be supplied horizontally by eddies. Eddies in the region primarily form at the coast and propagate offshore (Crawford et al., 2007). The most notable anticyclonic

eddies in the area are the Haida, Sitka, and Yakutat eddies (Tabata, 1982; Crawford and Whitney, 1999; Ladd et al., 2009), all of which have high sea surface height anomalies (e.g. Crawford, 2002). These eddies generally have higher chlorophyll within compared to outside based on satellite data (Crawford et al., 2005; Crawford et al., 2007) and bring iron-rich coastal waters from their region of formation (Johnson et al., 2005; Ladd et al., 2009). However, eddies do not always have higher chlorophyll associated with them (Crawford et al., 2007). The propagation of any of these eddies into the central Gulf of Alaska is considered rare (Crawford, 2002).

Eddies have almost no relationship to the mesoscale chlorophyll features we are considering here. In June 2015, mesoscale high chlorophyll features were not correlated with high SSHa, associated with anticyclonic eddies (Figure 4.3a,c). Conversely, high SSHa features are not associated with higher chlorophyll (top black box in Figure 4.3a,c). June 2016 also confirms that eddies cannot explain all variability in the area. The highest chlorophyll does not correspond to any particular SSHa eddy feature, but instead is similar to background SSHa (southern three black boxes in Figure 4.4a,c). A cyclonic eddy in June 2016 (north black box in Figure 4.4a,c) shows a hole in chlorophyll.

Eddies clearly cause some phytoplankton variability but are isolated features that do not explain the majority of variability in the HNLC area. An eddy was situated over P20 at the time of sampling during June 2016 based on SSHa (Figure 4.4c). This single instance of an anticyclonic eddy corresponded to higher chlorophyll concentrations (Figure 4.4a) but diatom relative abundance was normal (Figure 4.8a). Another example is the coastal cyclonic eddy (low SSHa) corresponding to a decrease in chlorophyll (Figure 4.4a,c) during June 2016. Within the eddy, chlorophyll is ~0.5 mg m^{-3} compared

to a maximum around the outside of ~3 mg m^{-3}. These are isolated features that do not explain the majority of variability.

4.4.5.3 Vertical iron supply via fronts

Finally, iron can be delivered to surface waters from below. We have shown that high chlorophyll is associated with colder and saltier water. In the Alaska Gyre, temperature decreases and salinity increases with depth, so colder saltier water is an indication of deeper water coming to the surface. For example, Lam et al. (2006) observed a diatom bloom in February 1996 at P26 that they link to deep wintertime mixing. Based on a tracer model, they hypothesized that iron was advected subsurface from the coast and then brought to the surface. However, in our study, the stations with higher productivity do not correlate with stronger winds leading up to sampling.

Instead of deep mixing by winds, we hypothesize that fronts cause vertical mixing or advection that brings a small amount of iron up from below. A front is characterized by strong horizontal temperature and/or salinity gradients at the surface (Franks, 1992). In our study region, fronts may form from meanders in the North Pacific Current. Typical fronts show upwelling on the less dense side; however, it is plausible that mixing occurs on the dense side as well. Molemaker et al. (2010) use a model to show that vertical mixing is not homogeneous along unstable fronts. Johnston et al. (2011) show elevated gradients and vertical mixing within 20 km on the dense side of a coastal upwelling front, though this is smaller scale and closer to shore than we are considering here. However, scale should not be an issue, because large scale fronts will produce cascading smaller scale gradients. Although neither example perfectly captures what we hypothesize is happening, none of the other mechanisms can explain the widespread variability in

chlorophyll that was observed in June 2015 and June 2016 and the link to colder, saltier water. To my knowledge, this is the first publication that cite fronts as a means of explaining phytoplankton variability in the offshore HNLC northeast Pacific, though Ribalet et al. (2010) suggested they may be important in the transition zone from coastal to HNLC conditions. If we assume phytoplankton need 8 iron molecules to every 108,000 carbon molecule (Morel et al., 2003) and a carbon to chlorophyll ratio of 50-80 (Burt et al., 2018), then a chlorophyll concentration of 1 mg m^{-3} would need 0.08 nM of iron. Based on the iron concentrations at P26, such a concentration is plausible at 50-100 m, much shallower than the base of the ferrocline near 500 m (Martin et al. 1989). The iron concentration profiles likely change cruise to cruise, but this does provide a rough estimate. This supports our hypothesis that a small amount of iron could be supplied from mesoscale vertical transport, fueling surface production.

Temperature fronts can loosely explain phytoplankton variability in June 2015-2017. We detected fronts based on a temperature gradient of 1°C over 5 data points (1/3 of a degree in latitude / longitude). In June 2015, fronts occur east of the area with the highest chlorophyll along a temperature of about 12°C (see arrows in Figure 4.3d). Fronts are also present throughout the area with patchy high chlorophyll during June 2016 (Figure 4.4d). However, not all apparent fronts result in higher chlorophyll; there are other factors such as the depth and strength of the vertical iron gradient. Unfortunately, we cannot evaluate depth profiles of iron from satellites. These sources of uncertainty mean that we do not expect high chlorophyll everywhere there is a front. Further supporting our hypothesis, no fronts are detected offshore in June 2017 using the same front criteria (Figure C3b), a time with low chlorophyll throughout the area. Lack of fronts explains

the steady and low chlorophyll concentration in this instance. We additionally considered the following parameters but did not find any correlation to the observed chlorophyll patterns: wind stress curl, Pacific Decadal Oscillation, geostrophic strain (Zhang and Qiu 2018), and current curl.

4.4.5.4 Summary of June 2015

We summarize our hypothesis using the June 2015 well-defined mesoscale feature as an example. At that time, two fronts (as defined by our temperature gradient criterion) located between 137°W to 142°W (see arrows in Figure 4.3d) caused water to upwell. We hypothesize the upwelled water contained elevated iron concentrations compared to surface water, fueling increased productivity and chlorophyll to the west (dense side) of the front. This higher chlorophyll tongue feature was sampled between 140°W and 136°W along Line P. The upwelled water also brought macronutrients into the surface water, causing nutrient drawdown along parts of Line P to be negative, with silicic acid drawdown (nitrate) starting negative (low) in the west and becoming more positive moving farther east through the feature (indicated by the bracket in Figure 4.8b). Negative drawdown indicates higher nutrient concentrations observed in June compared to February, suggesting newly upwelled water.

The longitudinal gradient in chlorophyll and in nutrient drawdown could indicate that waters to the east were less influenced by upwelling and/or that more time had elapsed since upwelling for phytoplankton to take up the upwelled nutrients. Geostrophic currents would have transported the upwelled water east, creating the tongue. Currents retrieved from the Mercator model show that geostrophic currents pulled the eastern front into the tongue shape (Figure 4.3b). Mercator SST supports this theory, where the western side of

the tongue had cooler temperatures than the east side, suggesting that the east side could be older water (Figure 4.3b). A different front further west was too distant from the currents, so there was no horizontal advection and no stretching like the other water mass (left arrow in Figure 4.3d). In summary, nutrients upwelled west of the front, causing increased chlorophyll. The highest chlorophyll feature was transported east while the water warmed and phytoplankton consumed the added nutrients.

It is unclear what causes fronts in the subarctic NE Pacific; however, the subtropical gyre provides some clues. Fronts (defined as 1°C change over 1/3 of a degree distance) are more common starting around 15°N and northward on 17 June 2015 (Figure C7a). This also corresponds to the region where water transitions from around 30°C to less than 25°C. Interestingly, even though this region appears to have more fronts compared to the NE Pacific, it does not have increased chlorophyll (Figure C7b). I suspect this difference is caused by the very different subsurface conditions in the two regions. The subtropical gyre is oligotrophic with a deep pycnocline and nutricline and shallow mixed layers (Karl and Lukas 1996). Fronts in the subtropics are unlikely to generate enough vertical mixing to bring nutrients from the deep nutricline into the surface layer. Any input of nutrients will be too deep in the water column for satellites to detect the change at the surface. In contrast, the subarctic NE Pacific has shallower euphotic zone and nutricline depths, so mixing or upwelling has the potential to have a surface expression that satellites can detect.

4.5 Conclusions

Using both shipboard and satellite data, we find that chlorophyll is more variable offshore (within the HNLC area) than historically considered. Phytoplankton productivity

and carbon export follow the same trends as surface chlorophyll. There is evidence that phytoplankton species shift from smaller phytoplankton to larger diatoms in the higher chlorophyll features, suggesting iron inputs. These higher chlorophyll areas are associated with higher salinity and lower temperature. Although eddies explain a small number of these features, they cannot explain the large majority of chlorophyll variability offshore observed during this study. The only possible iron source is from depth, and we hypothesize the mechanism is from vertical mixing at fronts. The required iron inputs are not large, unlike in coastal waters. Fronts need to be considered as a mechanism for iron inputs in the HNLC regions of the northeast subarctic Pacific.

This study draws attention to the spatial and temporal variation in offshore chlorophyll, which has broader implications. Many studies paint HNLC regions as having low and invariant chlorophyll concentrations. We suggest that is not the case. Spatial and temporal observations at finer scales are needed to more accurately capture mesoscale processes occurring due to fronts. Better understanding of the mechanisms that cause fronts, would allow us to predict how higher trophic levels may be impacted. Regional averages for the area may need to be reassessed.

To further explore the idea that offshore fronts can cause variability, iron concentrations need to be measured with higher resolution around the base of the euphotic zone. Nishioka et al., (2001) found that iron gradients vary from cruise to cruise, so one high resolution profile would not be sufficient to see if small gradients could explain front-based variability. Future studies could identify fronts in the region and do targeted sampling to further investigate our proposed mechanism.

4.6 Acknowledgements

We thank Marie Robert and Doug Yelland for accommodating sampling requests and assistance at sea. We also thank IOS personnel for help at sea and analyzing samples, especially Melissa Hennekes for counting phytoplankton cells and Debby Ianson and Lisa Miller for DIC samples. We thank the Captain and crew of the CCGS John P. Tully for assistance at sea. Thanks to Sarah Thornton for allowing us to borrow field gear. We thank Paul Quay and his lab for assistance with triple oxygen isotope analysis. We thank Frank Whitney, Erik Fields, Debby Ianson, and Noel Pelland for helpful conversations. Thanks to Ben Twining, Peter Morton, Moira Galbraith and Debby Ianson. GlobColour data (*http://globcolour.info*) used in this study has been developed, validated, and distributed by ACRI-ST, France. Thank you to Mercator Ocean for providing model output. Some analyses and visualizations used in this publication were produced with the Giovanni online data system, developed and maintained by the NASA GES DISC.

Chapter 5 Conclusions

5.1 Summary of individual chapters

The following are the four main points in each of the three chapters of this dissertation.

Chapter 2. Arctic conditions complicate comparison between in situ and in vitro productivity methods

1. ^{13}C and ^{14}C bottle incubations are not equivalent on a point-by-point basis during 24-hr incubations
2. Recently shoaled mixed layer can affect in situ versus in vitro method comparison
3. Chlorophyll-a concentration is highly correlated to ^{13}C-PP, ^{14}C-PP and ^{18}O-GPP
4. Primary production integrated to the bottom of the euphotic zone increased with decreasing latitude

Chapter 3. Phytoplankton response and upwelling cause productivity rate methods in the NE subarctic Pacific to disagree

1. When rates are low, strong correlations exist among different productivity rate methods
2. Methods disagreements occur at locations with high chlorophyll a
3. Three processes tend to cause methods to disagree: dissolved organic matter release, bloom dynamics, and upwelling.
4. Satellite net primary production is consistently different from carbon uptake in the NE subarctic Pacific

Chapter 4: Fronts potentially drive variability in phytoplankton productivity in the HNLC subarctic northeast Pacific

1. Challenging historical thought, HNLC chlorophyll a concentrations show mesoscale patchiness
2. Higher surface chlorophyll a is representative of increased productivity and carbon export rates
3. Higher surface chlorophyll a tends to occur in colder and saltier water, implying transport of water from below
4. Fronts as offshore iron input mechanisms can explain much of the chlorophyll a variability

5.2 Connecting chapters

Chapter 2 and 3 examine different biogeochemical regions, resulting in different conclusions from the method comparisons. Because the Arctic and North Atlantic have complicated oceanography with different water masses in close proximity to each other,

no one mechanism clearly dominates the comparison of methods. Instead, we suggest five mechanisms are likely to impact these methods simultaneously at each station. Although some of the mechanisms are speculative, it stands to reason that a dynamic system makes it challenging to identify only one reason for method disagreement. In contrast, the subarctic NE Pacific has simpler circulation, making it easier to determine the dominate process causing methods to disagree. At lower carbon export rates, excretion of dissolved organic matter likely causes in vitro methods to be underestimates. At higher rates, in vitro methods may be higher or lower relative to in situ methods due to upwelling and end of bloom dynamics, respectively. Ultimately, time of integration appears to have to greatest effect in the NE Pacific. Understanding the underlying mechanisms allows for a better understanding of the global carbon cycle and improves our ability to predict future changes.

Chapter 4 applies method comparison to understand what causes variability in phytoplankton primary production and carbon export in the offshore subarctic NE Pacific. We believe mesoscale front processes cause observed variability in chlorophyll. The increased chlorophyll is also directly correlated with higher productivity. This implies that the carbon to chlorophyll ratio is fairly constant and that zooplankton grazing (top down controls) do not dominate in June. Fronts should be considered when planning future research in the area.

The most important discovery from this dissertation is that horizontal gradients in the HNLC area in NE Pacific could be responsible for controlling primary production and carbon export rates.

5.3 Which productivity method is best

The best productivity method depends on the research question. Some considerations include: 1) Are you interested in what is happening now versus longer time scales (including possible episodic events)? 2) What fraction of production is most important to quantify in your study? 3) Are you interested in only particulate carbon export or both particulate and dissolved? 4) It is also important to be aware of issue surrounding your study region. Are conditions changing quickly? Is upwelling influencing your station? Is there mixing? How important is nitrification? Are dissolved organic matter production rates high? Is decoupling between splitting of oxygen and carbon fixation likely?

5.4 Future recommendations

My first set of recommendations focuses on better understanding method comparisons.

- Design and carry out a Lagrangian experiment over 2-3 weeks in a more dynamic region. It would be interesting to look at both in situ and in vitro methods to see how they change over time and to isolate specific changes that causes methods to disagree.
- Quantify DO^{13}C and DO^{15}N production from ^{13}C and ^{15}N incubations. This would allow quantification of both the labelled particulate matter and how much goes into the dissolved phase, closing a loop in the method.
- Include size fractionated chlorophyll a and primary production to identify which size class of organisms is responsible for what percentage of the total chlorophyll a and primary production.
- Perform incubations using additional ^{15}N labeled nitrogen sources such as urea and amino acids.

- Compare results on combusted and uncombusted filters from the same incubations. Alternatively, collect samples that to specifically measure how abundant phytoplankton that are less than 0.7 μm are in the subarctic NE Pacific.
- Track temperature and pCO_2 to better understand when upwelling is occurring independently of when methods disagree. This could work well for the La Perouse cruises.
- Specifically test bottle effects to determine their impact on incubations. For example, future studies could perform incubations in bottles made using different materials.
- Perform a series of incubations starting at different times. Most older studies do not start incubations at a specific time (like dawn). Doing a series of incubations starting at different times would help to determine the impact of start time on method comparison studies.
- Perform a time series of productivity rate measurements at a single location during upwelling and relaxation. This would allow us to better understand certain situations where methods did not agree (e.g. P4 in August 2016).

My second set of recommendations focuses on better understanding what causes phytoplankton variability in the subarctic NE Pacific. Using a combination of satellite, model, and in situ data is key to connecting different time and spatial scales.

- Explore whether mixing from below has the potential to introduce small amounts of iron. Implement higher resolution iron measurements at the base of the mixed

layer and euphotic zone. Using the observed vertical gradient, calculate how much mixing would be required to supply enough iron to the surface waters.

- Conduct iron enrichment experiments to see how the specific phytoplankton assemblage responds to very small iron additions.
- Explore the mechanisms that create fronts. Are the fronts a result of meanders in the North Pacific current? Or do fronts result from old eddies that no longer have a sea surface height anomaly? Could an eddy still transport iron far offshore without it all being consumed?
- Explore the possibility that fronts are a mechanism that controls phytoplankton variability offshore. Consider different times along Line P or other projects in the NE Pacific when primary production data exists. Couple the in situ data with satellites to determine where there is increased chlorophyll a in the area and see how it corresponds to productivity. Look at satellite and model based salinity, temperature, and density to identify associated fronts.
- Conduct a process study specifically targeting fronts, collecting measurements across and along front gradients. It would be especially interesting to measure vertical mixing and currents.

Bibliography

Acker, J.G. and Leptoukh, G., 2007. Online analysis enhances use of NASA earth science data. *Eos, Transactions American Geophysical Union*, *88*(2), pp.14-17.

Amante, C. and B.W. Eakins. 2009. ETOPO1 1 Arc-Minute Global Relief Model: Procedures, Data Sources and Analysis. NOAA Technical Memorandum NESDIS NGDC-24. National Geophysical Data Center, NOAA. doi:10.7289/V5C8276M 11Dec2018.

Anderson, L.A., 1995. On the hydrogen and oxygen content of marine phytoplankton. *Deep sea research part I: Oceanographic research papers*, *42*(9), pp.1675-1680.
Anderson, L.G. and Amon, R.M., 2015. DOM in the Arctic Ocean. In *Biogeochemistry of marine dissolved organic matter* (pp. 609-633). Academic Press.

Arrigo, K.R., van Dijken, G.L. and Bushinsky, S., 2008. Primary production in the Southern Ocean, 1997–2006. *Journal of Geophysical Research: Oceans*, *113*(C8).

Asher, E., Dacey, J.W., Ianson, D., Peña, A. and Tortell, P.D., 2017. Concentrations and cycling of DMS, DMSP, and DMSO in coastal and offshore waters of the Subarctic Pacific during summer, 2010-2011. *Journal of Geophysical Research: Oceans*, *122*(4), pp.3269-3286.

Babin, S.M., Carton, J.A., Dickey, T.D. and Wiggert, J.D., 2004. Satellite evidence of hurricane-induced phytoplankton blooms in an oceanic desert. *Journal of Geophysical Research: Oceans*, *109*(C3).

Banse, K. and English, D.C., 1999. Comparing phytoplankton seasonality in the eastern and western subarctic Pacific and the western Bering Sea. *Progress in Oceanography*, *43*(2-4), pp.235-288.

Barwell-Clarke, J. and Whitney, F., 1996. *Institute of Ocean Sciences nutrient methods and analysis*. Fisheries and Oceans Canada.

Bender, M., Grande, K., Johnson, K., Marra, J., Williams, P.J.L., Sieburth, J., Pilson, M., Langdon, C., Hitchcock, G., Orchardo, J. and Hunt, C., 1987. A comparison of four methods for determining planktonic community production1. *Limnology and Oceanography*, *32*(5), pp.1085-1098.

Bender, M., Orchardo, J., Dickson, M.L., Barber, R. and Lindley, S., 1999. In vitro O2 fluxes compared with 14C production and other rate terms during the JGOFS Equatorial Pacific experiment. *Deep Sea Research Part I: Oceanographic Research Papers*, *46*(4), pp.637-654.

Berelson, W.M., 2001. The flux of particulate organic carbon into the ocean interior: A

comparison of four US JGOFS regional studies. *Oceanography*, *14*(4), pp.59-67.

Bishop, J.K., Calvert, S.E. and Soon, M.Y., 1999. Spatial and temporal variability of POC in the northeast Subarctic Pacific. *Deep Sea Research Part II: Topical Studies in Oceanography*, *46*(11-12), pp.2699-2733.

Bond, N.A., Cronin, M.F., Freeland, H. and Mantua, N., 2015. Causes and impacts of the 2014 warm anomaly in the NE Pacific. *Geophysical Research Letters*, *42*(9), pp.3414-3420.

Boyd, P. and Harrison, P.J., 1999. Phytoplankton dynamics in the NE subarctic Pacific. *Deep Sea Research Part II: Topical Studies in Oceanography*, *46*(11-12), pp.2405-2432.

Boyd, P.W., Claustre, H., Levy, M., Siegel, D.A. and Weber, T., 2019. Multi-faceted particle pumps drive carbon sequestration in the ocean. *Nature*, *568*(7752), p.327.

Boyd, P.W., Muggli, D.L., Varela, D.E., Goldblatt, R.H., Chretien, R., Orians, K.J. and Harrison, P.J., 1996. In vitro iron enrichment experiments in the NE subarctic Pacific. *Marine Ecology Progress Series*, *136*, pp.179-193.

Boyd, P.W., Wong, C.S., Merrill, J., Whitney, F., Snow, J., Harrison, P.J. and Gower, J., 1998. Atmospheric iron supply and enhanced vertical carbon flux in the NE subarctic Pacific: is there a connection?. *Global Biogeochemical Cycles*, *12*(3), pp.429-441.

Brix, H., Gruber, N., Karl, D.M. and Bates, N.R., 2006. On the relationships between primary, net community, and export production in subtropical gyres. *Deep Sea Research Part II: Topical Studies in Oceanography*, *53*(5-7), pp.698-717.

Bronk, D.A. and Ward, B.B., 2000. Magnitude of dissolved organic nitrogen release relative to gross nitrogen uptake in marine systems. *Limnology and Oceanography*, *45*(8), pp.1879-1883.

Burt, W.J., Westberry, T.K., Behrenfeld, M.J., Zeng, C., Izett, R.W. and Tortell, P.D., 2018. Carbon: Chlorophyll ratios and net primary productivity of Subarctic Pacific surface waters derived from autonomous shipboard sensors. *Global Biogeochemical Cycles*, *32*(2), pp.267-288.

Cai, P., Rutgers Van Der Loeff, M., Stimac, I., Nöthig, E.M., Lepore, K. and Moran, S.B., 2010. Low export flux of particulate organic carbon in the central Arctic Ocean as revealed by 234Th: 238U disequilibrium. *Journal of Geophysical Research: Oceans*, *115*(C10).

Capone, D.G., Bronk, D.A., Mulholland, M.R. and Carpenter, E.J. eds., 2008. *Nitrogen in the marine environment*. Elsevier.

Carmack, E. and McLaughlin, F., 2011. Towards recognition of physical and

geochemical change in Subarctic and Arctic Seas. *Progress in Oceanography*, *90*(1-4), pp.90-104.

Carmack, E. and Wassmann, P., 2006. Food webs and physical–biological coupling on pan-Arctic shelves: unifying concepts and comprehensive perspectives. *Progress in Oceanography*, *71*(2-4), pp.446-477.

Caron, D.A., Dam, H.G., Kremer, P., Lessard, E.J., Madin, L.P., Malone, T.C., Napp, J.M., Peele, E.R., Roman, M.R. and Youngbluth, M.J., 1995. The contribution of microorganisms to particulate carbon and nitrogen in surface waters of the Sargasso Sea near Bermuda. *Deep Sea Research Part I: Oceanographic Research Papers*, *42*(6), pp.943-972.

Carpenter, J.H., 1965. The Chesapeake Bay Institute technique for the Winkler dissolved oxygen method. *Limnology and Oceanography*, *10*(1), pp.141-143.

Cassar, N., Nevison, C.D. and Manizza, M., 2014. Correcting oceanic O2/Ar-net community production estimates for vertical mixing using N2O observations. *Geophysical Research Letters*, *41*(24), pp.8961-8970.

Cassar, N., Wright, S.W., Thomson, P.G., Trull, T.W., Westwood, K.J., de Salas, M., Davidson, A., Pearce, I., Davies, D.M. and Matear, R.J., 2015. The relation of mixed-layer net community production to phytoplankton community composition in the Southern Ocean. *Global Biogeochemical Cycles*, *29*(4), pp.446-462.

Chipman, D.W., Marra, J. and Takahashi, T., 1993. Primary production at 47 N and 20 W in the North Atlantic Ocean: A comparison between the 14C incubation method and the mixed layer carbon budget. *Deep Sea Research Part II: Topical Studies in Oceanography*, *40*(1-2), pp.151-169.

Collos, Y. and Slawyk, G., 1985. On the compatibility of carbon uptake rates calculated from stable and radioactive isotope data: implications for the design of experimental protocols in aquatic primary productivity. *Journal of plankton research*, *7*(5), pp.595-603.

Coppola, L., Roy-Barman, M., Wassmann, P., Mulsow, S. and Jeandel, C., 2002. Calibration of sediment traps and particulate organic carbon export using 234Th in the Barents Sea. *Marine Chemistry*, *80*(1), pp.11-26.

Corno, G., Letelier, R.M., Abbott, M.R. and Karl, D.M., 2005. Assessing primary production variability in the north pacific subtropical gyre: a comparison of fast repetition rate fluorometry and 14C measurements. *Journal of Phycology*, *42*(1), pp.51-60.

Craig, H. and Hayward, T., 1987. Oxygen supersaturation in the ocean: Biological versus physical contributions. *Science*, *235*(4785), pp.199-202.

Crawford WR. 2002. Physical Characteristics of Haida Eddies. Journal of Oceanography. 58:703-713.

Crawford, W.R. and Whitney, F.A., 1999. Mesoscale eddy aswirl with data in Gulf of Alaska. *Eos, Transactions American Geophysical Union*, *80*(33), pp.365-370.
Crawford, W.R., Brickley, P.J. and Thomas, A.C., 2007. Mesoscale eddies dominate surface phytoplankton in northern Gulf of Alaska. *Progress in Oceanography*, *75*(2), pp.287-303.

Crawford, W.R., Brickley, P.J., Peterson, T.D. and Thomas, A.C., 2005. Impact of Haida eddies on chlorophyll distribution in the eastern Gulf of Alaska. *Deep Sea Research Part II: Topical Studies in Oceanography*, *52*(7-8), pp.975-989.

De La Rocha, CL. and Passow, U., 2007. Factors influencing the sinking of POC and the efficiency of the biological carbon pump. *Deep Sea Research Part II: Topical Studies in Oceanography*, *54*(5-7), pp.639-658.

Denman, K.L. and Gargett, A.E., 1988. Multiple thermoclines are barriers to vertical exchange in the subarctic Pacific during SUPER, May 1984. *Journal of Marine Research*, *46*(1), pp.77-103.

Dickson, A.G., Sabine, C.L. and Christian, J.R., 2007. *Guide to best practices for ocean CO2 measurements*. North Pacific Marine Science Organization.

DiFiore, P.J., Sigman, D.M. and Dunbar, R.B., 2009. Upper ocean nitrogen fluxes in the Polar Antarctic Zone: Constraints from the nitrogen and oxygen isotopes of nitrate. *Geochemistry, Geophysics, Geosystems*, *10*(11).

Di Lorenzo, E. and Mantua, N., 2016. Multi-year persistence of the 2014/15 North Pacific marine heatwave. *Nature Climate Change*, *6*(11), p.1042.

Dore, J.E. and Karl, D.M., 1996. Nitrification in the euphotic zone as a source for nitrite, nitrate, and nitrous oxide at Station ALOHA. *Limnology and Oceanography*, *41*(8), pp.1619-1628.

Dring, M.J. and Jewson, D.H., 1982. What does 14C uptake by phytoplankton really measure? A theoretical modelling approach. *Proceedings of the Royal Society of London. Series B. Biological Sciences*, *214*(1196), pp.351-368.

Ducklow, H.W., Steinberg, D.K. and Buesseler, K.O., 2001. Upper ocean carbon export and the biological pump. *Oceanography*, *14*(4), pp.50-58.

Dugdale, R.C. and Goering, J.J., 1967. Uptake of new and regenerated forms of nitrogen in primary productivity1. *Limnology and oceanography*, *12*(2), pp.196-206.

Dugdale, R.C. and Wilkerson, F.P., 1986. The use of 15N to measure nitrogen uptake in eutrophic oceans; experimental considerations 1, 2. *Limnology and Oceanography*, *31*(4), pp.673-689.

Emerson, S., 2014. Annual net community production and the biological carbon flux in the ocean. *Global Biogeochemical Cycles*, *28*(1), pp.14-28.

Emerson, S., Quay, P.D., Stump, C., Wilbur, D. and Schudlich, R., 1995. Chemical tracers of productivity and respiration in the subtropical Pacific Ocean. *Journal of Geophysical Research: Oceans*, *100*(C8), pp.15873-15887.

Emerson, S., Stump, C., Wilbur, D. and Quay, P., 1999. Accurate measurement of O2, N2, and Ar gases in water and the solubility of N2. *Marine Chemistry*, *64*(4), pp.337-347.

Emerson, S., Quay, P. and Wheeler, P.A., 1993. Biological productivity determined from oxygen mass balance and incubation experiments. *Deep Sea Research Part I: Oceanographic Research Papers*, *40*(11-12), pp.2351-2358.

Engida, Z., Monahan, A., Ianson, D. and Thomson, R.E., 2016. Remote forcing of subsurface currents and temperatures near the northern limit of the C alifornia C urrent S ystem. *Journal of Geophysical Research: Oceans*, *121*(10), pp.7244-7262.

Falkowski, P.G., Laws, E.A., Barber, R.T. and Murray, J.W., 2003. Phytoplankton and their role in primary, new, and export production. In *Ocean biogeochemistry* (pp. 99-121). Springer, Berlin, Heidelberg.

Falkowski, P. G., & Woodhead, A. D. (Eds.). (2013). *Primary productivity and biogeochemical cycles in the sea* (Vol. 43). Springer Science & Business Media.

Fanton d'Andon, O. and Mangin, A. and Lavender, S. and Antoine, D. and Maritorena, S. and Morel, A. and Barrot, G. et al. 2009. “GlobColour - the European Service for Ocean Colour”, in Proceedings of the 2009 IEEE International Geoscience & Remote Sensing Symposium, Jul 12-17 2009, Cape Town South Africa: IEEE Geoscience and Remote Sensing Society.

Ferrell, R.T. and Himmelblau, D.M., 1967. Diffusion coefficients of nitrogen and oxygen in water. *Journal of chemical and engineering data*, *12*(1), pp.111-115.

Field, C.B., Behrenfeld, M.J., Randerson, J.T. and Falkowski, P., 1998. Primary production of the biosphere: integrating terrestrial and oceanic components. *science*, *281*(5374), pp.237-240.

Fitzwater, S.E., Knauer, G.A. and Martin, J.H., 1982. Metal contamination and its effect on primary production measurements 1. *Limnology and Oceanography*, *27*(3), pp.544-551.

Franks, P.J., 1992. Phytoplankton blooms at fronts: patterns, scales, and physical forcing mechanisms. *Reviews in Aquatic Sciences*, *6*(2), pp.121-137.

Freeland, H.J., 1982. A topographically controlled upwelling center off southern Vancouver Island. *J. Mar. Res.*, *40*, pp.1069-1093.

Freeland, H., 2007. A short history of Ocean Station Papa and Line P. *Progress in Oceanography*, *75*(2), pp.120-125.

Freeland, H. and Whitney, F., 2014. Unusual warming in the Gulf of Alaska. *PICES press*, *22*(2), p.51.

Fu, W., Randerson, J., & Moore, J. K. (2015). Climate change impacts on net primary production (NPP) and export production (EP) regulated by increasing stratification and phytoplankton community structure in CMIP5 models. *Biogeosciences Discussions*, *12*(15).

Gaarder, T. and Grann, H.H., 1927. Investigation of plankton production in the Oslo Fjord. *Rapp. Cons. Perm. Int. Explor. Afar 144: 56*, *60*.

Garcia, H.E. and Gordon, L.I., 1992. Oxygen solubility in seawater: Better fitting equations. *Limnology and oceanography*, *37*(6), pp.1307-1312.

Giesbrecht, K.E., Hamme, R.C. and Emerson, S.R., 2012. Biological productivity along Line P in the subarctic northeast Pacific: In situ versus incubation-based methods. *Global Biogeochemical Cycles*, *26*(3).

Gieskes, W.W.C., Kraay, G.W. and Baars, M.A., 1979. Current 14C methods for measuring primary production: gross underestimates in oceanic waters. *Netherlands Journal of Sea Research*, *13*(1), pp.58-78.

Gocke, K. and Lenz, J., 2004. A new 'turbulence incubator'for measuring primary production in non-stratified waters. *Journal of Plankton Research*, *26*(3), pp.357-369.

Gosselin, M., Levasseur, M., Wheeler, P.A., Horner, R.A. and Booth, B.C., 1997. New measurements of phytoplankton and ice algal production in the Arctic Ocean. *Deep Sea Research Part II: Topical Studies in Oceanography*, *44*(8), pp.1623-1644.

Grande, K.D., Williams, P.J.L., Marra, J., Purdie, D.A., Heinemann, K., Eppley, R.W. and Bender, M.L., 1989. Primary production in the North Pacific gyre: a comparison of rates determined by the 14C, O2 concentration and 18O methods. *Deep Sea Research Part A. Oceanographic Research Papers*, *36*(11), pp.1621-1634.

Grundle, D.S., Juniper, S.K. and Giesbrecht, K.E., 2013. Euphotic zone nitrification in the NE subarctic Pacific: Implications for measurements of new production. *Marine*

Chemistry, *155*, pp.113-123.

Guy, R.D., Fogel, M.L. and Berry, J.A., 1993. Photosynthetic fractionation of the stable isotopes of oxygen and carbon. *Plant Physiology*, *101*(1), pp.37-47.

Halsey, K.H. and Jones, B.M., 2015. Phytoplankton strategies for photosynthetic energy allocation. *Annual review of marine science*, *7*, pp.265-297.

Hama, T., Miyazaki, T., Ogawa, Y., Iwakuma, T., Takahashi, M., Otsuki, A. and Ichimura, S., 1983. Measurement of photosynthetic production of a marine phytoplankton population using a stable 13 C isotope. *Marine Biology*, *73*(1), pp.31-36.

Hama, T.A.K.E.O., Hama, J.U.N.K.O. and Handa, N.O.B.U.H.I.K.O., 1993. 13C tracer methodology in microbial ecology with special reference to primary production.

Hamme, R.C. and Emerson, S.R., 2006. Constraining bubble dynamics and mixing with dissolved gases: Implications for productivity measurements by oxygen mass balance. *Journal of Marine Research*, *64*(1), pp.73-95.

Hamme, R.C., Cassar, N., Lance, V.P., Vaillancourt, R.D., Bender, M.L., Strutton, P.G., Moore, T.S., DeGrandpre, M.D., Sabine, C.L., Ho, D.T. and Hargreaves, B.R., 2012. Dissolved O2/Ar and other methods reveal rapid changes in productivity during a Lagrangian experiment in the Southern Ocean. *Journal of Geophysical Research: Oceans*, *117*(C4).

Hamme, R.C., Webley, P.W., Crawford, W.R., Whitney, F.A., DeGrandpre, M.D., Emerson, S.R., Eriksen, C.C., Giesbrecht, K.E., Gower, J.F., Kavanaugh, M.T. and Peña, M.A., 2010. Volcanic ash fuels anomalous plankton bloom in subarctic northeast Pacific. *Geophysical Research Letters*, *37*(19).

Hamme, R.C., 2003. *Applications of Neon, Nitrogen, Argon, and Oxygen to Physical, Chemical, and Biological Cycles in the Ocean* (Doctoral dissertation, University of Washington).

Hansell, D.A., Carlson, C.A., Repeta, D.J. and Schlitzer, R., 2009. Dissolved organic matter in the ocean: A controversy stimulates new insights. *Oceanography*, *22*(4), pp.202-211.

Harrison, P.J., Boyd, P.W., Varela, D.E., Takeda, S., Shiomoto, A. and Odate, T., 1999. Comparison of factors controlling phytoplankton productivity in the NE and NW subarctic Pacific gyres. *Progress in Oceanography*, *43*(2-4), pp.205-234.

Harrison, W.G., Platt, T. and Irwin, B., 1982. Primary production and nutrient assimilation by natural phytoplankton populations of the eastern Canadian Arctic. *Canadian journal of fisheries and aquatic sciences*, *39*(2), pp.335-345.

Haskell II, W.Z., Prokopenko, M.G., Hammond, D.E., Stanley, R.H., Berelson, W.M., Baronas, J.J., Fleming, J.C. and Aluwihare, L., 2016. An organic carbon budget for coastal Southern California determined by estimates of vertical nutrient flux, net community production and export. *Deep Sea Research Part I: Oceanographic Research Papers*, *116*, pp.49-76.

Helbling, E.W., Villafane, V., Ferrario, M. and Holm-Hansen, O., 1992. Impact of natural ultraviolet radiation on rates of photosynthesis and on specific marine phytoplankton species. *Marine Ecology Progress Series*, pp.89-100.

Hendricks, M.B., Bender, M.L., Barnett, B.A., Strutton, P. and Chavez, F.P., 2005. Triple oxygen isotope composition of dissolved O2 in the equatorial Pacific: A tracer of mixing, production, and respiration. *Journal of Geophysical Research: Oceans*, *110*(C12).

Henson, S.A., Sanders, R. and Madsen, E., 2012. Global patterns in efficiency of particulate organic carbon export and transfer to the deep ocean. *Global Biogeochemical Cycles*, *26*(1).

Henson, S.A., Sanders, R., Madsen, E., Morris, P.J., Le Moigne, F. and Quartly, G.D., 2011. A reduced estimate of the strength of the ocean's biological carbon pump. *Geophysical Research Letters*, *38*(4).

Hertz, E., Trudel, M., Tucker, S., Beacham, T.D., Parken, C., Mackas, D. and Mazumder, A., 2016. Influences of ocean conditions and feeding ecology on the survival of juvenile Chinook Salmon (Oncorhynchus tshawytscha). *Fisheries oceanography*, *25*(4), pp.407-419.

Hill, V.J., Matrai, P.A., Olson, E., Suttles, S., Steele, M., Codispoti, L.A. and Zimmerman, R.C., 2013. Synthesis of integrated primary production in the Arctic Ocean: II. In situ and remotely sensed estimates. *Progress in Oceanography*, *110*, pp.107-125.

Ho, D.T., Law, C.S., Smith, M.J., Schlosser, P., Harvey, M. and Hill, P., 2006. Measurements of air-sea gas exchange at high wind speeds in the Southern Ocean: Implications for global parameterizations. *Geophysical Research Letters*, *33*(16).

Holm-Hansen, O., Lorenzen, C.J., Holmes, R.W. and Strickland, J.D., 1965. Fluorometric determination of chlorophyll. *ICES Journal of Marine Science*, *30*(1), pp.3-15.

Holmes, R.M., Aminot, A., Kérouel, R., Hooker, B.A. and Peterson, B.J., 1999. A simple and precise method for measuring ammonium in marine and freshwater ecosystems. *Canadian Journal of Fisheries and Aquatic Sciences*, *56*(10), pp.1801-1808.

Horrigan, S.G., Carlucci, A.F., Williams, P.M., 1981. Light inhibition of nitrification in sea-surface films. *Journal of Marine Research,* 39, pp.557-565.

Houghton, R.A., 2007. Balancing the global carbon budget. *Annu. Rev. Earth Planet. Sci.*, *35*, pp.313-347.

Hughes, K.G., Klymak, J.M., Williams, W.J. and Melling, H., 2018. Tidally modulated internal hydraulic flow and energetics in the central Canadian Arctic Archipelago. *Journal of Geophysical Research: Oceans*, *123*(8), pp.5210-5229.

Ianson, D., Allen, S.E., Harris, S.L., Orians, K.J., Varela, D.E. and Wong, C.S., 2003. The inorganic carbon system in the coastal upwelling region west of Vancouver Island, Canada. *Deep Sea Research Part I: Oceanographic Research Papers*, *50*(8), pp.1023-1042.

Ianson, D., Feely, R.A., Sabine, C.L. and Juranek, L.W., 2009. Features of coastal upwelling regions that determine net air-sea CO 2 flux. *Journal of oceanography*, *65*(5), pp.677-687.

Izett, R.W., Manning, C.C., Hamme, R.C. and Tortell, P.D., 2018. Refined estimates of net community production in the Subarctic Northeast Pacific derived from ΔO2/Ar measurements with N2O-based corrections for vertical mixing. *Global Biogeochemical Cycles*, *32*(3), pp.326-350.

Johnson, W.K., Miller, L.A., Sutherland, N.E. and Wong, C.S., 2005. Iron transport by mesoscale Haida eddies in the Gulf of Alaska. *Deep Sea Research Part II: Topical Studies in Oceanography*, *52*(7-8), pp.933-953.

Johnson, K.S., Coletti, L.J. and Chavez, F.P., 2006. Diel nitrate cycles observed with in situ sensors predict monthly and annual new production. *Deep Sea Research Part I: Oceanographic Research Papers*, *53*(3), pp.561-573.

Johnston, T.M., Rudnick, D.L. and Pallàs-Sanz, E., 2011. Elevated mixing at a front. *Journal of Geophysical Research: Oceans*, *116*(C11).

Jonsson, B.F., Doney, S.C., Dunne, J. and Bender, M., 2013. Evaluation of the Southern Ocean O2/Ar-based NCP estimates in a model framework. *Journal of Geophysical Research: Biogeosciences*, *118*(2), pp.385-399.

Juranek, L.W. and Quay, P.D., 2005. In vitro and in situ gross primary and net community production in the North Pacific Subtropical Gyre using labeled and natural abundance isotopes of dissolved O2. *Global Biogeochemical Cycles*, *19*(3).

Juranek, L.W. and Quay, P.D., 2013. Using triple isotopes of dissolved oxygen to evaluate global marine productivity. *Annual Review of Marine Science*, *5*, pp.503-524.

Juranek, L.W., Quay, P.D., Feely, R.A., Lockwood, D., Karl, D.M. and Church, M.J., 2012. Biological production in the NE Pacific and its influence on air-sea CO2 flux:

Evidence from dissolved oxygen isotopes and O2/Ar. *Journal of Geophysical Research: Oceans*, *117*(C5).

Kaiser, J., 2011. Consistent calculation of aquatic gross production from oxygen triple isotope measurements. *Biogeosciences*, *8*(7), pp.1793-1811.

Karl, D.M. and Lukas, R., 1996. The Hawaii Ocean Time-series (HOT) program: Background, rationale and field implementation. *Deep Sea Research Part II: Topical Studies in Oceanography*, *43*(2-3), pp.129-156.

Keeling, C.D., Rakestraw, N.W. and Waterman, L.S., 1965. Carbon dioxide in surface waters of the Pacific Ocean: 1. Measurements of the distribution. *Journal of Geophysical Research*, *70*(24), pp.6087-6097.

Kirchman, D.L., Keil, R.G. and Wheeler, P.A., 1989. The effect of amino acids on ammonium utilization and regeneration by heterotrophic bacteria in the subarctic Pacific. *Deep Sea Research Part A. Oceanographic Research Papers*, *36*(11), pp.1763-1776.

Kirchman, D.L. and Wheeler, P.A., 1998. Uptake of ammonium and nitrate by heterotrophic bacteria and phytoplankton in the sub-Arctic Pacific. *Deep Sea Research Part I: Oceanographic Research Papers*, *45*(2-3), pp.347-365.

Knutson, T.R., McBride, J.L., Chan, J., Emanuel, K., Holland, G., Landsea, C., Held, I., Kossin, J.P., Srivastava, A.K. and Sugi, M., 2010. Tropical cyclones and climate change. *Nature geoscience*, *3*(3), p.157.

Kolber, Z., and P. G. Falkowski.1993 Use of active fluorescence to estimate phyto-plankton photosynthesis in situ, Limnol. Oceanogr., 38(8), 1646–1665, doi:10.4319/lo.1993.38.8.1646.

Krause, J.W., Nelson, D.M. and Brzezinski, M.A., 2011. Biogenic silica production and the diatom contribution to primary production and nitrate uptake in the eastern equatorial Pacific Ocean. *Deep Sea Research Part II: Topical Studies in Oceanography*, *58*(3-4), pp.434-448.

La Roche, J., Boyd, P.W., McKay, R.M.L. and Geider, R.J., 1996. Flavodoxin as an in situ marker for iron stress in phytoplankton. *Nature*, *382*(6594), p.802.

Ladd, C., Crawford, W.R., Harpold, C.E., Johnson, W.K., Kachel, N.B., Stabeno, P.J. and Whitney, F., 2009. A synoptic survey of young mesoscale eddies in the Eastern Gulf of Alaska. *Deep Sea Research Part II: Topical Studies in Oceanography*, *56*(24), pp.2460-2473.

Lam, P.J., Bishop, J.K., Henning, C.C., Marcus, M.A., Waychunas, G.A. and Fung, I.Y., 2006. Wintertime phytoplankton bloom in the subarctic Pacific supported by continental margin iron. *Global Biogeochemical Cycles*, *20*(1).

Landry, M.R., Monger, B.C. and Selph, K.E., 1993. Time-dependency of microzooplankton grazing and phytoplankton growth in the subarctic Pacific. *Progress in Oceanography*, *32*(1-4), pp.205-222.

Laws, E.A., 1991. Photosynthetic quotients, new production and net community production in the open ocean. *Deep Sea Research Part A. Oceanographic Research Papers*, *38*(1), pp.143-167.

Laws, E.A., Falkowski, P.G., Smith, W.O., Ducklow, H. and McCarthy, J.J., 2000. Temperature effects on export production in the open ocean. *Global Biogeochemical Cycles*, *14*(4), pp.1231-1246.

Laws, E.A., DiTullio, G.R. and Redalje, D.G., 1987. High phytoplankton growth and production rates in the North Pacific subtropical gyre 1, 2. *Limnology and Oceanography*, *32*(4), pp.905-918.

Le Moigne, F.A., Poulton, A.J., Henson, S.A., Daniels, C.J., Fragoso, G.M., Mitchell, E., Richier, S., Russell, B.C., Smith, H.E., Tarling, G.A. and Young, J.R., 2015. Carbon export efficiency and phytoplankton community composition in the Atlantic sector of the Arctic Ocean. *Journal of Geophysical Research: Oceans*, *120*(6), pp.3896-3912.

Lean, D.R.S. and Burnison, B.K., 1979. An evaluation of errors in the 14C method of primary production measurement. *Limnology and Oceanography*, *24*(5), pp.917-928.

Legendre, L. and Gosselin, M., 1989. New production and export of organic matter to the deep ocean: consequences of some recent discoveries. *Limnology and Oceanography*, *34*(7), pp.1374-1380.

Levy, R.C., Mattoo, S., Munchak, L.A., Remer, L.A., Sayer, A.M., Patadia, F. and Hsu, N.C., 2013. The Collection 6 MODIS aerosol products over land and ocean. *Atmospheric Measurement Techniques*, *6*(11), p.2989.

Luz, B. and Barkan, E., 2000. Assessment of oceanic productivity with the triple-isotope composition of dissolved oxygen. *Science*, *288*(5473), pp.2028-2031.

Luz, B. and Barkan, E., 2009. Net and gross oxygen production from O2/Ar, 17O/16O and 18O/16O ratios. *Aquatic Microbial Ecology*, *56*(2-3), pp.133-145.

Luz, B. and Barkan, E., 2011. The isotopic composition of atmospheric oxygen. *Global Biogeochemical Cycles*, *25*(3).

Luz, B., Barkan, E., Bender, M.L., Thiemens, M.H. and Boering, K.A., 1999. Triple-isotope composition of atmospheric oxygen as a tracer of biosphere productivity. *Nature*, *400*(6744), p.547.

Luz, B. and Barkan, E., 2005. The isotopic ratios 17O/16O and 18O/16O in molecular oxygen and their significance in biogeochemistry. *Geochimica et Cosmochimica Acta*, *69*(5), pp.1099-1110.

Mackas, D.L., 1992. Seasonal cycle of zooplankton off southwestern British Columbia: 1979–89. *Canadian Journal of Fisheries and Aquatic Sciences*, *49*(5), pp.903-921.

Manning, C.C., Howard, E.M., Nicholson, D.P., Ji, B.Y., Sandwith, Z.O. and Stanley, R.H., 2017. Revising estimates of aquatic gross oxygen production by the triple oxygen isotope method to incorporate the local isotopic composition of water. *Geophysical Research Letters*, *44*(20), pp.10-511.

Marchetti, A., Sherry, N.D., Kiyosawa, H., Tsuda, A. and Harrison, P.J., 2006. Phytoplankton processes during a mesoscale iron enrichment in the NE subarctic Pacific: Part I—Biomass and assemblage. *Deep Sea Research Part II: Topical Studies in Oceanography*, *53*(20-22), pp.2095-2113.

Maritorena, S., d'Andon, O.H.F., Mangin, A. and Siegel, D.A., 2010. Merged satellite ocean color data products using a bio-optical model: Characteristics, benefits and issues. *Remote Sensing of Environment*, *114*(8), pp.1791-1804.

Marra, J., 2009. Net and gross productivity: weighing in with 14C. *Aquatic Microbial Ecology*, *56*(2-3), pp.123-131.

Marra, J., 2002. Approaches to the measurement of plankton production. *Phytoplankton productivity: Carbon assimilation in marine and freshwater ecosystems*, pp.78-108.

Matrai, P.A., Olson, E., Suttles, S., Hill, V., Codispoti, L.A., Light, B. and Steele, M., 2013. Synthesis of primary production in the Arctic Ocean: I. Surface waters, 1954–2007. *Progress in Oceanography*, *110*, pp.93-106.

Maritorena, S., Siegel, D.A. and Peterson, A.R., 2002. Optimization of a semianalytical ocean color model for global-scale applications. *Applied optics*, *41*(15), pp.2705-2714.

Martin, J.H., Gordon, R.M., Fitzwater, S. and Broenkow, W.W., 1989. VERTEX: phytoplankton/iron studies in the Gulf of Alaska. *Deep Sea Research Part A. Oceanographic Research Papers*, *36*(5), pp.649-680.

Miller, C.B., Frost, B.W., Wheeler, P.A., Landry, M.R., Welschmeyer, N. and Powell, T.M., 1991. Ecological dynamics in the subarctic Pacific, a possibly iron-limited ecosystem. *Limnology and Oceanography*, *36*(8), pp.1600-1615.

Molemaker, M.J., McWilliams, J.C. and Capet, X., 2010. Balanced and unbalanced routes to dissipation in an equilibrated Eady flow. *Journal of Fluid Mechanics*, *654*, pp.35-63.

Moran, S.B., Ellis, K.M. and Smith, J.N., 1997. 234Th/238U disequilibrium in the central Arctic Ocean: implications for particulate organic carbon export. *Deep Sea Research Part II: Topical Studies in Oceanography*, *44*(8), pp.1593-1606.

Mousseau, L., Dauchez, S., Legendre, L. and Fortier, L., 1995. Photosynthetic carbon uptake by marine phytoplankton: comparison of the stable (13C) and radioactive (14C) isotope methods. *Journal of plankton research*, *17*(7), pp.1449-1460.

Munro, D.R., Quay, P.D., Juranek, L.W. and Goericke, R., 2013. Biological production rates off the Southern California coast estimated from triple O2 isotopes and O2: Ar gas ratios. *Limnology and Oceanography*, *58*(4), pp.1312-1328.

Nayar, S. and Chou, L.M., 2003. Relative efficiencies of different filters in retaining phytoplankton for pigment and productivity studies. *Estuarine, Coastal and Shelf Science*, *58*(2), pp.241-248.

Nicholson, D., Stanley, R.H. and Doney, S.C., 2014. The triple oxygen isotope tracer of primary productivity in a dynamic ocean model. *Global Biogeochemical Cycles*, *28*(5), pp.538-552.

Nicholson, D.P., Stanley, R.H., Barkan, E., Karl, D.M., Luz, B., Quay, P.D. and Doney, S.C., 2012. Evaluating triple oxygen isotope estimates of gross primary production at the Hawaii Ocean Time-series and Bermuda Atlantic Time-series Study sites. *Journal of Geophysical Research: Oceans*, *117*(C5).

Nielsen, E.S., 1952. The use of radio-active carbon (C^) for measuring organic production in the sea. *Journal de Conseil*, *18*, pp.117-140.

Nier, A.O. and Gulbransen, E.A., 1939. Variations in the relative abundance of the carbon isotopes. *Journal of the American Chemical Society*, *61*(3), pp.697-698.

Nishioka, J., Takeda, S., Wong, C.S. and Johnson, W.K., 2001. Size-fractionated iron concentrations in the northeast Pacific Ocean: distribution of soluble and small colloidal iron. *Marine Chemistry*, *74*(2-3), pp.157-179.

O'Reilly, J.E., and 24 Coauthors, 2000: SeaWiFS Postlaunch Calibration and Validation Analyses, Part 3. NASA Tech. Memo. 2000-206892, Vol. 11, S.B. Hooker and E.R. Firestone, Eds., NASA Goddard Space Flight Center.
http://oceancolor.gsfc.nasa.gov/cms/reprocessing/r2009/ocv6

Palevsky, H.I., Quay, P.D., Lockwood, D.E. and Nicholson, D.P., 2016. The annual cycle of gross primary production, net community production, and export efficiency across the North Pacific Ocean. *Global Biogeochemical Cycles*, *30*(2), pp.361-380.

Parslow, J.S., 1981. *Phytoplankton-zooplankton interactions: data analysis and modelling (with particular reference to Ocean Station P (50ºN, 145ºW) and controlled*

ecosystem experiments) (Doctoral dissertation, University of British Columbia).

Parsons, T. R., Y. Maita, and C. M. Lalli. 1984. A manual of chemical and biological methods for seawater analysis. Pergamon Press.

Passow, U. and Carlson, C.A., 2012. The biological pump in a high CO2 world. *Marine Ecology Progress Series*, *470*, pp.249-271.

Pawan K. Bhartia (2012), OMI/Aura TOMS-Like Ozone, Aerosol Index, Cloud Radiance Fraction L3 1 day 1 degree x 1 degree V3, NASA Goddard Space Flight Center, Goddard Earth Sciences Data and Information Services Center (GES DISC), Accessed: **[*5July2017*]**, 10.5067/Aura/OMI/DATA3001.

Pelland, N.A., Eriksen, C.C. and Cronin, M.F., 2016. Seaglider surveys at Ocean Station Papa: Circulation and water mass properties in a meander of the North Pacific Current. *Journal of Geophysical Research: Oceans*, *121*(9), pp.6816-6846.

Pelland, N.A., Eriksen, C.C., Emerson, S.R. and Cronin, M.F., 2018. Seaglider Surveys at Ocean Station Papa: Oxygen Kinematics and Upper-Ocean Metabolism. *Journal of Geophysical Research: Oceans*, *123*(9), pp.6408-6427.

Peña, M.A. and Varela, D.E., 2007. Seasonal and interannual variability in phytoplankton and nutrient dynamics along Line P in the NE subarctic Pacific. *Progress in Oceanography*, *75*(2), pp.200-222.

Peña, M.A., Nemcek, N. and Robert, M., 2019. Phytoplankton responses to the 2014–2016 warming anomaly in the northeast subarctic Pacific Ocean. *Limnology and Oceanography*, *64*(2), pp.515-525.

Platnick, S., P. Hubanks, K. Meyer, and M. D. King, 2015: MODIS Atmosphere L3 Monthly Product (08_L3). NASA MODIS Adaptive Processing System, Goddard Space Flight Center.

Platt, T., Harrison, W.G., Lewis, M.R., Li, W.K., Sathyendranath, S., Smith, R.E. and Vezina, A.F., 1989. Biological production of the oceans: the case for a consensus. *Marine Ecology Progress Series*, pp.77-88.

Portner, H.-O., Karl, D., Boyd, P. W., Cheung, W., Lluch-Cota, S. E., Nojiri, Y., et al. (2014). "Ocean systems," in *Climate Change 2014: Impacts, Adaptation, and Vulnerability. Part A: Global and Sectoral Aspects. Contribution of Working Group II to the Fifth Assessment Report of the Intergovernmental Panel on Climate Change,* eds C. B. Field, V. R. Barros, D. J. Dokken, K. J. Mach, M. D. Mastrandrea, T. E. Bilir et al. (Cambridge, UK; New York, NY: Cambridge University Press), 411–484.

Power, M.E., 1992. Top-down and bottom-up forces in food webs: do plants have primacy. *Ecology*, *73*(3), pp.733-746.

Prokopenko, M.G., Pauluis, O.M., Granger, J. and Yeung, L.Y., 2011. Exact evaluation of gross photosynthetic production from the oxygen triple-isotope composition of O2: Implications for the net-to-gross primary production ratios. *Geophysical research letters*, *38*(14).

Quay, P.D., Peacock, C., Björkman, K. and Karl, D.M., 2010. Measuring primary production rates in the ocean: Enigmatic results between incubation and non-incubation methods at Station ALOHA. *Global Biogeochemical Cycles*, *24*(3).

Rao, D.S. and Platt, T., 1984. Primary production of Arctic waters. *Polar Biology*, *3*(4), pp.191-201.

Regaudie-de-Gioux, A., Lasternas, S., Agustí, S. and Duarte, C.M., 2014. Comparing marine primary production estimates through different methods and development of conversion equations. *Frontiers in Marine Science*, *1*, p.19.

Reuer, M.K., Barnett, B.A., Bender, M.L., Falkowski, P.G. and Hendricks, M.B., 2007. New estimates of Southern Ocean biological production rates from O2/Ar ratios and the triple isotope composition of O2. *Deep Sea Research Part I: Oceanographic Research Papers*, *54*(6), pp.951-974.

Ribalet, F., Marchetti, A., Hubbard, K.A., Brown, K., Durkin, C.A., Morales, R., Robert, M., Swalwell, J.E., Tortell, P.D. and Armbrust, E.V., 2010. Unveiling a phytoplankton hotspot at a narrow boundary between coastal and offshore waters. *Proceedings of the National Academy of Sciences*, *107*(38), pp.16571-16576.

Robinson, C., Tilstone, G.H., Rees, A.P., Smyth, T.J., Fishwick, J.R., Tarran, G.A., Luz, B., Barkan, E. and David, E., 2009. Comparison of in vitro and in situ plankton production determinations. *Aquatic microbial ecology*, *54*(1), pp.13-34.

Sakshaug, E., 2004. Primary and secondary production in the Arctic Seas. In *The organic carbon cycle in the Arctic Ocean* (pp. 57-81). Springer, Berlin, Heidelberg.

Sharqawy, M.H., Lienhard, J.H. and Zubair, S.M., 2010. Thermophysical properties of seawater: a review of existing correlations and data. *Desalination and water treatment*, *16*(1-3), pp.354-380.

Siegel, D.A., Buesseler, K.O., Doney, S.C., Sailley, S.F., Behrenfeld, M.J. and Boyd, P.W., 2014. Global assessment of ocean carbon export by combining satellite observations and food-web models. *Global Biogeochemical Cycles*, *28*(3), pp.181-196.

Slawyk, G., Collos, Y. and Auclair, J.C., 1977. The use of the 13C and 15N isotopes for the simultaneous measurement of carbon and nitrogen turnover rates in marine phytoplankton 1. *Limnology and Oceanography*, *22*(5), pp.925-932.

Smith, J.M., Chavez, F.P. and Francis, C.A., 2014. Ammonium uptake by phytoplankton regulates nitrification in the sunlit ocean. *PLoS One*, *9*(9), p.e108173.

Stanley, R.H., Sandwith, Z.O. and Williams, W.J., 2015. Rates of summertime biological productivity in the Beaufort Gyre: A comparison between the low and record-low ice conditions of August 2011 and 2012. *Journal of Marine Systems*, *147*, pp.29-44.

Sydeman, W.J., Thompson, S.A., Field, J.C., Peterson, W.T., Tanasichuk, R.W., Freeland, H.J., Bograd, S.J. and Rykaczewski, R.R., 2011. Does positioning of the North Pacific Current affect downstream ecosystem productivity?. *Geophysical Research Letters*, *38*(12).

Tabata, S., 1982. The anticyclonic, baroclinic eddy off Sitka, Alaska, in the northeast Pacific Ocean. *Journal of Physical Oceanography*, *12*(11), pp.1260-1282.

Tang, C.C., Ross, C.K., Yao, T., Petrie, B., DeTracey, B.M. and Dunlap, E., 2004. The circulation, water masses and sea-ice of Baffin Bay. *Progress in Oceanography*, *63*(4), pp.183-228.

Teeter, L., Hamme, R.C., Ianson, D. and Bianucci, L., 2018. Accurate estimation of net community production from O2/Ar measurements. *Global Biogeochemical Cycles*, *32*(8), pp.1163-1181.

Thiemens, M.H., Jackson, T., Zipf, E.C., Erdman, P.W. and van Egmond, C., 1995. Carbon dioxide and oxygen isotope anomalies in the mesosphere and stratosphere. *Science*, *270*(5238), pp.969-972.

Torres-Valdés, S., Tsubouchi, T., Bacon, S., Naveira-Garabato, A.C., Sanders, R., McLaughlin, F.A., Petrie, B., Kattner, G., Azetsu-Scott, K. and Whitledge, T.E., 2013. Export of nutrients from the Arctic Ocean. *Journal of Geophysical Research: Oceans*, *118*(4), pp.1625-1644.

Tortell, P.D., Merzouk, A., Ianson, D., Pawlowicz, R. and Yelland, D.R., 2012. Influence of regional climate forcing on surface water pCO2, ΔO2/Ar and dimethylsulfide (DMS) along the southern British Columbia coast. *Continental Shelf Research*, *47*, pp.119-132.

Tremblay, J.É., Anderson, L.G., Matrai, P., Coupel, P., Bélanger, S., Michel, C. and Reigstad, M., 2015. Global and regional drivers of nutrient supply, primary production and CO2 drawdown in the changing Arctic Ocean. *Progress in Oceanography*, *139*, pp.171-196.

Ulfsbo, A., Cassar, N., Korhonen, M., van Heuven, S., Hoppema, M., Kattner, G. and Anderson, L.G., 2014. Late summer net community production in the central Arctic Ocean using multiple approaches. *Global Biogeochemical Cycles*, *28*(10), pp.1129-1148.

Varela, D.E. and Harrison, P.J., 1999. Seasonal variability in nitrogenous nutrition of

phytoplankton assemblages in the northeastern subarctic Pacific Ocean. *Deep Sea Research Part II: Topical Studies in Oceanography*, *46*(11-12), pp.2505-2538.

Varela, D.E., Crawford, D.W., Wrohan, I.A., Wyatt, S.N. and Carmack, E.C., 2013. Pelagic primary productivity and upper ocean nutrient dynamics across Subarctic and Arctic Seas. *Journal of Geophysical Research: Oceans*, *118*(12), pp.7132-7152.

Verity, P.G. and Smetacek, V., 1996. Organism life cycles, predation, and the structure of marine pelagic ecosystems. *Marine Ecology Progress Series*, *130*, pp.277-293.

Volk, T., & Hoffert, M. I. (1985). Ocean carbon pumps: Analysis of relative strengths and efficiencies in ocean- driven atmospheric CO2 changes. *The Carbon Cycle and Atmospheric CO: Natural Variations Archean to Present*, 99-110.

Watson, A.J., Robinson, C., Robinson, J.E., Williams, P.L.B. and Fasham, M.J.R., 1991. Spatial variability in the sink for atmospheric carbon dioxide in the North Atlantic. *Nature*, *350*(6313), p.50.

Welschmeyer, N.A., Strom, S., Goericke, R., DiTullio, G., Belvin, M. and Petersen, W., 1993. Primary production in the subarctic Pacific Ocean: Project SUPER. *Progress in Oceanography*, *32*(1-4), pp.101-135.

Westberry, T., Behrenfeld, M.J., Siegel, D.A. and Boss, E., 2008. Carbon-based primary productivity modeling with vertically resolved photoacclimation. *Global Biogeochemical Cycles*, *22*(2).

Whitney, F.A., Wong, C.S. and Boyd, P.W., 1998. Interannual variability in nitrate supply to surface waters of the Northeast Pacific Ocean. *Marine Ecology Progress Series*, *170*, pp.15-23.

Whitney, F.A. and Freeland, H.J., 1999. Variability in upper-ocean water properties in the NE Pacific Ocean. *Deep Sea Research Part II: Topical Studies in Oceanography*, *46*(11-12), pp.2351-2370.

Whitney, F.A., 2015. Anomalous winter winds decrease 2014 transition zone productivity in the NE Pacific. *Geophysical Research Letters*, *42*(2), pp.428-431.

Wilson, S.E., Ruhl, H.A. and Smith, Jr, K.L., 2013. Zooplankton fecal pellet flux in the abyssal northeast Pacific: A 15 year time-series study. *Limnology and Oceanography*, *58*(3), pp.881-892.

Wong, C.S., Whitney, F.A., Iseki, K., Page, J.S. and Zeng, J., 1995. Analysis of trends in primary productivity and chlorophyll-a over two decades at Ocean Station P (50 N, 145 W) in the subarctic northeast Pacific Ocean. *Canadian Special Publication of Fisheries and Aquatic Sciences*, pp.107-117.

Yamamoto-Kawai, M., Carmack, E. and McLaughlin, F., 2006. Nitrogen balance and Arctic throughflow. *Nature*, *443*(7107), p.43.

Yang, B., Emerson, S.R. and Peña, M.A., 2018. The effect of the 2013–2016 high temperature anomaly in the subarctic Northeast Pacific (the "Blob") on net community production. *Biogeosciences*, *15*(21), pp.6747-6759.

Yoder, J.A., 1979. Effect of temperature on light-limited growth and chemical composition of Skeletonema costatum (Bacillariophyceae) 1. *Journal of Phycology*, *15*(4), pp.362-370.

Yool, A., Martin, A.P., Fernández, C. and Clark, D.R., 2007. The significance of nitrification for oceanic new production. *Nature*, *447*(7147), p.999.

Yumimoto, K., Tanaka, T. Y., Oshima, N., and Maki, T., 2017. JRAero: the Japanese Reanalysis for Aerosol v1.0, *Geosci. Model Dev.*, 10, pp. 3225-3253, doi:10.5194/gmd-10-3225-2017.

Zlotnicki, Victor; Qu, Zheng; Willis, Joshua. 2016. JPL MEaSUREs Gridded Sea Surface Height Anomalies Interim Version 1609. Ver. 1609. PO.DAAC, CA, USA. Dataset accessed [YYYY-MM-DD] at http://dx.doi.org/10.5067/SLINT-CDRV1.

Appendix A. Weighted gas transfer velocity

A.1 Objective

The objective of this section is to assess how different wind products for the Arctic affect the gas transfer velocity, k. There are no wind stations near the study site to assess wind product accuracy, so we use the average of several wind products help to account for variation in this parameter, used in both of the in situ methods.

A.2 Results

Considerable variation exists among the different products, particularly with the Canadian Arctic Archipelago. However, none of the wind products is uniformly biased high or low (Figure A1). Final gas transfer velocities were insensitive to 30 day versus 60 day weighting (Table A1).

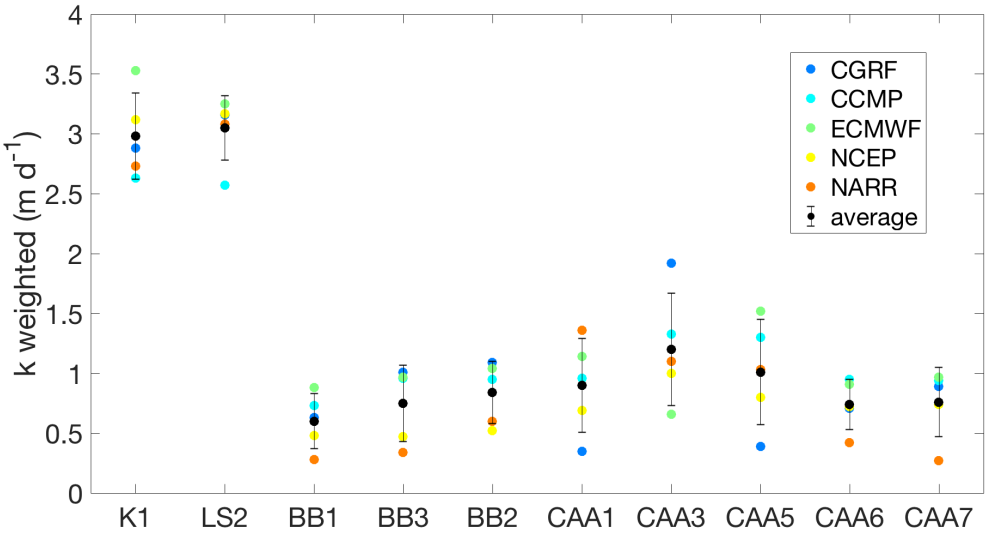

Figure A1. The weighted gas transfer velocity (30 day) for 5 wind products (CGRF, CCMP, ECMWF, NCEP and NARR) across the cruise track. The average of the 5 with standard deviation is also plotted.

Table A1. Weighted gas transfer velocities (k) using CCMP and NCEP wind products with both 30 or 60 day weighting at each station for the sampling time.

		K1	LS2	BB1	BB3	BB2	CAA1	CAA3	CAA5	CAA6	CAA7
CCMP	K_weight (30 days)	2.63	2.57	0.73	0.96	0.95	0.96	1.33	1.31	0.95	0.94
	K_weight (60 days)	2.63	2.52	0.73	0.94	1.00	0.98	1.31	1.29	0.95	0.94
NCEP	K_weight (30 days)	3.12	3.17	0.48	0.47	0.52	0.69	1.00	0.81	0.72	0.74
	K_weight (60 days)	3.10	3.06	0.48	0.47	0.59	0.75	0.99	0.83	0.72	0.74

Appendix B-1. Calculating new production

B-1.1 Objective

To compare the two methods for calculating new production and assess the effect on method comparison.

B-1.2 Results

There are two ways to calculate new production, each with different assumptions, so differences between them may help to explain observed biases. This study calculated new production by converting nitrate uptake to carbon uptake using the measured C:N ratios from each sample. This method ignores how much production came from other nitrogen

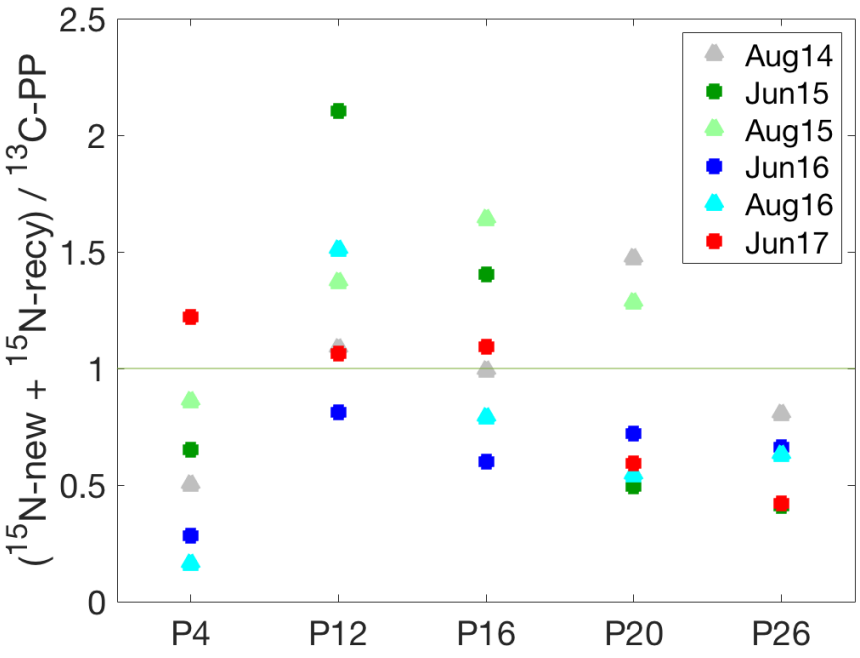

Figure B1. The ratio of the sum of nitrate and ammonium uptake (in C units using the measured C:N ratio of the particles) to carbon uptake across Line P. When below 1, the sum is less than carbon uptake, indicating other fixed nitrogen species are likely important. When above 1, the sum is more than carbon uptake, indicating a bias of some sort.

sources as a function of the total amount of carbon uptake. There are four instances where the sum of nitrate and ammonium uptake is at least 1.5 times more than carbon uptake (Figure B1). In this case, perhaps phytoplankton were taking up and storing nitrogen but not using it for primary production. There are 6 instances where the sum of nitrate and ammonium uptake is less than 0.5 times the carbon uptake.

New production can also be calculated by multiplying carbon uptake by the f-ratio. For this study, only nitrate and ammonium species were included so the f-ratio is an

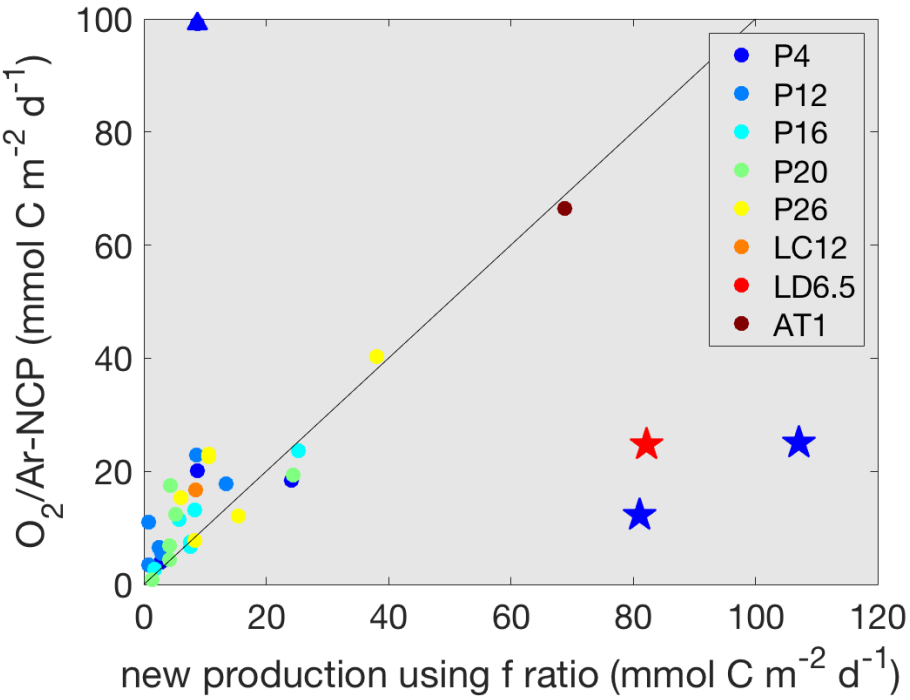

Figure B2. O_2/Ar-NCP versus new production versus where new production was calculated by multiplying ^{13}C-PP by the f-ratio. Stations likely influenced by recent upwelling are indicated by stars. P4 from August 2016 is indicated by a triangle.

overestimate. Varela and Harrison (1999) found uptake for ammonium, urea, and nitrate was 55%, 24%, and 21%, respectively in this region. When urea is ignored, the f-ratio is overestimated by about 36% (Varela and Harrison, 1999). Since our study did not

measure all nitrogen species, using the f-ratio likely adds more uncertainty. On the other hand, when only using nitrate uptake, there are no assumptions about what the total nitrogen sources contribute. When using the f-ratio to calculate ^{15}N-new, ^{15}N-new$_{f\text{-}ratio}$ tends to be higher when rates are higher and to lie closer to the 1:1 relationship with O_2/Ar-NCP, implying that the error due to not considering other nitrogen sources is similar to the error due to excretion of DON (Figure B2). Interestingly, the P4 station that was at the end of the bloom (Section 3.4.5) has lower ^{15}N-new when calculated this way. However, two outliers where O_2/Ar-NCP was higher than ^{15}N-new now fall on the 1:1 line. Upwelling conditions and station P4 in August 2016 still stand out as outliers.

Appendix B-2. Trace metals

B-2.1 Objective

To explore the effect of trace metal contamination during sampling and incubation.

B-2.2 Results

Contamination by trace metals and toxins from sampling can have an impact on productivity rates. Rubber and metal can be toxic to phytoplankton (Laws et al., 1987). Most Niskin closure mechanisms are made of coated metal springs, which could introduce trace metals to the sample water. Black rubber is used for Niskin O-rings, which is a larger source of contamination. Chavez and Barber (1987) show severe primary production inhibition from samples collected using Niskins compared to buckets and Go-FLO bottles. Further, Martin et al. (1993) found increased Zn concentrations in samples collected using standard Niskins compared to other methods, resulting in about a 25% decrease in primary production. This Zn poisoning likely results from the ZnO used in the manufacturing process of the rubber (Martin et al., 1993). We collected trace metal measurements from standard Niskin bottles before modification and compared to trace metal clean collection using pumps during June 2015. At P26, dissolved Zn and Fe concentrations from the ship's CTD Niskin system were 9.62±0.2 nmol/L and 223±29 pmol/L, respectively, compared to concentrations of 0.16±0.01 nmol/L and 54±18 pmol/L, respectively, using the trace metal clean sampling system (personal communication-Ben Twining and Peter Morton).

Studies show that 24 hours (the time of our incubations) is too short for phytoplankton to alter their physiology enough to affect incubation results. We found an order of magnitude increase in iron concentrations in the incubations even with acid washing all

sampling and incubation supplies. Schuback et al. (2015) shows that parameters such as the maximum quantum yield of PSII photochemistry and the fraction of irradiance absorbed by PSII change during iron addition experiments along Line P; however, chlorophyll did not respond rapidly in these experiments. Boyd et al. (1996) also show no change in chlorophyll for all size fractions until day 4 after an iron fertilization. In fact, some studies use 24 hours after addition as the first time point for a control for iron enrichment Lagrangian studies (Marchetti et al., 2006). Even if enough iron was added to cause a physiological change in phytoplankton, the incubations should not have been impacted within 24 hours. Maldonado et al. (1999) suggests a greater iron stimulation effect on ^{13}C-PP deeper in the water column. However, since the majority of our work is depth integrated only to the mixed layer, we expect little impact.

The standard Niskins were modified starting in June 2016 with Niskin closure mechanisms of silicon tubing and with the black O-rings replaced by non-toxic Viton O-rings. A comparison between unmodified and modified Niskins for ^{13}C-PP showed no statistical difference between the modified and unmodified Niskins based on the Wilcoxon statistic.

Appendix B-3. ^{18}O-GPP and ^{13}C-PP

B-3.1 Objective

This section explores whether ^{18}O-GPP and ^{13}C-PP converge at depth, similar to other studies.

B-3.2 Results

In our study, the specific light level of the incubation appears less important to the difference between the ^{18}O-GPP and ^{13}C-PP than the absolute rate (Figure B3). There is a strong linear relationship between the difference between methods and the absolute ^{18}O-GPP rate, such that the closer a point is to 0, the more similar the two rates are to each other. The one exception is at higher rates that correspond to P4 from August 2016 (see Section 3.4.5). However, the strong linearity with an intercept near zero demonstrates that the relationship between the two methods where ^{18}O-GPP is about twice ^{13}C-PP is maintained to the lowest rates in our study, in contrast to observations at Hawaii Ocean Time-series (Juranek and Quay, 2005; Quay et al., 2010).

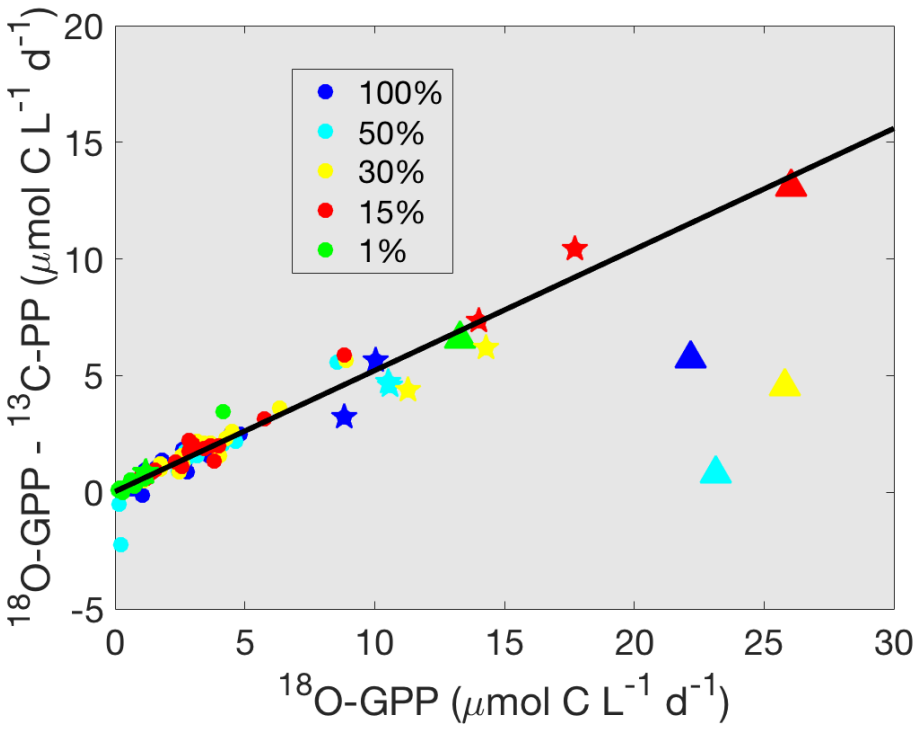

Figure B3. The difference between ^{18}O-GPP and ^{13}C-PP as a function of ^{18}O-GPP, where color indicates light level. These data are on a volumetric depth by depth basis and show the five different light levels for the incubations. ^{18}O-GPP was converted to oxygen units using a PQ of 1.25. The black line is the best fit line excluding the three outliers.

Appendix C. Satellite and model data

C.1 Objective

The first goal of this section is to assess satellite data accuracy by comparing to shipboard data. The second goal is to further examine June 2017 for chlorophyll-a (GlobColor) and the location of fronts, similar to the analysis in the main paper for June 2015/2016. The third goal is to explore multiple satellite measurements to see if dust deposition could have caused the variability in chlorophyll-a that was observed offshore during this study.

C.2 Results

GlobColor's estimate of surface chlorophyll-a was not biased high or low compared to shipboard data (Figure C1). The Mercator model SST is highly correlated with shipboard sea surface temperature (Figure C2). There was very little surface chlorophyll-a offshore and no fronts were present offshore as defined in the methods (Figure C3). Dust deposition cannot explain the variability in chlorophyll-a that was observed offshore (Figures C4-6).

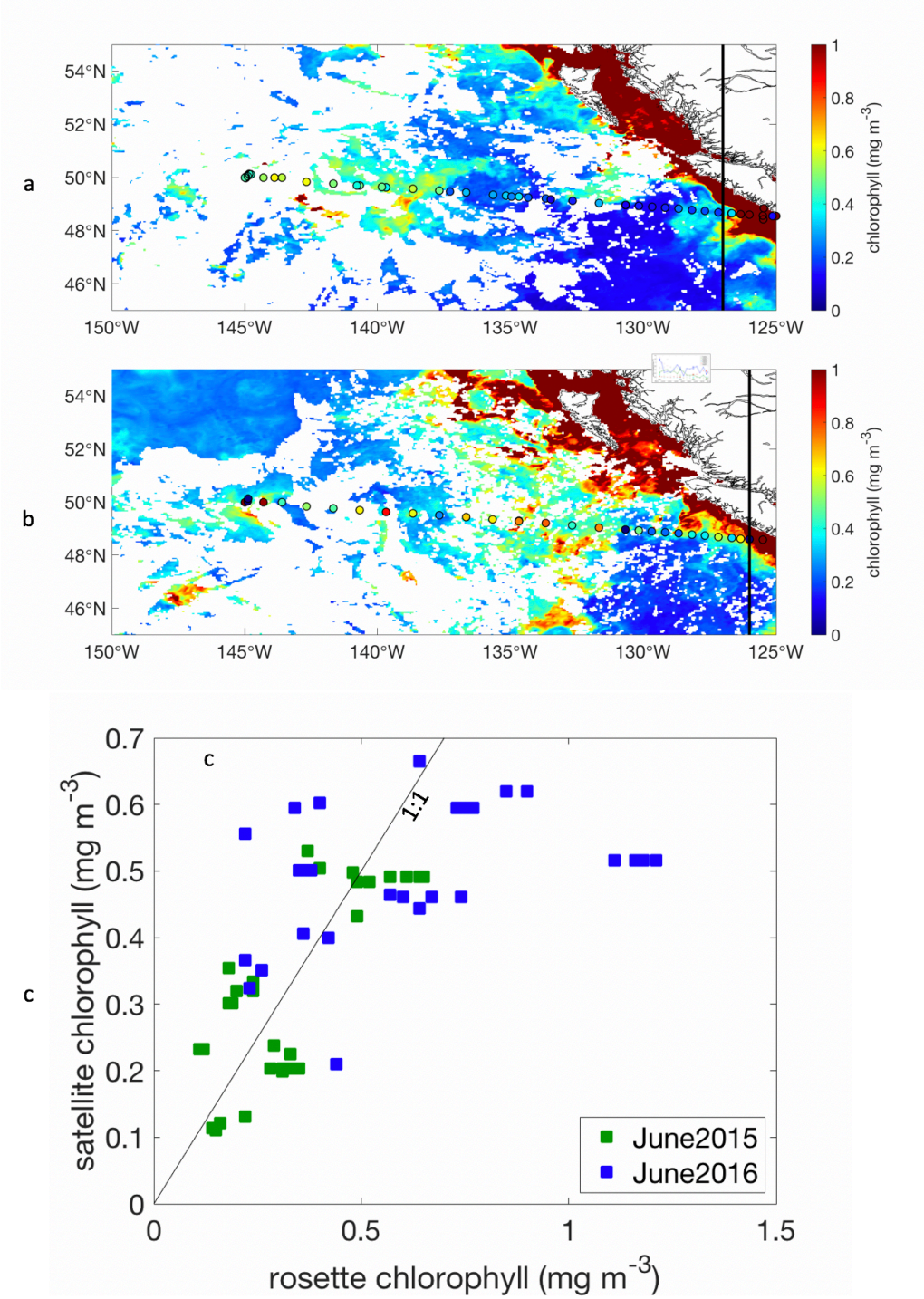

Figure C1. The background color is surface chlorophyll from GlobColour with colored circled from shipboard chlorophyll for (a) June 2015 (b) June 2016. When the circles disappear into the background, the satellite agrees well with shipboard. (c) Rosette compared to satellite chlorophyll comparison show the satellite chlorophyll is not biased high or low. The black line is the 1:1. R^2 for both years combined is 0.45. For each cast where rosette chlorophyll samples were collected,

one satellite chlorophyll was determined. However, when multiple rosette chlorophyll samples were some collected at one station, the same satellite data point applies to each. This explains the appearance of horizontal lines in the data, reflecting the chlorophyll variability at one station.

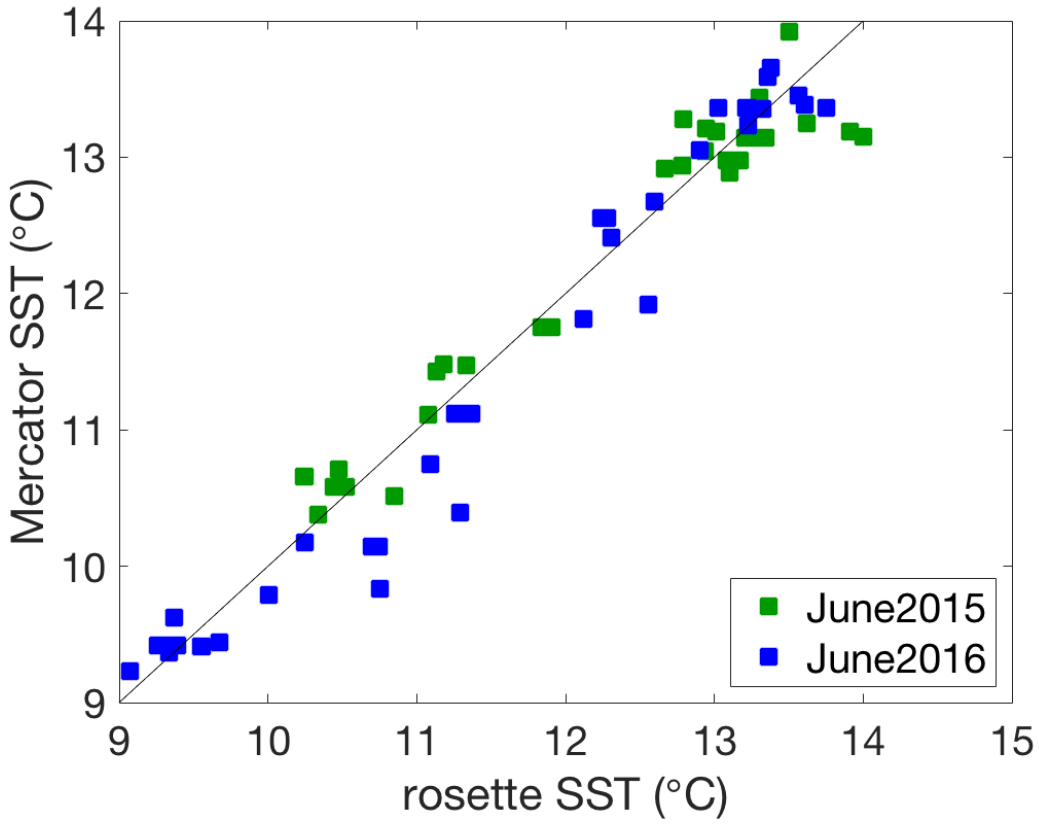

Figure C2. Rosette surface temperature versus Mercator sea surface temperature for all stations west of 127.5°W and 126°W during June 2015 and June 2016, respectively. June 2015 and June 2016 had strong relationship with R^2 of 0.97 and 0.96, respectively.

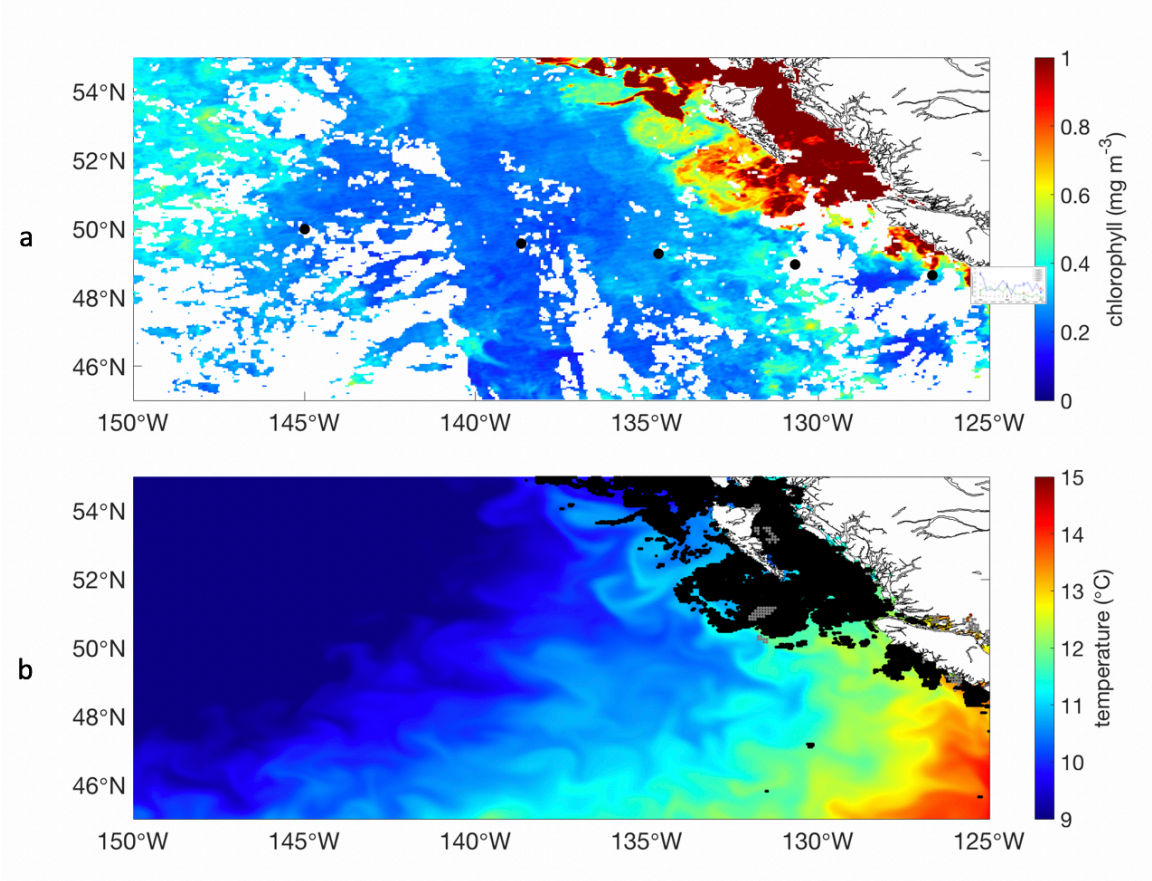

Figure C3. (a) 8 day average surface chlorophyll satellite data from GlobColour for 10-17 June 2017. (b) Background colours are Mercator sea surface temperature for 13June2017. Black dots indicate surface chlorophyll above 0.6 mg m^{-3}. Grey dots indicate front locations based on a criterion of 1°C temperature change over 1/3 degree distance.

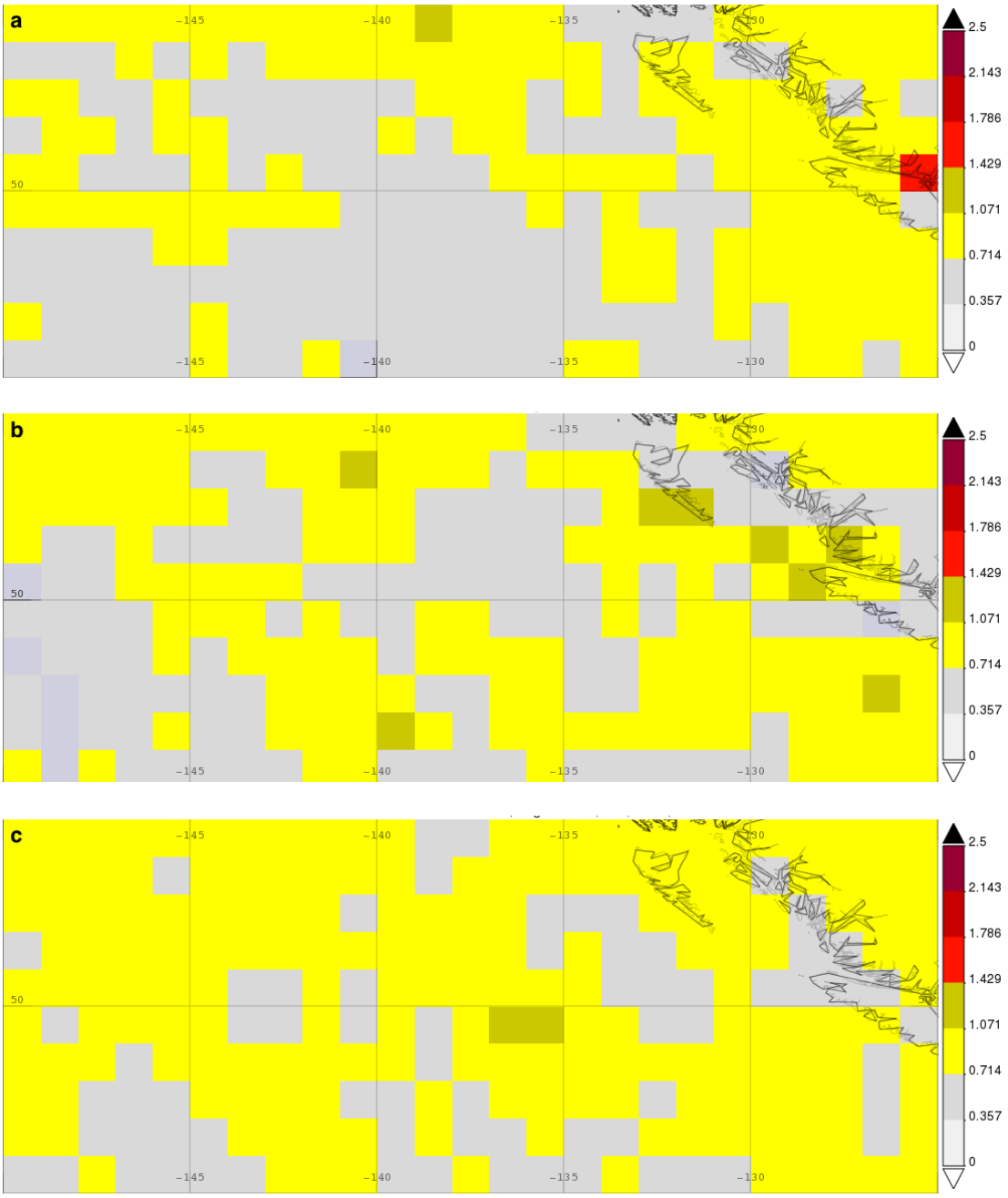

Figure C4. June averaged OMI aerosol index for (a) 2015, (b) 2016, and (c) 2017. Data were downloaded from NASA's Giovanni website.

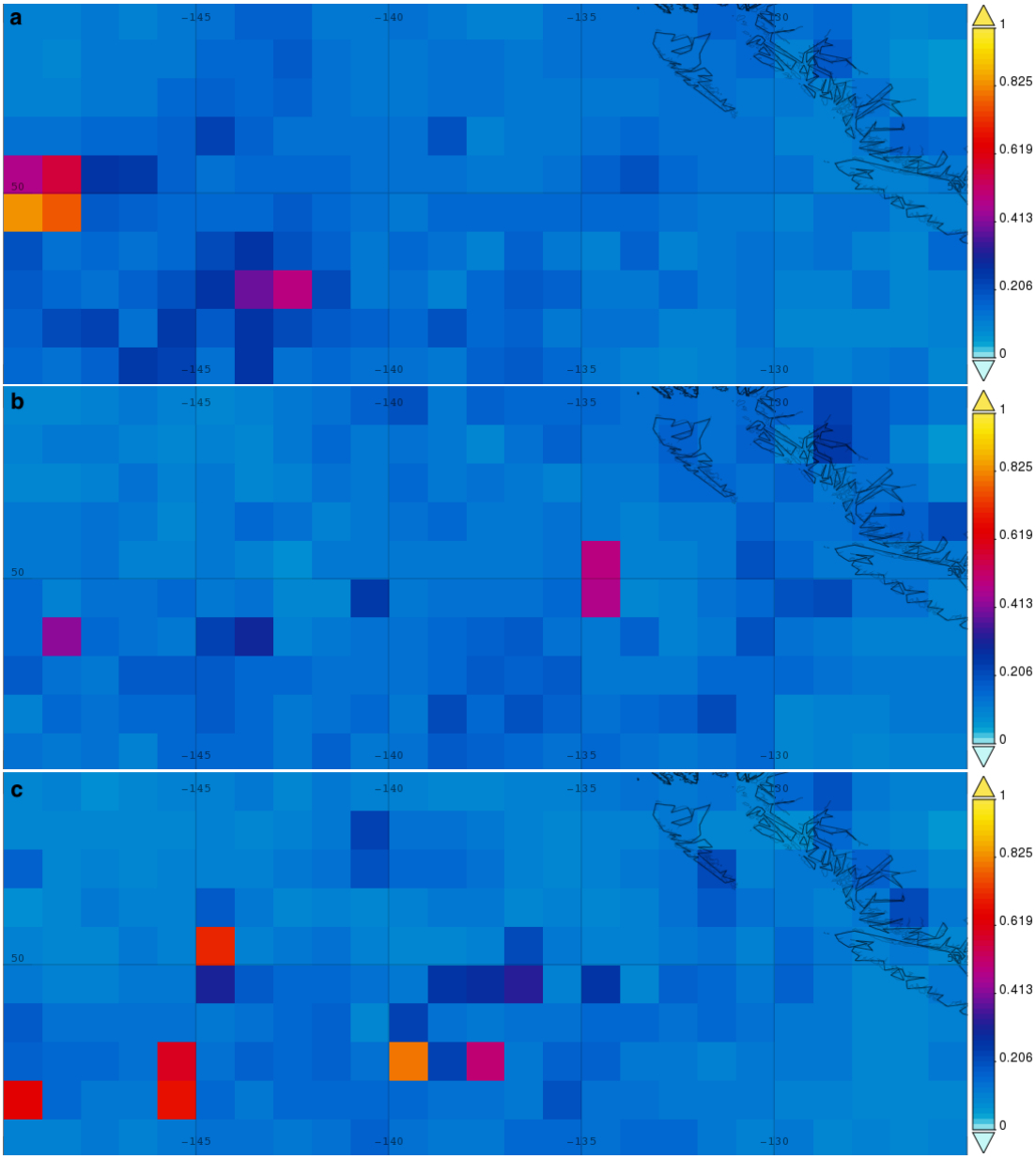

Figure C5. June averaged MODIS aerosol optical depth for (a) 2015, (b) 2016, and (c) 2017. Data were downloaded from NASA's Giovanni website.

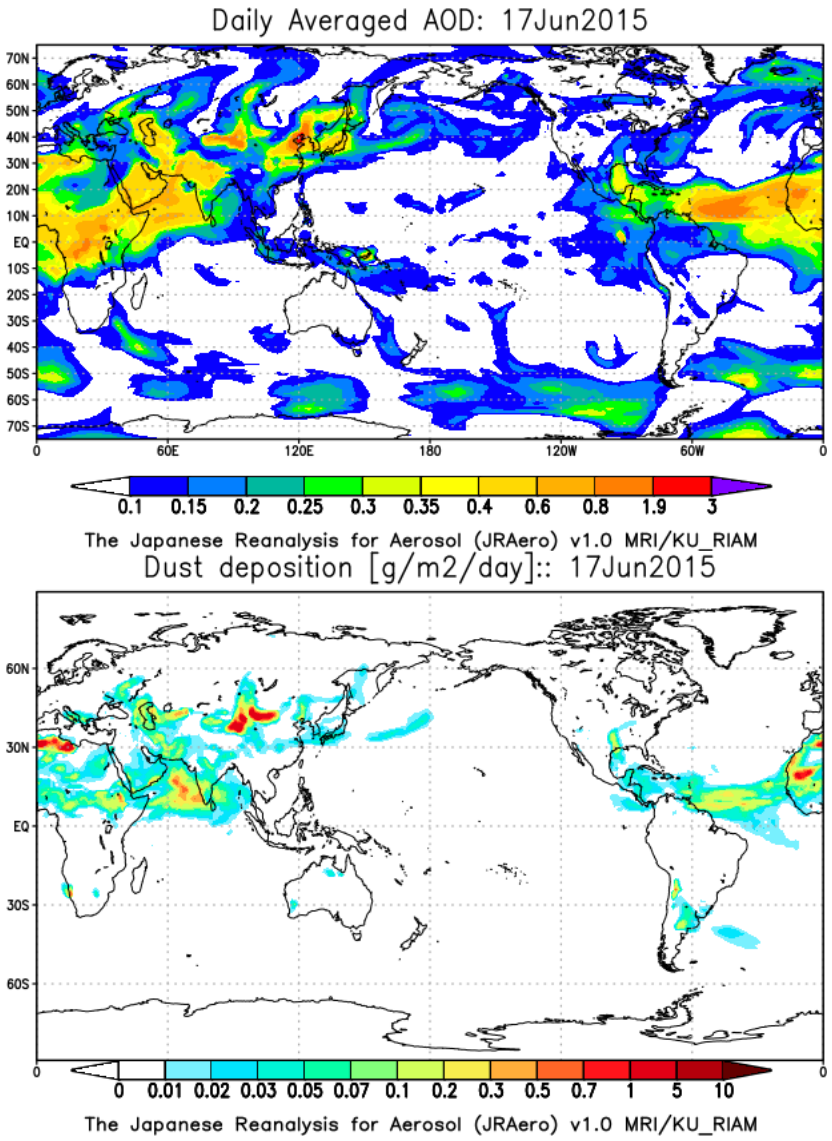

Figure C6. Japanese Reanalysis for (a) daily averaged aerosol optical depth and (b) dust deposition (g m^{-2} d^{-1}) on 17 June 2015. Data were downloaded from https://www.riam.kyushu-u.ac.jp/taikai/JRAero/atlas.html. Only 2015 data were available.

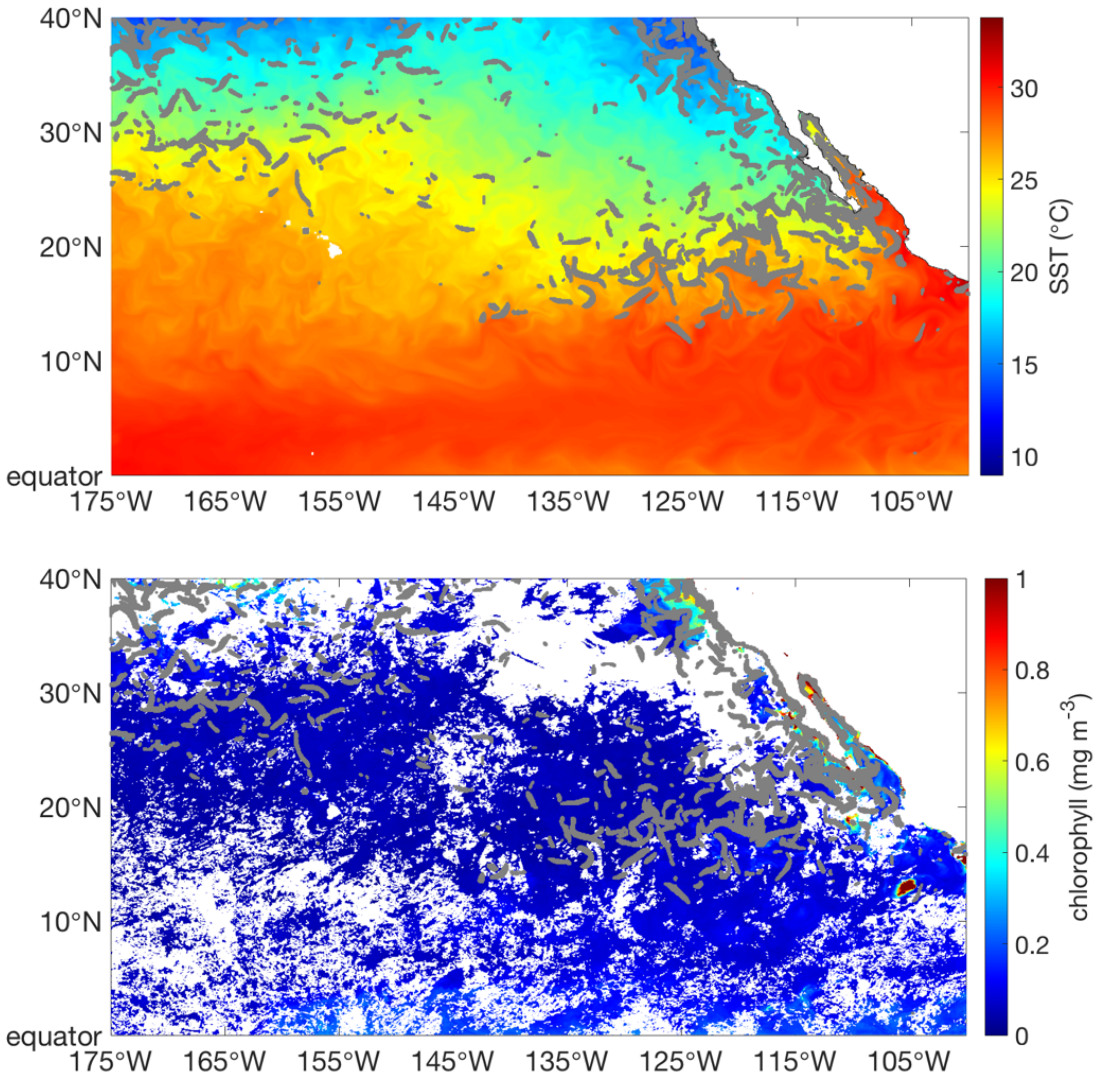

Figure C7. (a) Background colours are Mercator sea surface temperature for 17 June 2017 (b) 8 day average surface chlorophyll satellite data from GlobColour for 10-17 June 2017. Grey dots indicate front locations based on a criterion of 1°C temperature change over 1/3 degree distance.